



**Calhoun: The NPS Institutional Archive**  
**DSpace Repository**

---

Theses and Dissertations

1. Thesis and Dissertation Collection, all items

---

2000-09

Evaluation of tactical decision aid programs  
for prediction of field performance of IR sensors

Goksin, Celalettin

Monterey, California. Naval Postgraduate School

---

<https://hdl.handle.net/10945/7688>

---

*Downloaded from NPS Archive: Calhoun*



Calhoun is the Naval Postgraduate School's public access digital repository for research materials and institutional publications created by the NPS community. Calhoun is named for Professor of Mathematics Guy K. Calhoun, NPS's first appointed -- and published -- scholarly author.

**Dudley Knox Library / Naval Postgraduate School**  
**411 Dyer Road / 1 University Circle**  
**Monterey, California USA 93943**

<http://www.nps.edu/library>

**NPS ARCHIVE**  
**2000.09**  
**GOKSIN, C.**









# NAVAL POSTGRADUATE SCHOOL Monterey, California



## THESIS

**EVALUATION OF TACTICAL DECISION AID  
PROGRAMS FOR PREDICTION OF FIELD  
PERFORMANCE OF IR SENSORS**

by

Celalettin Goksin

September 2000

Thesis Advisor:  
Co-Advisor:

Alfred W. Cooper  
Andreas K. Goroeh

**Approved for public release; distribution is unlimited.**



# REPORT DOCUMENTATION PAGE

Form Approved  
OMB No. 0704-0188

Public reporting burden for this collection of information is estimated to average 1 hour per response, including the time for reviewing instruction, searching existing data sources, gathering and maintaining the data needed, and completing and reviewing the collection of information. Send comments regarding this burden estimate or any other aspect of this collection of information, including suggestions for reducing this burden, to Washington headquarters Services, Directorate for Information Operations and Reports, 1215 Jefferson Davis Highway, Suite 1204, Arlington, VA 22202-4302, and to the Office of Management and Budget, Paperwork Reduction Project (0704-0188) Washington DC 20503.

1. AGENCY USE ONLY (Leave blank)		2. REPORT DATE September 2000	3. REPORT TYPE AND DATES COVERED Master's Thesis	
4. TITLE AND SUBTITLE Evaluation of Tactical Decision Aid Programs for Prediction of Field Performance of IR Sensors.			5. FUNDING NUMBERS	
6. AUTHOR(S) Goksin, Celalettin			8. PERFORMING ORGANIZATION REPORT NUMBER	
7. PERFORMING ORGANIZATION NAME(S) AND ADDRESS(ES) Naval Postgraduate School Monterey, CA 93943-5000			10. SPONSORING / MONITORING AGENCY REPORT NUMBER	
9. SPONSORING / MONITORING AGENCY NAME(S) AND ADDRESS(ES)			11. SUPPLEMENTARY NOTES The views expressed in this thesis are those of the author and do not reflect the official policy or position of the Department of Defense or the U.S. Government.	
12a. DISTRIBUTION / AVAILABILITY STATEMENT Approved for public release; distribution is unlimited.			12b. DISTRIBUTION CODE	
13. ABSTRACT (maximum 200 words) The diversity of infrared system performance prediction models currently used by different services conflict with the concept of 'joint operations' where all services must share the common resources to survive. In this respect this study presents an analysis and a comparison of two operational performance models, the U.S. Army's ACQUIRE and the infrared module of the Navy/Air Force Tactical Decision Aid (TDA), WinEOTDA. Differences in the modeling of underlying physical principles, input parameters, and treatments are analyzed. A comparison of the predicted detection ranges is made using a data set collected in the Gulf of Oman as the meteorological input. Suggestions are sought for the modification of the codes that will lead to the same outputs. Finally the possibility of adopting one of the codes as a standard TDA is analyzed. For the same scenario inputs and with a user-defined sensor model WinEOTDA predicted longer ranges for 100% of the time. WinEOTDA was observed to be more accurate in predicting detection ranges than ACQUIRE because of the improved target modeling.				
14. Subject Terms Tactical Decision Aids, FLIR92, SeaRad, ACQUIRE, WinEOTDA, TAWS.			15. NUMBER OF PAGES 164	
			16. PRICE CODE	
17. SECURITY CLASSIFICATION OF REPORT Unclassified	18. SECURITY CLASSIFICATION OF THIS PAGE Unclassified	19. SECURITY CLASSIFICATION OF ABSTRACT Unclassified	20. LIMITATION OF ABSTRACT UL	

NSN 7540-01-280-5500

Standard Form 298 (Rev. 2-89)  
Prescribed by ANSI Std. Z39-18298-102



THIS PAGE INTENTIONALLY LEFT BLANK

**Approved for public release; distribution is unlimited**

**EVALUATION OF TACTICAL DECISION AID PROGRAMS FOR  
PREDICTION OF FIELD PERFORMANCE OF IR SENSORS**

Celalettin Goksin  
1<sup>st</sup> Lieutenant, Turkish Army  
B.S., Turkish War College, 1993

Submitted in partial fulfillment of the  
requirements for the degree of

**MASTER OF SCIENCE IN SYSTEMS ENGINEERING**

from the

**NAVAL POSTGRADUATE SCHOOL  
September 2000**

NPS ARCHIVE  
2000.09  
GOKSIN, C.

~~Thesis~~  
~~G5833~~  
C.1

THIS PAGE INTENTIONALLY LEFT BLANK

## ABSTRACT

The diversity of infrared system performance prediction models currently used by different services conflict with the concept of 'joint operations' where all services must share the common resources to survive. In this respect this study presents an analysis and a comparison of two operational performance models, the U.S. Army's ACQUIRE and the infrared module of the Navy/Air Force Tactical Decision Aid (TDA), WinEOTDA. Differences in the modeling of underlying physical principles, input parameters, and treatments are analyzed. A comparison of the predicted detection ranges is made using a data set collected in the Gulf of Oman as the meteorological input. Suggestions are sought for the modification of the codes that will lead to the same outputs. Finally the possibility of adopting one of the codes as a standard TDA is analyzed. For the same scenario inputs and with a user-defined sensor model WinEOTDA predicted longer ranges for 100% of the time. WinEOTDA was observed to be more accurate in predicting detection ranges than ACQUIRE because of the improved target modeling.

THIS PAGE INTENTIONALLY LEFT BLANK



## TABLE OF CONTENTS

I.	INTRODUCTION.....	1
II.	THEORY AND BACKGROUND.....	5
	A. ELECTROMAGNETIC AND IR SPECTRUM.....	5
	B. THERMAL RADIATION LAWS.....	7
	1. Planck's Law.....	9
	2. Wien's Displacement Law.....	9
	3. Stefan-Boltzmann Law.....	10
	4. Total Power Law.....	11
	5. Kirchoff's Law.....	11
	C. ATMOSPHERIC PROPAGATION.....	12
	D. TARGET SIGNATURE.....	15
	E. DETECTION CRITERION.....	20
	F. FLIR SYSTEM PERFORMANCE PARAMETERS.....	22
	1. Physical Parameters.....	22
	2. Noise Equivalent Temperature Difference (NETD).....	24
	3. Minimum Resolvable Temperature Difference (MRTD).....	26
	4. Minimum Detectable Temperature Difference (MDTD).....	28
III.	MODELS.....	31
	A. GENERAL INFORMATION ABOUT TDAs.....	31
	B. FLIR92 MODEL.....	32
	C. SEARAD RADIANCE MODEL.....	36
	D. WINEOTDA MODEL.....	37
	1. Target Model.....	38
	2. Atmospheric Model.....	41
	3. Sensor Model.....	43
	4. Output Files.....	44
	E. ACQUIRE MODEL.....	44
	1. Target Model.....	46
	2. Atmospheric Model.....	47
	3. Sensor Model.....	48
	4. Output Files.....	48
IV.	COMPUTATIONS AND RESULTS.....	51
	A. SCENARIO INPUT PARAMETERS.....	51
	B. FLIR92 MODEL OUTPUTS.....	53
	1. Comparison of FLIR92 Model Sensor Outputs With The Other Sensors in WinEOTDA Model.....	53
	C. SEARAD RADIANCE MODEL OUTPUTS.....	55
	D. WINEOTDA MODEL INPUTS.....	55
	1. Target Model.....	56
	2. Atmospheric Model.....	58
	3. Sensor Model.....	59

E. WINEOTDA MODEL OUTPUTS .....	60
F. ACQUIRE MODEL INPUTS .....	61
1. Target Model .....	61
2. Atmospheric Model .....	65
3. Sensor Model .....	66
G. ACQUIRE MODEL OUTPUTS .....	68
H. COMPARISON OF WINEOTDA AND ACQUIRE MODEL OUTPUTS ....	70
I. COMPARISON OF WINEOTDA AND ACQUIRE OUTPUTS WITH THE MODIFIED WINEOTDA METEOROLOGICAL DATA.....	73
J. COMPARISON OF WINEOTDA AND ACQUIRE OUTPUTS WITH THE USE OF BEER'S LAW APPROXIMATION IN ACQUIRE MODEL .....	74
<b>V. CONCLUSIONS AND RECOMMENDATIONS .....</b>	<b>79</b>
A. COMMON SET OF INPUT PARAMETERS .....	80
B. DIFFERENCES IN THE PREDICTIONS OF CODES WITH THE COMMON INPUT PARAMETERS .....	81
C. DIFFERENCES IN THE TREATMENT OF CODE INPUTS.....	82
D. SUGGESTIONS FOR THE MODIFICATION OF CODES.....	87
E. CODE SELECTION FOR INTER-SERVICE USE .....	89
F. RECOMMENDATIONS FOR FURTHER RESEARCH .....	90
<b>APPENDIX A. FLIR92 MODEL OUTPUTS.....</b>	<b>93</b>
<b>APPENDIX B. FIGURES OF COMPARISON OF FLIR92 MODEL SENSOR OUTPUTS WITH THE OTHER SENSORS IN WINEOTDA MODEL .....</b>	<b>97</b>
<b>APPENDIX C. SEARAD INPUTS.....</b>	<b>101</b>
<b>APPENDIX D. SEARAD OUTPUTS.....</b>	<b>103</b>
<b>APPENDIX E. WINEOTDA MODEL DATA ENTRY FORMS.....</b>	<b>105</b>
<b>APPENDIX F. WINEOTDA MODEL OUTPUTS.....</b>	<b>109</b>
<b>APPENDIX G. ACQUIRE MODEL INPUTS .....</b>	<b>115</b>
<b>APPENDIX H. CRITICAL DIMENSION ANALYSIS OF ACQUIRE TARGET MODEL .....</b>	<b>117</b>
<b>APPENDIX I. ACQUIRE MODEL OUTPUTS.....</b>	<b>121</b>
<b>APPENDIX J. COMPARISON OF BEER'S LAW AND SEARAD OUTPUTS .....</b>	<b>139</b>
<b>APPENDIX K. COMPARISON TABLES OF WINEOTDA AND TAWS OUTPUTS .....</b>	<b>141</b>
A. TAWS OVERVIEW .....	141
B. COMPARISON OF TAWS AND WINEOTDA OUTPUTS .....	142
<b>LIST OF REFERENCES.....</b>	<b>145</b>
<b>INITIAL DISTRIBUTION LIST .....</b>	<b>149</b>

## **ACKNOWLEDGMENT**

The support of this project by Naval Sea Systems Command through the Thesis and Curriculum Support Project is gratefully acknowledged.

I want to thank my thesis advisors for everything they provided for my work. First, I would like to thank Dr. Andreas Goroch of Naval Research Laboratory for his active participation and help during all phases of this work.

I have special thanks for Professor Alfred Cooper, whose vast knowledge and experience led me to finish this thesis successfully. His cooperation and guidance made everything easier to work with.

Finally, I would like to thank my parents for their support in any means during the development of this work.

THIS PAGE INTENTIONALLY LEFT BLANK

## I. INTRODUCTION

Thermal imaging systems are often used for detection, recognition, and identification of targets from ground based or aerial platforms by the military. The availability of these performance predictions to a decision maker or an operator in advance or at the time of operation has vital importance for the timely deployment of weapon systems on the battlefield. A reliable prediction of performance in the target area is also very significant in the mission-planning phase of a tactical operation. Tactical Decision Aids (TDAs), which can have various forms such as nomographs, manuals and computer codes, are tools currently used for these purposes to provide predicted detection and lock-on ranges to decision makers or operators. The performance predictions are currently available in the form of computer codes from either the Naval Research Laboratory (NRL), the Air Force Research Laboratory (AFRL), or the U.S. Army Night Vision and Electronic Systems Directorate (NVESD).

Current and future modern warfare, which utilizes high technology in every means to have the desired impact on the enemy, can be analyzed within the concept of joint



operations. As opposed to the old style battlefield where each service had its own opponent, today every service requires joint resources and joint support to survive. This requires a cooperative effort, which leads to the concept of joint operations. In this respect the existence of two different infrared system TDA programs currently used by the military conflicts with this idea. This work will seek a solution to this problem by comparing the infrared modules of the Navy/Air Force TDA, WinEOTDA Version 1.3.3 dated 1998 and the Army FLIR TDA, ACQUIRE Version 1 dated 1995, with respect to different means the programs use to model target, atmosphere and sensor.

The objective of this thesis is to determine the differences in the modeling of underlying physical principles, in the input parameters, and in the predicted target detection ranges; provide suggestions for modification of the codes that will lead to equivalent outputs for the same inputs. Finally the possibility of using one of them as a standard TDA for all services will be examined. We will start Chapter II by presenting some fundamentals of infrared radiation theory. This will be followed by an analysis and comparison of the ways in which this theory is implemented by the two programs. Then the

analysis of the results will be presented in Chapter IV.  
Finally Chapter V will summarize and conclude this work.

THIS PAGE INTENTIONALLY LEFT BLANK

## II. THEORY AND BACKGROUND

The purpose of this Chapter is to give a short summary of those basic principles of Infrared Radiation which are related to the topics addressed in this thesis.

### A. ELECTROMAGNETIC AND IR SPECTRUM

The electromagnetic spectrum can be described in terms of propagating electromagnetic fields that are characterized by frequency and amplitude. The optical spectrum can be defined as that subset of the electromagnetic spectrum covering optical wavelengths. However there are no exact boundaries for the separation of these wavelengths.

The optical spectrum covers the ultraviolet (UV), visible, and infrared (IR) portions of the electromagnetic spectrum. Figure 2.1 shows the electromagnetic spectrum and identifies various sub-regions of the optical spectrum. It can be seen that the visible light spectrum bounds the infrared region on the short-wavelength side and the microwave bounds it on the long-wavelength side. The ultraviolet portion ranges from about 0.1 to 0.38

micrometer while the visible portion is from approximately 0.38 to 0.76 micrometer in wavelength.

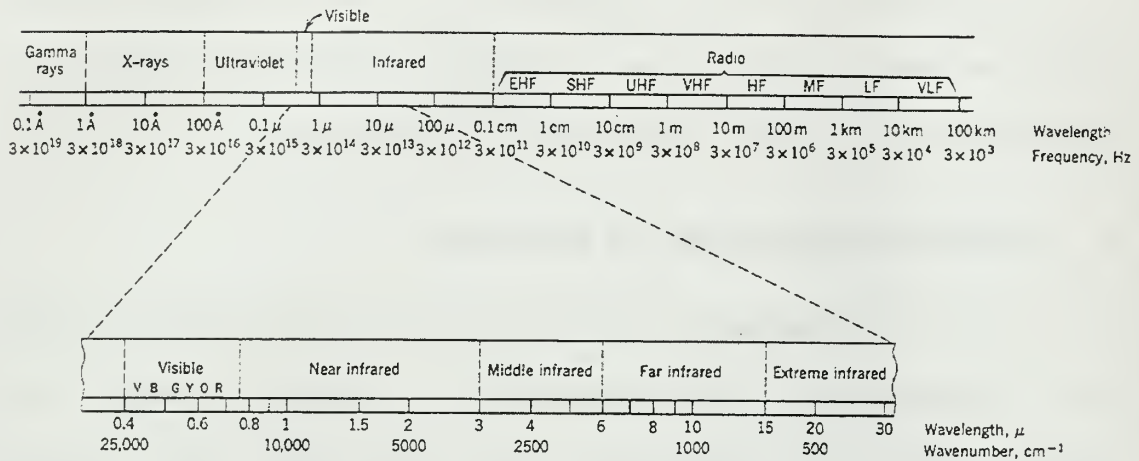


Figure 2.1 - The Electromagnetic Spectrum "From [Ref. 6]".

The infrared portion is further divided into four different sub-regions; the near infrared or short-wavelength infrared (SWIR) region (from 0.77 to 3 micrometer), the mid-wavelength infrared (MWIR) region (from 3 to 8 micrometer), the long-wavelength infrared (LWIR) region (from 8 to 14 micrometer), and the far and extreme infrared regions (from 14 to 1000 micrometer) respectively [Ref. 5].

Imagers operating in the infrared region of the electromagnetic spectrum sense the radiation emanating from the targets and the background scene. Unlike night vision devices working in the near infrared region, which sense the ambient radiation reflected from the targets and the background, thermal devices (e.g., Forward Looking



Infrared, FLIR) basically take advantage of the thermal energy emitted by the objects in the infrared to detect the signatures.

## B. THERMAL RADIATION LAWS

It is necessary to define some important parameters to clarify the basic laws of thermal radiation. The following definitions are taken from Seyrafi [Ref. 5].

- Absorptivity ( $\alpha$ ): the ratio of the absorbed radiant power to the incident radiant power.
- Reflectivity ( $\rho$ ): the ratio of the reflected radiant power to the incident radiant power.
- Transmissivity ( $\tau$ ): the ratio of the transmitted radiant power to the incident radiant power.
- Emissivity ( $\varepsilon$ ): the ratio of the radiant power emitted per unit area from a surface to the radiance emitted per unit area from a blackbody.
- Blackbody: defined as an ideal body or surface that absorbs all radiant energy incident upon it at any wavelength and at any angle of incidence, so that none of the radiant energy is reflected or

transmitted. Blackbodies also have emissivity equal to one ( $\epsilon=1$ ).

- Gray body: a radiation source with an emissivity less than unity, and the emissivity is constant over all wavelengths [Ref. 1].

Table 2.1 gives basic definitions of a few most commonly used radiometric quantities.

Name	Symbol	Units	Description
Energy	$Q$	$J$	Total radiant energy contained in a radiation field. ( $Q$ )
Radiant Flux(Power)	$\Phi$	$W$	Radiant power traversing a surface. ( $\partial Q/\partial t$ )
Radiant flux Density (Exitance)	$M$	$W - cm^{-2}$	Radiant flux leaving an infinitesimal area of surface divided by that area. ( $\partial\Phi/\partial A$ )
Irradiance	$E$	$W - cm^{-2}$	Radiant power per unit area incident on a surface. ( $\partial\Phi/\partial A$ )
Radiant Intensity	$I$	$W - sr^{-1}$	Radiant power leaving a Point Source per unit Solid Angle. ( $\partial\Phi/\partial\Omega$ )
Radiance	$L$	$W - sr^{-1} - cm^{-2}$	Radiant power leaving or arriving at a surface at a point in a given direction per unit solid angle and per unit area projected normal to that direction. ( $\partial^2\Phi/\partial A \cos\theta \partial\Omega$ )

Table 2.1 - Radiometric Units "After [Ref. 3]".

## 1. Planck's Law

This law gives the spectral distribution of radiant emittance of a blackbody radiation source, and can be formulated as:

$$M(\lambda, T) = \frac{c_1}{\lambda^5 (e^{c_2/\lambda T} - 1)} \quad (2.1)$$

where:

$M(\lambda, T)$  = the blackbody spectral radiant emittance at wavelength  $\lambda$  (Watt/cm<sup>2</sup>  $\mu$ m)

$$c_1 = 3.7418 \times 10^4 \text{ Watt-}\mu\text{m}^4 / \text{cm}^2$$

$$c_2 = 1.4388 \times 10^4 \mu\text{m-Kelvin}$$

$$T = \text{absolute temperature of the blackbody (K)}$$

$$\lambda = \text{wavelength (m)}$$

## 2. Wien's Displacement Law

Wien's law is simply the derivative of Equation 2.1 and gives the peak wavelength of the spectral emission for a given blackbody temperature by:

$$\lambda_{\max} T = 2897 \quad (2.2)$$

where:

$\lambda_{\max}$  = wavelength where the peak of radiation occurs ( $\mu$ m).

$T$  = temperature (K).

As the temperature of a source increases, this equation indicates a shift in the wavelength of the maximum radiation toward a shorter wavelength. This can be observed graphically in Figure 2.2.

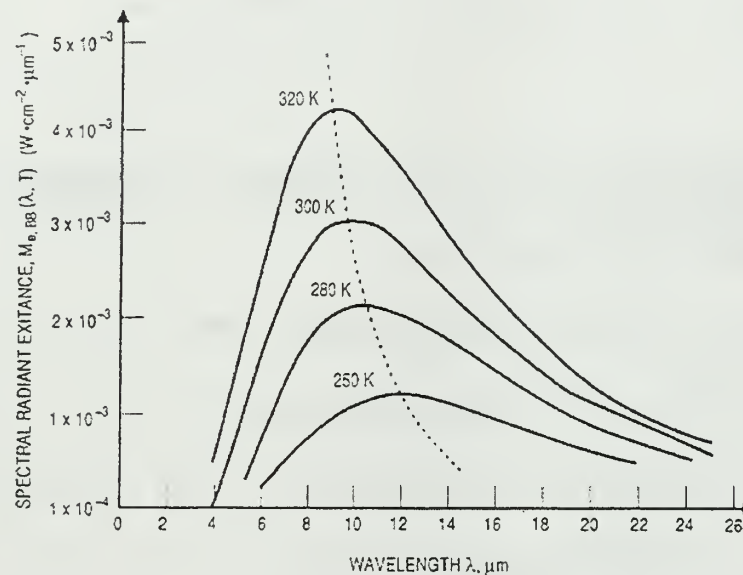


Figure 2.2 - Spectral Radiant Exitance of Blackbodies at Various Temperatures "From [Ref. 5]".

### 3. Stefan-Boltzmann Law

This law is simply the integral of Equation 2.1 and provides the total radiant emittance by integrating Planck's law over the entire spectrum. The following equation applies only to blackbody and graybody sources [Ref. 1], and is formulated as:

$$M = \epsilon \sigma T^4 \quad (2.3)$$

where:

$\epsilon$  = emissivity

$M$  = total radiant emittance of a blackbody

$\sigma$  = the Stefan-Boltzmann constant ( $5.7 \times 10^{-8}$  Watt/m<sup>2</sup>)

#### **4. Total Power Law**

The radiation incident upon a body may be transmitted, absorbed, or reflected and by conservation of energy the sum of the ratios of each of these components to the incident power must be one.

$$\alpha + \rho + \tau = 1 \quad (2.4)$$

where:

$\alpha$  = absorptivity

$\rho$  = reflectivity

$\tau$  = transmissivity

#### **5. Kirchoff's Law**

This law states that the bodies emit as well as they absorb at any wavelength; this can be expressed as [Ref. 2]:

$$\alpha_{\lambda} = \epsilon_{\lambda} \quad (2.5)$$



### C.    **ATMOSPHERIC PROPAGATION**

The optical signal radiated from an object must pass through the Earth's atmosphere before it reaches a receiver. No matter how strong the target signature is, the intervening atmosphere always attenuates the thermal signal. This attenuation is due to the individual or collective effects of the following phenomena:

- Molecular absorption,
- Molecular scattering,
- Aerosol absorption and,
- Aerosol scattering.

Molecular absorption is due to the ability of certain molecules to go from one vibration-rotation state to another. It is generally characterized by discrete absorption lines arising from the quantal nature of the absorption, modified by broadening processes, including pressure and Doppler broadening. Water vapor is the most important of these molecules. It limits the useful range of infrared wavelength to the 3-5 and 8-14 micrometer bands. Other molecular absorbers include carbon dioxide, carbon monoxide, ozone, methane and nitrous oxides.

Scattering, on the other hand, is the redistribution of the incident energy into all propagation directions. The scattering processes are generally related to the ratio of wavelength to particle size, resulting in broad absorption spectra, generally maximum when wavelength is pi times particle size. When wavelength is much shorter than particle radius, Rayleigh scattering is dominant; when wavelength is much longer than particle radius scattering becomes small. Scattering differs from absorption in that the scattered radiant energy remains in the same form as the incident radiation [Ref. 1]. Water droplets suspended in the air are the most important source of scattering. Other sources of scattering include dust, smoke, smog, rain, or snow [Ref. 10].

Extinction, the sum of absorption and scattering, is the process of attenuation of the radiant flux in passing through the atmosphere. It can be expressed in terms of an exponential coefficient used in the following formula, called Beer's law, where  $\mu$  is the extinction coefficient and  $R$  is the path length:

$$\tau = e^{-\mu R} \quad (2.6)$$

$\tau$  is the transmittance of a path length  $R$  through the atmosphere. The spectral transmittance for 1 km path length

at sea level under "typical" conditions is shown in Figure 2.3.

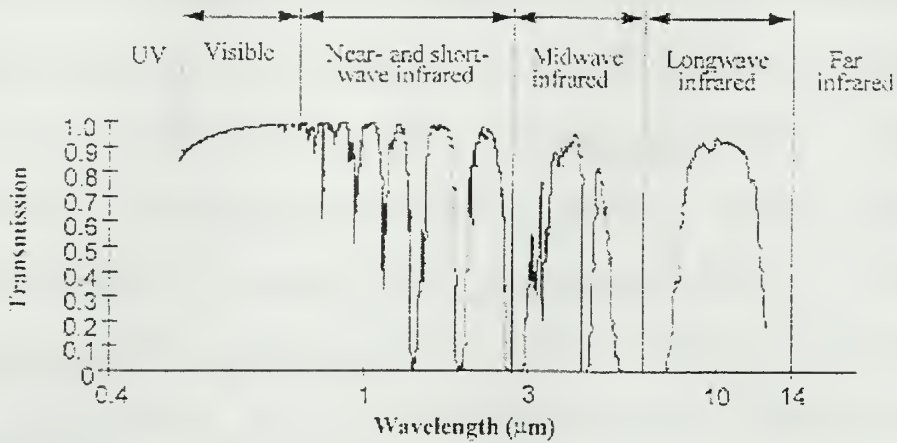


Figure 2.3 - Typical Atmospheric Transmission for a 1 Km Path Length "From [Ref. 1]".

It can be observed that atmospheric extinction is a strong function of wavelength, which severely affects the transmittance through the atmosphere, and 3-5  $\mu\text{m}$  (MWIR) and 8-12  $\mu\text{m}$  (LWIR) wavelength regions are the only ranges valid for atmospheric propagation.

The large number of parameters involved in optical transmission through the atmosphere makes numerical calculations of atmospheric transmission inevitable. The aim of the numerical calculation is to predict with a high degree of accuracy the transmittance through the atmosphere, given a path, atmospheric conditions, wavelength, and a set of measured or predicted

meteorological parameters [Ref. 5]. For an accurate atmospheric transmission calculation all molecular, aerosol, and precipitation effects must be considered, and a detailed model must be used to get precise results when necessary. Three such models are LOWTRAN [Ref. 17], FASCODE [Ref. 3], and MODTRAN [Ref. 18] that are used to obtain the atmospheric transmittance  $\tau(\lambda)$ .

The SEARAD Radiance Model, which is a surface radiance model integrated with the MODTRAN2 transmission model, will be used to predict the atmospheric transmittance required by the sensor performance model in this thesis, and will be described in that context.

#### **D. TARGET SIGNATURE**

Infrared sensors respond to the difference in radiance between target and background. From Equation 2.3 it is evident that the target-background radiance difference can be related to an equivalent temperature difference ( $\Delta T$ ), which appears as a thermal quantity. The equivalent temperature difference is defined as the temperature difference of two blackbody sources required to produce the actual radiance difference between target and background.

Figure 2.4 shows the geometry, which can be used to obtain  $\Delta T$  for an extended target.

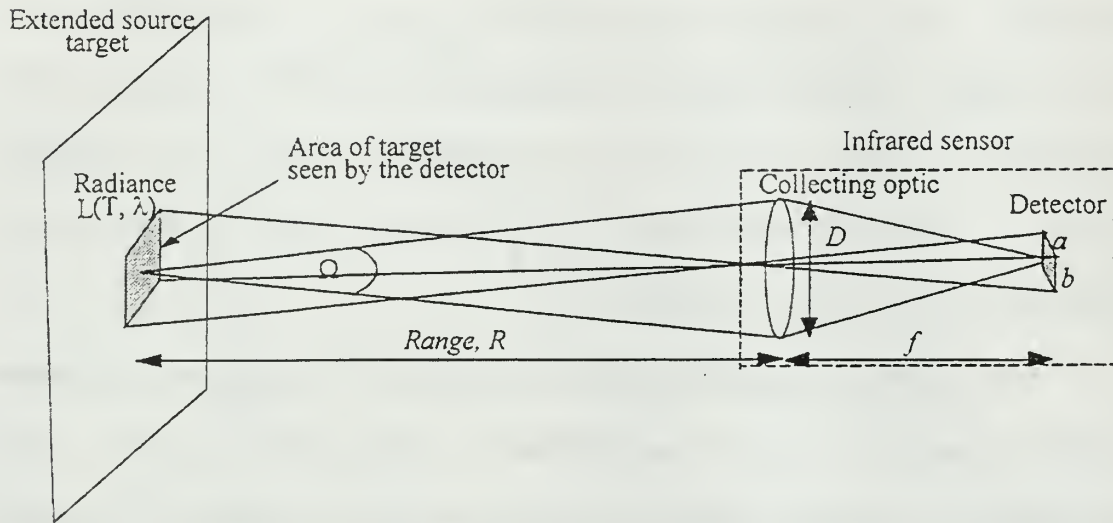


Figure 2.4 - Differential temperature geometry "From [Ref.1]" .

However, a more important quantity than temperature difference is the apparent temperature difference ( $\Delta T_{app}$ ). This is the equivalent blackbody temperature difference seen through an atmospheric path that produces the same sensor output voltage difference as the real target and background. The following figure pictures the difference between the concept of temperature difference at zero range ( $\Delta T_{tgt}$ ) and the temperature difference seen at the entrance aperture of the sensor (apparent delta T,  $\Delta T_{app}$ ).

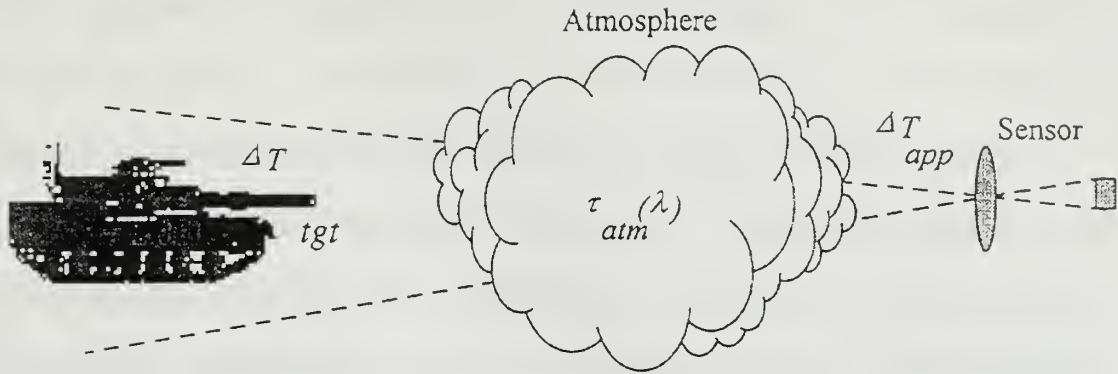


Figure 2.5 - Apparent delta T "From [Ref. 1]".

There are various computational techniques available to determine the apparent target-to-background temperature difference at the entrance aperture of a broadband infrared sensor. In this thesis the following two techniques will be used for calculating the apparent delta T where necessary.

The first technique estimates an apparent temperature difference as the product of the target-to-background temperature ( $\Delta T_{tgt}$ ) and the atmospheric broadband Beer's law transmittance ( $\tau_{1Km}^R$ ), using an extinction coefficient averaged over the system bandwidth. That is:

$$\Delta T_{app} = \Delta T_{tgt} \tau_{1Km}^R \quad (2.7)$$



The broadband transmittance ( $\tau_{1Km}^R$ ) is defined for a one-kilometer path length and R is the target-to-sensor range in km.

While Beer's law is valid for monochromatic (single wavelength) sources, infrared imaging sensors typically operate with a broad bandwidth of several micrometers. Propagation of broadband radiation presents significant computational difficulty, since Beer's Law is not generally valid for broadband transmission of light [Ref. 1]. In the broadband Beer's Law approximation, a band averaged extinction coefficient is computed from the transmittance at a reference path length. The transmittance is found by averaging the spectral transmittance over the wave band for that path length. In this computation the reference extinction coefficient is then taken to be constant over that bandwidth for all ranges. However, in actuality the spectral extinction coefficient varies within the bandpass, and the band averaged extinction coefficient will be a function of the range. Thus in broadband transmission, absorption is not characterized by a constant exponential coefficient as in Beer's Law, and the exponential range dependence does not hold.

The second technique is different from the first in that a broadband Beer's law assumption is not used to determine the atmospheric transmittance. Instead an atmospheric transmission program is used to find the broadband transmittance directly as a function of range. Then as in the following equation the product of target-to-background temperature ( $\Delta T_{igr}$ ) and the output transmittance values of the atmospheric transmission program,  $\tau(R)$ , is taken to determine the apparent temperature.

$$\Delta T_{app} = \Delta T_{igr} \tau(R) \quad (2.8)$$

It must be noted that differential target temperature ( $\Delta T_{igr}$ ) used in Equation 2.7 and 2.8 is referenced to two blackbody sources required to provide the same differential flux as that of actual target and background. Thus the temperature is not in fact attenuated through the atmosphere; energy or radiance is attenuated [Ref. 1].

This technique is the one presently used in the system performance program ACQUIRE [Ref. 16] in this thesis. This technique eliminates the errors associated with a broadband Beer's law assumption [Ref. 1].

## E. DETECTION CRITERION

Target detection refers to different levels of distinguishing an object from background. The lowest level is simply a detection of the object. The highest level is the identification of a specific object. These levels can be gathered into two groups: pure detection and discrimination detection. In pure detection locating an object in the scene is sufficient to declare detection. On the other hand, in discrimination detection where the scene contains many non-targets, objects cannot be detected as targets until sufficient shape information can be obtained to distinguish the target from non-targets or clutter.

The traditional FLIR analysis describes the interaction of the FLIR-aided eye with two types of simple targets: an isolated rectangle, characterized by uniform temperature difference from the background and a periodic bar pattern, also characterized by a temperature difference from the background [Ref. 10]. The minimum temperature difference required for detection of the rectangle is known as the minimum detectable temperature difference (MDTD). The temperature required to resolve the four bars is known as the minimum resolvable temperature difference (MRTD). It

is common to represent operational targets with equivalent bar targets for evaluation. Johnson [Ref. 19] conducted a number of experiments with a number of trained observers at the U.S. Army's Night Vision and Electronic Sensor's Directorate to develop resolution requirements for detection, recognition and identification of objects by using these bar patterns. He determined the average number of line pairs required for different discrimination levels as listed in Table 2.2. Today these are known as the "Johnson Criteria". The cycle criteria in Table 2.2 correspond to the necessary number of resolution elements on the critical dimension of the object with a two-dimensional cycle requirement and to a probability of 50% for a given discrimination task. In this table,  $n_{50}$  is the number of cycles required to be resolved in order to achieve a 50% probability of discrimination.

Detection $n_{50} = 0.75$	An object within the sensor FOV is a target of potential military interest
Classification $n_{50} = 1.5$	The target belongs to a general class of vehicles: tracked or wheeled
Recognition $n_{50} = 3$	The target is a specific object within a class of similar objects: tank or APC
Identification $n_{50} = 6$	The target is a specific vehicle: T72

Table 2.2 - Johnson Cycle Criteria "From [Ref. 13]".

In the detection process the Johnson criterion is used after finding the target, where the target size and shape provide information for detection, recognition, and identification. It provides the connection between the MRTD and field performance of the sensor.

In two-dimensional discrimination, also used in this thesis, target area is more important than the minimum dimension used in one-dimensional detection, as first used by Johnson. The "critical dimension" as used in two-dimensional resolution is defined as the square root of the target area.

The two-dimensional FLIR92 model uses the critical dimension approach in the same manner [Ref. 9]. In this thesis Shumaker's [Ref. 10] approach, which takes into account the aspect angles will be used to calculate the critical dimension of the target.

## **F. FLIR SYSTEM PERFORMANCE PARAMETERS**

The following section describes the physical parameters which determine the MRT and MDT.

### **1. Physical Parameters**

The physical parameters of a FLIR system are defined as follows:

**a) Field-of-View (FOV)**

The FOV of an IR system is the angular space in which the system accepts radiation. The system FOV and the distance, or range, from sensor to the object determine the area that a system will image [Ref. 1].

**b) Instantaneous Field-of-View (IFOV)**

The instantaneous FOV is the angular cone through which a detector senses radiation; it depends upon the optical design. It includes both the optical blur diameter and the DAS. When the blur diameter is small compared to the DAS, the IFOV and DAS are approximately equal [Ref. 9].

**c) Detector Angular Subtense (DAS)**

The detector angular subtense is used to describe the resolution limitations of the detector size. DASs in the in-scan ( $\Delta x$ ) and cross-scan ( $\Delta y$ ) directions are given by the detector width or height divided by the focal length. It describes the best resolution that can be achieved by an EO system due to the detector size limitations [Ref. 1].

**d) Modulation Transfer Function (MTF)**

The MTF of a system is a primary measure of the overall system resolution. The system MTF gives the



transfer of input spatial frequencies, and it can be in both horizontal and vertical directions.

The modulation transfer function is the magnitude of the optical transfer function, which actually alters the image as it passes through the optics and circuitry of the system. It can be formulated as the output modulation produced by the system divided by the input modulation at that spatial frequency:

$$MTF = \frac{OUTPUT\_MODULATION}{INPUT\_MODULATION} \quad (2.10)$$

## **2. Noise Equivalent Temperature Difference (NETD)**

NETD is the temperature difference between a large target and its background, which produces a SNR of one in the video signal. In performance predictions, it is used as an intermediate sensitivity parameter for simplification of formulations of performance parameters such as MRT, and MDT. NETD can also be described as a system's ability to detect small signals in noise. It does not account for the spatial and temporal integration effects of the eye.

Shumaker [Ref. 10] gives NETD for a scanning system as:

$$NETD = \frac{10(FOV_x FOV_y F_r N_{os} N_{ss})^{1/2}}{(\pi N_D \eta_{sc})^{1/2} D^2 \Delta x \Delta y D^* \partial N / \partial T} \quad (2.11)$$

where:

D is the aperture diameter (m)

D\* is the band average detectivity of the detector  
with no cold shield (cm Hz<sup>1/2</sup> W<sup>-1</sup>)

N<sub>D</sub> is the number of detectors

η<sub>sc</sub> is the scan efficiency

Δx is the in-scan detector angular subtense (mRad)

Δy is the cross-scan detector angular subtense  
(mRad)

∂N/∂T is the derivative of Planck's Law (the "Thermal  
gradient".) (watt cm<sup>-2</sup> K<sup>-1</sup> sr<sup>-1</sup>)

FOV<sub>x</sub> is the in-scan field of view (mRad)

FOV<sub>y</sub> is the cross-scan field of view (mRad)

N<sub>os</sub> is the overscan ratio

N<sub>ss</sub> is the serial scan ratio

F<sub>r</sub> is the frame rate

However the concept of three-dimensional noise, which has been successfully integrated into the U.S. Army's Night Vision and Electronics Sensor Directorate's FLIR92 sensor model, will be used for defining the infrared system noise

in this thesis. This method eliminates the limitation of NETD on defining only the temporal detector noise, and characterizes the noise both spatially and temporally from various sources.

### **3. Minimum Resolvable Temperature Difference (MRTD)**

Minimum resolvable temperature difference (MRTD) is the most used and useful FLIR specification parameter. It is defined as the temperature difference between the background and a set of four standard bars (7:1 aspect ratio) required to make the bars just resolvable, as a function of the spatial frequency of the bars. [Ref. 10]

There are several important features of MRTD. First, it is an end-to-end system measure including both resolution and sensitivity, and it is subjective since it involves the judgment of the human observer. Second, the temperature difference that is required to resolve the four bars increases as the bars become smaller, as can be seen from Figure 2.6. Finally the MRT curve is asymptotic at a spatial frequency near  $1/DAS$ , where the MTF becomes zero.

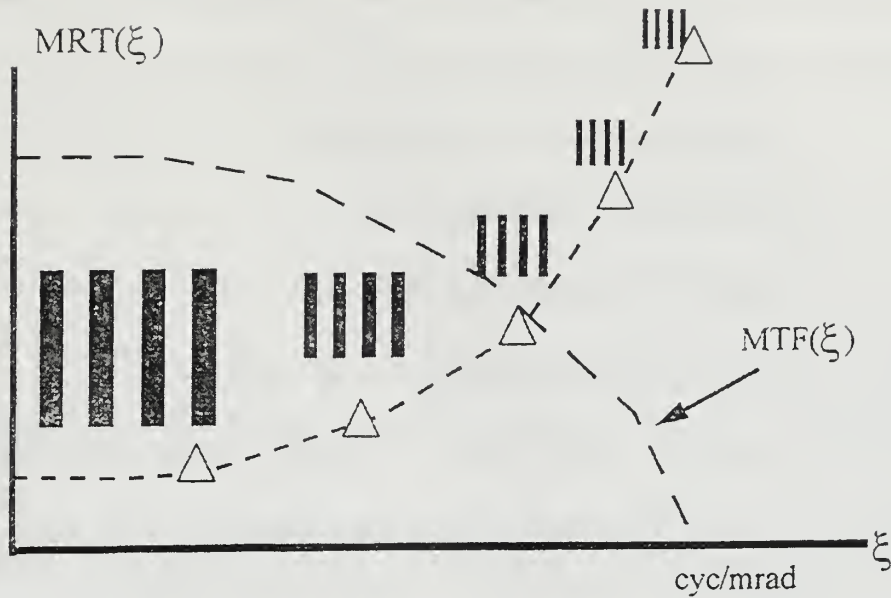


Figure 2.6 - MRTD Patterns of Differing Spatial Frequency ( $\xi$ )  
[Ref. 1]

There are several formulations used and various authors have proposed some alternative expressions for the MRTD. Shumaker [Ref. 8] gives the following formula:

$$MRT(v) = \frac{20SNRT(FOV_x FOV_y v^2)^{1/2} \rho_x^{1/2}}{\tau_0 DD^{**} (\pi N_D \eta_{sc})^{1/2} \eta_{cs} (\Delta x \Delta y)^{1/2} MTF_S(v) (Lt_e)^{1/2} \partial N / \partial T} \quad (2.12)$$

where:

SNRT is the perceived signal-to-noise threshold

$v$  is the spatial frequency (cycles/mRad)

$D$  is the aperture diameter (m)

$D^{**}$  is the band-average detectivity of the detector  
with no cold shield ( $\text{cm Hz}^{1/2} \text{W}^{-1}$ )

$N_D$  is the number of detectors

$\eta_{sc}$  is the scan efficiency

$\eta_{cs}$  is the cold shield efficiency

$\tau_o$  is the transmittance of the optics

$\Delta x$  is the in-scan detector angular subtense (mRad)

$\Delta y$  is the cross-scan detector angular subtense  
(mRad)

$MTF_s$  is the system modulation transfer function

$L$  is the length-to-width ratio for the bar chart

$t_e$  is the eye integration time (0.2s)

$\partial N/\partial T$  is the thermal derivative of Planck's Law (watt  
 $\text{cm}^{-2} \text{K}^{-1} \text{sr}^{-1}$ )

$FOV_x$  is the in-scan field of view (mRad)

$FOV_y$  is the cross-scan field of view (mRad)

$\rho_x$  is the noise filter factor

#### **4. Minimum Detectable Temperature Difference (MDTD)**

The description is almost the same as the MRTD of a FLIR system. The difference between the two is the representation of the target, which for MDTD a square rather than a four-bar target. MDTD of a FLIR gives the

temperature difference between an isolated square and a uniform background that renders the square just detectable, as a function of the dimension of square in spatial frequency. As in the case of MRT it has an element of subjectivity since the judgment of an observer is involved in the process. In the observation process the observer approximately knows the target location. MDT is given as:

$$MDT(v) = \frac{20SNRT(FOV_x FOV_y \Delta x \Delta y)^{1/2} (\Omega_T + r_S^2)}{\pi \tau_0 D \Delta x \Delta y D^{**} \partial N / \partial T \eta_{cs} (N_D \eta_{sc} t_e)^{1/2} \Omega_T (r_S^2 + r_B^2 + \Omega_T)^{1/2}} \quad (2.13)$$

where:

SNRT is the perceived signal-to-noise threshold

v is the spatial frequency (cycles/mRad)

$\Omega_T$  is the solid angular subtense of the target  
(mRad)<sup>2</sup>

D is the aperture diameter (m)

D\*\* is the band average detectivity of the detector  
with no cold shield (cm Hz<sup>1/2</sup> W<sup>-1</sup>)

N<sub>D</sub> is the number of detectors

$\eta_{sc}$  is the scan efficiency

$\eta_{cs}$  is the cold shield efficiency



$\tau_0$  is the transmittance of the optics

$\Delta x$  is the in-scan detector angular subtense (mRad)

$\Delta y$  is the cross-scan detector angular subtense  
(mRad)

$t_e$  is the eye integration time (0.2s)

$\partial N/\partial T$  is the thermal derivative of the Planck's Law  
(watt  $\text{cm}^{-2} \text{K}^{-1} \text{sr}^{-1}$ )

$\text{FOV}_x$  is the in-scan field of view (mRad)

$\text{FOV}_y$  is the cross-scan field of view (mRad)

$r_s$  is the resolution of the system that includes the  
front-end resolution and back-end resolution (mRad)

$r_B$  is the resolution of the back-end that includes  
the detector electronics resolution, preamp resolution,  
resolution of the multiplexer, resolution of the display,  
resolution of the eye, and the resolution due to image  
motion (mRad)

As seen from the above equation MDT has no first-order  
linear dependence on MTF, which means that it does not show  
the asymptotic behavior that MRT does.

### III. MODELS

#### A. GENERAL INFORMATION ABOUT TDAS

Tactical Decision Aids (TDAs) are tools that assist a decision maker or an operator in planning or performing a task. They can be in such various forms as nomographs, manuals or computer codes, which is the form used in this thesis. They are designed to aid a decision maker by assimilation and convenient presentation of data and analysis of a tactical problem beyond what is feasible by humans in timely fashion [Ref. 8].

In parallel with the rapid development in technology of new weapon systems, it is becoming more complex to plan or decide on the timely deployment of these systems on the battlefield. In order to have the desired impact on the targets, TDA codes used by the personnel must be quick and user-friendly to accelerate the planning or operational process. These models can also be used in the design or testing phase of a new system.

Each code contains the following three fundamental parts; a) Target Model which determines the inherent signal emanating from the target and background and converts the radiance difference between them into a temperature

difference ( $\Delta T$ ) at zero range. b) Atmospheric Model, which is the module that calculates the apparent delta T by estimating the degradation of signal due to the atmosphere at the entrance aperture of the sensor. c) Sensor Model which describes the sensor performance in terms of MRTD or MDTD as a function of spatial frequency. This model determines the detection or the lock-on range of an electro-optical system when applied to the apparent target signature. In this thesis the Johnson criterion will be applied for specifying a detection decision where necessary.

The following two sections will cover the models used to design and calculate the performance parameters (i.e., MRTD and MDTD) of a sensor and the calculation of atmospheric transmission, as required by the WinEOTDA and ACQUIRE models. In the remaining sections TDAs under study will be described according to the fundamental parts listed above.

## **B. FLIR92 MODEL**

FLIR92 is a system evaluation tool that uses basic sensor parameters to predict overall system performance for thermal imaging systems. It is a desktop computer model

working in the DOS environment. The model calculates modulation transfer function (MTF), noise equivalent temperature difference (NETD), minimum resolvable temperature difference (MRTD), and minimum detectable temperature difference (MDTD) by using basic system parameters. The principal function of the model is to predict whether or not a system achieves the required MTF, system noise, MRTD, and MDTD determined necessary to meet a target acquisition and discrimination task.

FLIR92 models parallel scan, serial scan, and staring thermal imagers operating in the mid and long-wave infrared regions. It can be used for thermal imagers only and cannot predict the performance of other kinds of electro-optical sensors. The model does not predict target acquisition and discrimination range performance. [Ref. 11]

In FLIR92, there are two different outputs: an MRTD commonly used for which a discrimination decision is made, and an MDTD commonly used for which an acquisition decision is made.

FLIR92 calculates the system's overall MTF by using linear filter theory. The MTFs for the components are multiplied together. Instead of including an MTF for each component, MTFs of common system components are gathered in

three main groups: a) Prefilter MTFs, b) Temporal Postfilter MTFs, and c) Spatial Postfilter MTFs. The components may vary according to the design and the users can add new MTFs into these groups.

FLIR92 ignores signal and noise aliasing in the MRTD and MDTD predictions, for thermal imaging systems are assumed to be well designed, so that image artifacts due to under-sampling do not significantly degrade the system. Thus, the model is implemented with enough flexibility to accommodate most system designs through user determined pre- and post-sampling MTFs. Also, MRTD is not predicted at spatial frequencies exceeding the Nyquist frequency [Ref. 11].

As opposed to the first generation thermal imaging systems where NETD was used to predict the system performance, in second generation systems noise was defined in a three dimensional coordinate system (temporal, horizontal spatial, and vertical spatial) by the FLIR92 model. The model calculates the full temporal noise, and the spatial noise is incorporated into the MRTD prediction via the three dimensional noise model and summary noise factors. "Noise calculations are made relative to a



measuring port that is assumed to be located at a video port prior to the system display." [Ref. 11].

FLIR92 calculates the horizontal and vertical MRTDs depending on the direction of the standard four bar pattern. As mentioned in Chapter I the MRTD depends directly on the system transfer function, which is represented by the system overall MTF, and the system sensitivity that is described by NETD. To predict MRTD and MDTD, the spatial integration of the eye/brain system must be modeled. FLIR92 uses a synchronous integrator model for MRTD predictions as opposed to a matched filter model. "With this method, the eye/brain system is assumed to spatially integrate over the image of a bar, ignoring blurring of the target caused by finite apertures in the system." [Ref. 11]. In the case of periodic targets, synchronous integrator and matched filter methods give the same results. However, since the algorithms required to implement are simpler than matched filter algorithms, FLIR92 uses the synchronous integrator method. On the other hand, MDTD prediction is based on the matched filter concept, in which the eye/brain filter is matched to the signal in order to maximize the signal to noise ratio.



### C. SEARAD RADIANCE MODEL

SeaRad is a FORTRAN computer code used in predicting the radiance of the ocean surface. It includes a more accurate description of the sea surface including effects of solar heating and reflection and wind modification of the sea surface. For transmission it uses a modified version of the U.S. Air Force program MODTRAN2, which uses a card input system to compute atmospheric transmittance and path radiance. SeaRad is DOS-compatible and runs on a personal computer. In this thesis a Matlab shell for input and output of this code [Ref. 4] was used to compute the atmospheric transmittance values required by the ACQUIRE model.

The SeaRad surface state model is based on the Cox-Munk statistical model for wind-driven capillary wave facets. It operates exactly like the original MODTRAN2 code with an additional new logical parameter that is required in the input file. "Sun glint is included in the sea radiance prediction provided that the user has chosen to execute SeaRad in radiance mode with solar scattered radiance included." [Ref. 7]. The program is valid for the spectral range from the visible to far infrared regions.

#### D. WINEOTDA MODEL

Windows Electro-Optical Tactical Decision Aid (WinEOTDA) is a computer model developed by the Naval Research Laboratory (NRL), in Monterey, CA [Ref. 22]. It was derived from the Electro-Optical Tactical Decision Aid Mark III (EOTDA III), which was originally an EOTDA model running in DOS. The USAF Philips Laboratory first created Mark III, and then NRL incorporated Navy sensors into this model. NRL developed the Windows version of this program to make it user friendly and simplify the prediction process.

WinEOTDA predicts the performance of electro-optical weapon systems and night vision goggles (NVG), working in the infrared (8-12 micrometer), visible (0.4-0.9 micrometer), and laser (1.06 micrometer) wavelengths region of the optical spectrum. The prediction is based on environmental and tactical information, which includes meteorological data, time over target, target location and characteristics, sensor specifications and height, and background characteristics.

WinEOTDA uses a Graphical User Interface (GUI) design to display the maximum information on the screen and present the inputs and outputs in a single window. This

allows the user to reach the details just by clicking on the links on the main screen. Using the main menu and toolbar on the same screen can also make the selection. All meteorological and operational data can be input via the drop down menus and links.

WinEOTDA consists of three basic components: target model, atmospheric transmittance model, and sensor performance model. In the following three sections each of these components will be explained and a summary description of output files will be given.

### **1. Target Model**

Target model calculates the strength of the electro-optical signal at zero range using target and background characteristics entered by the user. The radiance difference between the target and background is converted to an equivalent blackbody temperature difference via the thermal model Target Contrast Model #2 (TCM2). TCM2 is a very powerful and accurate target signature model developed by Georgia Tech Research Institute. It is based on heat transfer and treats the target as a distinctive three-dimensional network of nodes that exchange heat with one another as well as with their environment [Ref. 12]. The model provides a very detailed target signature.

The TCM2 model continuously calculates a new temperature for all nodes during the period between the beginning and the end of the operation at various time intervals determined by the user. For each interval TCM2 computes a mean temperature and identifies the hottest and coldest of the visible nodes [Ref. 12]. Then the one with the greater contrast to the background is identified and the sensor model uses the temperature and projected area of this facet in MDTD based range detection. The target mean temperature and total projected area are used to compute MRTD based detection range.

The WinEOTDA version 1.3.3 dated 1998, the version used in this thesis, includes 20 different targets in its target menu, containing land vehicles and buildings, aircraft, and naval ships. Target heading, operating state, and speed of these targets provide the necessary input for the TCM2 model to calculate internal heat sources as well as surface heating and cooling. Target heading affects the perceptible solar heating on target, as the target operating state gives information about the heat interaction with the environment, and the surface heating of the target. The movement of the target, represented by

its speed and the wind speed, provides a cooling effect on the target.

The backgrounds in the model are grouped under two different categories, as general backgrounds and specific backgrounds. The general background offers five subcategories: continental, urban, desert, ocean, and snow. It describes the dominant terrain feature of the target area, which gives the information used to calculate the solar reflection by the model. The background, which is the immediate area surrounding the target, consists of eight different structures: vegetation, soil, snow, water, concrete, asphalt, swamp and rocky field, which are further described by the composition, coverage or depth of the surface type. Three different backgrounds used in this thesis are water, soil, and vegetation, so as to represent a beach scenario for joint operations. Despite the use of multiple backgrounds in the model, the program uses the one entered first as the primary background to calculate the solar heating and reflection of the ground. However these backgrounds are not considered to be independent and the program directs the user to enter the most representative one first. In the case of water background the depth affects the heat capacity of the water body and clarity



affects the heat flow from the surface [Ref. 12]. Soil types also define the heat capacity and reflectivity, as the moisture affects cooling rate, which is also an issue for the vegetation model.

## **2. Atmospheric Model**

The atmospheric model calculates the degradation of the signal in transit from target to sensor. A limited version of the LOWTRAN atmospheric propagation model is used in calculations to predict the transmittance through the atmosphere. The path radiance is not included in this modeling. The model for a range of four kilometers is used to evaluate the transmittance and thus the band averaged extinction coefficient. Then the Beer's Law approximation is used to calculate the other transmittance values for different ranges.

WinEOTDA uses the two-layer model, which calculates two extinction coefficients for below and above the boundary layer height. A weighted average of transmission is used for sensors above the boundary layer.

The aerosol modeling consists of 19 aerosols from LOWTRAN 5,6,7 [Ref. 17], and the Navy Aerosol Size Distribution Model (NAM). WinEOTDA aerosol models include: rural, urban, maritime, tropospheric, desert, navy



maritime, advective fog, radiative fog, and camouflage smokes. The navy maritime model, which is used in this thesis, describes aerosols found in the boundary layer of oceanic environments. WinEOTDA includes nine different aerosols in the Navy maritime model, defined by air mass history, and the 24 hour average and local wind speeds, a distinguishing factor from the standard maritime model in LOWTRAN.

Meteorological data are input by using the Met input screen for the transmission calculations in WinEOTDA. The following parameters of the target scene are required by the model on an hourly basis: surface temperature, surface dew point temperature, aerosol, battlefield induced contaminants (BICs), visibility, precipitation index, rain rate, wind speed and direction, boundary layer height, low, middle and high cloud data.

The surface temperature and dew point are used to compute the relative humidity. Then relative humidity, aerosol and visibility parameters are used to calculate an extinction coefficient. In Navy Maritime, the model calculates visibility.

### 3. Sensor Model

The sensor performance model evaluates the range at which the signal received by the sensor equals the threshold value for detection. The target apparent size (angular subtense) as viewed from the sensor determines this threshold value as where the angular subtense is equal to the critical dimension of the target divided by the range to sensor.

WinEOTDA supplies the user with a number of sensor data files identified by a unique three-digit index. The operator selects the sensor according to this number from the sensor list. The program offers two kinds of sensor IDs: standard IDs reserved for sensors supplied with the program and additional IDs for user-defined sensors. The physical and performance parameters of the supplied sensors are encrypted into separate data files and kept in the program in pure ASCII code. The identifications of these sensors are not available to the user. In this thesis a user-defined model using the standard SADA II scanning focal plane array was designed as a second generation FLIR sensor by the FLIR92 model using the basic sensor parameters found in the literature.

#### **4. Output Files**

WinEOTDA outputs are displayed in three different formats that can be selected via the main menu or toolbar. Alphanumeric, graphic, and tabular outputs are created automatically after each run. An alphanumeric output is designed with the following parameters: MRT Range, MDT Range, Lock-on Range, MRT Delta T, MDT Delta T, Lock-on Delta T, Background Temperature, MRT Target Temperature, MDT Target Temperature and Lock-on Target Temperature. Graphic output includes the output range, target temperatures, and delta T values while the tabular output displays only the output ranges according to different viewing directions. In addition to these outputs the model displays the maximum ranges for each target on the main screen. The units of the ranges can be changed via the main screen, which has the options of kilo-feet (kft), kilometers (km), and nautical miles (nm). WinEOTDA gives maximum range predictions for detection only, for both Narrow and Wide FOVs.

#### **E. ACQUIRE MODEL**

ACQUIRE is a range performance program that was developed by the US Army CECOM, Night Vision and Electronic

Sensors Directorate (NVESD). The version used in this thesis is dated May 1995. It runs on IBM compatible personal computers in a DOS environment and on Unix workstations.

ACQUIRE predicts target detection and discrimination range performance for systems working in the visible, near infrared, and infrared spectral bands. There are two different range prediction tasks in ACQUIRE: target discrimination and target spot detection. Two-dimensional Johnson cycle criteria along with MRTD predict the target discrimination ranges, while target spot detection (star detection) ranges are predicted by utilizing SNR theory and using MDTD.

As explained in ACQUIRE's User's Guide "ACQUIRE is intended for experienced systems analysts who are knowledgeable of 1) the principles of imaging electro-optical systems and their application to target acquisition tasks, 2) the parameterization of target acquisition scenarios for the purpose of evaluating targeting systems, and 3) the basic methodologies applied in the model." [Ref. 13].

## 1. Target Model

ACQUIRE uses the target information given by target signature and dimensions to calculate the probability of target discrimination. The target signature is represented by target contrast in the visible or near infrared regions while it is defined to be the temperature difference between target and background at zero range in the infrared spectral bands. The probability of target discrimination is a function of the number of equivalent cycles resolved on the target by the sensor. The number of cycles resolved is determined by minimum resolvable temperature difference (MRTD) for a target at a given range and apparent signature [Ref. 13] and is given by:

$$n = \frac{c_d}{r} f_f \quad (3.1)$$

where

$c_d$  is the characteristic size of the target (m),

$r$  is the range to the target (km), and

$f_f$  is the frequency (cycles/mRad) resolved by the sensor for the target at range  $r$ .

Then the probability of discrimination is calculated by utilizing the following target transfer probability function (TTPF) used by ACQUIRE as a curve fit:

$$P = \frac{(n/n_{50})^E}{1 + (n/n_{50})^E} \quad (3.2)$$

where

$E$  is equal to  $2.7 + 0.7(n/n_{50})$ ,

$n_{50}$  is the number of cycles required to be resolved in order to achieve a 50% probability of discrimination.

ACQUIRE offers 23 land targets in its target look-up table file. For targets that are not represented in the internal lookup table, a data file is built with the target dimensions and signature. When the target signature is not entered in the model, a thermal default of 1.25 degrees C is used for it.

## **2. Atmospheric Model**

ACQUIRE offers two different methods of modeling atmospheric transmittance. The first uses the Beer's Law approximation calculated from the atmospheric transmittance over a one-kilometer path; the second method (recommended by the ACQUIRE's User's Guide) is to specify broadband atmospheric transmittance as a function of range. In the latter method the data may be obtained from measurements or predicted by using an atmospheric propagation model (e.g., LOWTRAN). In this thesis the SeaRad radiance model will be



used for predicting atmospheric transmittance. Then outputs of this model will be included in the ACQUIRE data file.

### **3. Sensor Model**

The ACQUIRE model permits sensor definition in two formats: either the sensor parameters are written in the ACQUIRE data file, or a separate sensor data file is included in the sensor look-up table. In both methods, required performance parameters (i.e., MRTD and MDTD), horizontal field-of-view (HFOV), and wide field-of-view - narrow field-of-view (WFOV-NFOV) ratio are included in the format. A data file name is required when using a look-up table in the main ACQUIRE file. This allows the user to define their own sensors and attach these user-defined sensors to the look-up table.

### **4. Output Files**

ACQUIRE outputs are displayed in two formats. The first output file with the extension r1 is automatically written for target discrimination performance after each run. It lists the target discrimination ranges for different probability levels in a tabular form. The second one with the extension r2 is written when the user enters the appropriate command as explained in the User's Guide. The format resembles the first one except that it lists the

target discrimination probabilities according to different detection ranges. The r1 file is used to verify performance with respect to a specific probability requirement and "obtained by linearly interpolating the results listed in the r2 file, and, therefore subject to interpolation errors if the probabilities are changing rapidly with respect to the range increment." [Ref. 13]

The program can also write the r2 output file with all headers and labels removed. Thus these files can be imported by plotting software and the outputs can be displayed in graphic form.

THIS PAGE INTENTIONALLY LEFT BLANK

#### IV. COMPUTATIONS AND RESULTS

##### A. SCENARIO INPUT PARAMETERS

The scenario parameters were chosen to represent a beach environment for a joint operation. The parameters are related to air-to-ground weapon systems, which is the case that the TDAs under study deal with. These parameters were utilized to reach the ultimate goal of this thesis; that is, to give ideas or make recommendations for a common TDA code that can be used in all services (Army, Navy and Air Force).

The target was chosen to be "Gunboat", which is one of the targets in the WinEOTDA target look-up table. After studying its physical dimensions, it was noted that Gunboat has the same dimensions as R/V POINT SUR, which was used in the PREOS 92 Experiment in Monterey Bay in 1992.

The atmospheric data were chosen to fit the properties of a typical operational environment of a naval target. An atmospheric data set collected from the Gulf of Oman, which was extracted from the EOTDA III model test data [Ref. 14], was used in this work.

The published parameters of the SADA II Focal Plane Array (FPA) system were used to build a second-generation

FLIR sensor using the FLIR92 model. The data relating to the physical parameters of the FPA were given by Ludwiszewski [Ref. 15]. The remaining input data required by the FLIR92 model were gathered from Ludwiszewski [Ref. 15], on second-generation sensor structure, and the textbook by Driggers et al [Ref. 1]. The data set was used along with NETD and IFOV parameters as input to the FLIR92 model to obtain MRT and MDT outputs.

The following table summarizes the input data used in the WinEOTDA and ACQUIRE models.

Target Target Dimensions (m) Sensor		Gunboat H:8.8 L:41.5 W:9.75 User-defined SADAI
Date/time (GMT) Latitude Longitude		07 Jan 1993, 1055 24deg 15min N 59deg 45min W
Temperature (min) Temperature (max) Temperature (F) Dew Point Temperature (F) Sea Surface Temperature (F)		71 78 76 50 69
Aerosol Model Index Visibility (mi) Wind Direction (deg) Wind Speed (kts)		6 (Navy Maritime) 15 (24.14 km) 120 5
Low Cloud	Type Height Amount	Sc 2000 1
Inversion Height (ft)		2000

Table 4.1 - Scenario Input Parameters [Ref. 14].

## **B. FLIR92 MODEL OUTPUTS**

The sensor model was formed using the input parameters included in a data file that was later saved in pure ASCII text mode. The model was run in the DOS environment for prediction of both MRTD and MDTD performance parameters, which would later form the input for ACQUIRE and WinEOTDA. The output of this model containing the MRTD and MDTD predictions along with NETD and IFOV data is included in Appendix A.

### **1. Comparison of FLIR92 Model Sensor Outputs With The Other Sensors in WinEOTDA Model**

The WinEOTDA sensors and the sensor built by the FLIR92 model were tabulated according to their physical and performance parameters. Later a comparison analysis between these sensors was performed to verify that the sensor built by FLIR92 had reasonable input and output data. The comparison charts are given in Appendix B, which includes NETD, horizontal and vertical IFOVs and MRTD at min and max spatial frequency comparisons. The sensor #127 represents the user-defined sensor, while the WinEOTDA standard sensor numbers range from 100 to 126.

In the case of NETD it can be observed that the NETD parameter of the user-defined sensor is within the



theoretical limit, which is stated as 0.02 to 0.2 degree C by Driggers [Ref. 1], and in agreement with the other sensor NETDs.

Horizontal and vertical IFOVs, which are equal due to the square detector usage in the design process, are also reasonable when compared to the other sensor IFOVs. Since the user-defined sensor had a Narrow Field of View (NFOV), the comparison was made between the sensors of the WinEOTDA model.

The maximum and minimum MRTD values showed an agreement between the sensors. However although the minimum spatial frequency of the user defined sensor's MRTD matched to the other sensor MRTDs, the maximum value was noticeably greater than those in the WinEOTDA model. This is because the sensor built by FLIR92 used the second-generation sensor (SADAI) parameters. Sensors of this generation offer increased resolution limits with a smaller detector size. Thus the MRTD values show an asymptotic behavior at higher spatial frequencies.

The above comparisons allowed the conclusion that both physical and performance parameters of the sensor built by the FLIR92 model were reasonable and within theoretical limits.

### **C. SEARAD RADIANCE MODEL OUTPUTS**

The SeaRad Radiance model was used to calculate the atmospheric transmittance values required by ACQUIRE. The atmospheric data given in scenario input parameters were used as input to this model. The template and input data given in Appendix C were used in the model, and transmissivities for 0.5, 0.75, 1...28 km ranges were obtained. An example output file along with a tabular and graphical form of all transmissivities is shown in Appendix D.

The maritime scenario used in this work represents the atmospheric conditions during winter in the Gulf of Oman, located in the sub-tropical region. Due to the location of the Gulf, even though the conditions were described for winter the mid-latitude summer model was chosen in SeaRad. The winter in the sub-tropics has almost the same atmospheric parameters as summertime in mid-latitude regions.

### **D. WINEOTDA MODEL INPUTS**

The WinEOTDA model requires meteorological and tactical inputs before the model can be run. The meteorological data can be entered by selecting the MET

data summary from the main menu or by clicking on the descriptor picture on the main screen. It includes the target location, surface weather characteristics at a specified time, and information about the boundary layer along with cloud data.

The tactical information or Operations and Intelligence (Ops) data include the inputs for sensor, target and backgrounds. The main menu or main screen can be used to enter the input data by selecting sensor, target, time over target or background.

The detailed descriptions of the input parameters used in WinEOTDA can be found in Ref.12 and the WinEOTDA (Version 1.3.3) model's help menu.

### **1. Target Model**

Target and background information form this model. The target defines the size and physical characteristics used in WinEOTDA. Background data give information about general background, which is the dominant terrain feature of the target area, and the immediate area of the target.

The target selected from the target menu was 'Gunboat'. For discriminating the output ranges for different viewing directions the heading, which refers to the direction of the target front aspect with respect to

north was entered as zero degrees. The operating state that gives the condition of the target at time over target (TOT) was selected 'Off', which meant that the target was heated by the environment alone. The entry form in Appendix E (Figure E.1) was used to enter the target data.

The scenario conditions were described as a beach environment in the sub-tropical region. The background for this environment was selected as water, soil and vegetation respectively along with an ocean general background. Since the composition of the background has an effect on its heating and reflective properties, detailed information was entered for each background type by using the entry form in Appendix E (Figure E.2).

The target location and time data are also used in the target model. They were entered according to the scenario input parameters. For time over target WinEOTDA offers two different options for decision makers and operators. The model can calculate the output ranges for either the execution phase or the planning phase of the scenario. While the execution phase needs the exact operation time and computes the output ranges according to varying viewing directions, the planning phase uses time intervals to calculate the detection ranges. Both parameters can be

entered by using the TOT entry form in Appendix E (Figure E.3). The execution phase was chosen in this thesis for comparison purposes of WinEOTDA to ACQUIRE.

## **2. Atmospheric Model**

The atmospheric model uses the input Meteorological and Site (Met) data to calculate the atmospheric transmittance. The Met information is entered using the input form in Appendix E (Figure E.5) via the main menu or the main screen. The entry form offers more options that can be seen after clicking on the individual parameter labels. Furthermore, the graphical view of each entry can be displayed by right clicking on the individual parameters. The weather forecast data can be entered as a spot entry, which is the case in this thesis, or as 24-hour cycle data.

The following set of meteorological data from the scenario parameters was used in WinEOTDA model.



Date/time (GMT)		07 Jan 1993, 1055
Latitude		24deg 15min N
Longitude		59deg 45min W
Temperature (min)		71
Temperature (max)		78
Temperature (F)		76
Dew Point Temperature (F)		50
Sea Surface Temperature (F)		69
Aerosol Model Index		6 (Navy Maritime)
Visibility (mi)		15 (24.14 km)
Weather		
Wind Direction (deg)		120
Wind Speed (kts)		5
Low Cloud	Type	Sc
	Height	2000
	Amount	1
Inversion Height (ft)		2000
Upper Level (UL)		Yes
UL Temperature (F)		10
UL Dew Point Temperature (F)		-1
UL Aerosol		4
UL Visibility		20

Table 4.2 - Meteorological Input Parameters [Ref. 14].

### 3. Sensor Model

The sensor entry form that can be reached via the main screen or the main menu, included in Appendix E (Figure E.4), offers a numbered sensor list to the operator. The user-defined SADAI second generation FLIR sensor was attached to this list as sensor #127. The NETD, XIFOV and YIFOV, MRTD and MDTD outputs of the FLIR92 model formed the sensor data file.

The remaining parameters for the entry form include the sensor height, viewing direction and scene complexity.



The sensor height was entered as 500, 2000, and 4000 ft respectively, along with a zero degree viewing direction. The scene complexity input describing the number of objects in the immediate vicinity that can be mistaken for the targets was chosen to be 'None'.

#### **E. WINEOTDA MODEL OUTPUTS**

The scenarios as previously defined were run for each of three different sensor altitudes: 500, 2000, and 4000 ft. After each successful run an indication of a 'successful run' was presented at the bottom of the screen and the maximum detection ranges for different targets with different backgrounds were displayed in tabular form on the main screen. The other output files mentioned in Chapter III were also automatically generated. The examples of these output files along with a main screen output table are given in Appendix F. The alphanumeric output summarizes some of the input parameters and displays the calculated Detection Ranges, Thermal Contrast, and Target Temperature for the permutation of targets #1 and #2 and three input backgrounds, where target#1 and target#2 are the same. The same results are also displayed in graphical (Figure F.1) and tabular (Figure F.2) formats along with a main screen

output (Figure F.3). These outputs were obtained with the original scenario input parameters for the sensor at 2000 ft altitude.

In these scenarios the heading of the target and the viewing direction of the sensor were chosen to be zero degrees. This information was utilized to determine the front and side aspect angles in the output files as: 000 for Front and 090 for Side views. Although the model gives outputs for 45 degree intervals in viewing direction, only the 000 and 090 degree directions were used to compare the results with the ACQUIRE outputs.

## **F. ACQUIRE MODEL INPUTS**

The ACQUIRE model uses a data file which includes target, sensor, and atmospheric information to predict the discrimination ranges. This file must be in pure ASCII code and written before the model is run. The data file format can be seen in Appendix G, where the section between the header line and 'end' of the file forms the input data file format.

### **1. Target Model**

The ACQUIRE has two different ways of defining a target in the model: The target look-up table, which

consists of a number of land targets, can be used, or user-defined data can be entered. The latter was used to specify the size of the naval target, Gunboat, which was not represented in the internal look-up table of the model, and the following format was used to enter target data:

```
>target  
  
    characteristic_dimension      0.0  meters  
  
    signature                      0.0  degrees_C
```

The signature parameter, which is the temperature difference between the target and its surrounding background, was taken from Shumaker et al [Ref. 10] where the representative values of ship differential temperatures were readily available for summer conditions at the specified operation time (10.55 AM). The selection procedure from the same reference was followed and the signature was determined to be 7.71 degrees C.

The selection of a proper target size, represented by 'characteristic\_dimension', is critical. For discrimination the target size directly affects the number of spatial cycles that can be resolved across the target. In the ACQUIRE User Guide a characteristic dimension that is equal to the square root of the projected area of the target in meters is recommended for calculations. This necessitates

the proper calculation of the projected area of the target. The program allows alternative definitions for target-projected area to be applied for off-menu targets. For this thesis the following equations given by Shumaker [Ref. 10] were used in projected area ( $A_T$ ) and critical dimension ( $D_c$ ) calculations with the following target orientation model:

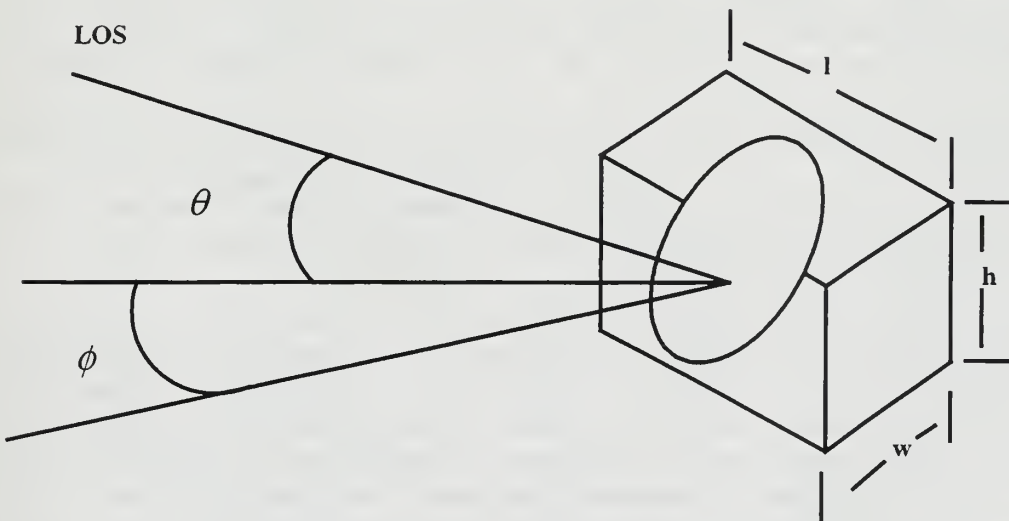


Figure 4.1 - Orientation of Targets "After [Ref. 10]".

$$A_T = lh \cos \theta \cos \phi + wh \cos \theta \sin \phi + lw \sin \theta \quad (4.1)$$

where

$l$  is the actual target length (m)

$w$  is the actual target width (m)

$h$  is the actual target height (m)

$\theta$  is the elevation angle (deg)

$\phi$  is the azimuth angle (deg)

$$D_c = \sqrt{A_r} \quad (4.2)$$

Due to the importance of the subject the following section will cover an analysis of critical dimension calculation.

#### ***a) Critical Dimension Analysis***

The ACQUIRE code uses a critical dimension parameter calculated off-line for user-defined targets. This value is entered as a constant in the model and is not calculated continuously within different time intervals for varying ranges and altitudes.

The orientation model in Figure 4.1 and the Equations 4.1 and 4.2 were used to calculate critical dimension values for different ranges (between one and 30 km) and altitudes (500, 2000, and 4000 ft). The altitudes were chosen to represent a descending aircraft carrying the sensor.

The calculations in Appendix H showed that the critical dimension is very similar for longer ranges at different altitudes, but at short ranges the results for different altitudes are dramatically different. Varying

ranges and altitudes definitely affects the aspect angle, which causes a change in apparent target size. The critical dimensions were calculated for front (F) and side (S) views of the targets, which are represented by the azimuth aspect angle '90' and '0' degrees.

To evaluate the impact of the changes in aspect ratio due to altitude changes, critical dimension values for 500, 2000, and 4000 ft sensor heights and 25 km range were calculated. These were used as input parameters for the target model.

## **2. Atmospheric Model**

The SeaRad Radiance model outputs in Appendix D were used in building the ACQUIRE data file. This is the recommended method in the ACQUIRE User's Guide for calculating atmospheric transmittance and the following format is the only way of entering these data:

```
>band_averaged_atmosphere
#_points: 0          km____transmittance
                0.0      0.0
```

The km array holds the range in kilometers and requires at least three and not more than fifty points with the data ordered by increasing range. The transmissivity



array holds atmospheric transmittance with the same number of points as the km array.

### 3. Sensor Model

ACQUIRE models the sensor in two ways as mentioned earlier in Chapter III. In this work the second method was adopted in which a separate sensor data file that is later included in a sensor look-up table was used. The outputs of the FLIR92 model, which include horizontal, vertical, and 2D MRTD values, were utilized to build the sensor data file with the following format:

```
Header line
>systemA
    hfov: 0.0 vfov: 0.0 w/nfov_ratio: 0.0
    @MRTD_2d
    #_points: 0    cy/mr..... MRTD
                0.0          0.0
```

The first line of the file is a 'Header line' that is always required. The second line is the name of the sensor system and remaining lines contain sensor physical and performance parameters. For discrimination purposes 2D MRTD outputs of the FLIR92 model were used in this thesis. This externally built sensor data file was included in the

ACQUIRE data file to determine the sensor system with the following format:

```
>sensor_lookup
```

```
data_file_name : is the name of the file in  
which sensor performance curve data is stored in  
lookup tables.
```

```
sensor_id      : identifies which sensor to  
select from the lookup table.
```

```
performance_mode: selects the performance data  
to read from the lookup table.
```

The target discrimination criteria listed in Table 2.2 in Chapter II were entered using the following format for the MRT 'performance\_mode' of the sensor model:

```
>cycle_criteria
```

```
detection_n50      0.0 :for WFOV
```

```
detection_n50      0.0 :for NFOV
```

```
classification_n50 0.0 :for NFOV
```

```
recognition_n50    0.0 :for NFOV
```

```
identification_n50 0.0 :for NFOV
```

WFOV is only used for detection purposes. After detection of the target NFOV is used to resolve the details for discrimination purposes.

## G. ACQUIRE MODEL OUTPUTS

The input parameters including target, atmosphere and sensor data along with the varying characteristic size of the target according to different altitudes were entered into the following ACQUIRE data files:

- SadaIIfa: is the ACQUIRE data file for front view of Gunboat seen from the sensor at 500 ft altitude and 25 km range,
- SadaIIfb: is the ACQUIRE data file for front view of Gunboat seen from the sensor at 2000 ft altitude and 25 km range,
- SadaIIfc: is the ACQUIRE data file for front view of Gunboat seen from the sensor at 4000 ft altitude and 25 km range,
- SadaIIsa: is the ACQUIRE data file for side view of Gunboat seen from the sensor at 500 ft altitude and 25 km range,
- SadaIIsb: is the ACQUIRE data file for side view of Gunboat seen from the sensor at 2000 ft altitude and 25 km range,

- SadaIIsc: is the ACQUIRE data file for side view of Gunboat seen from the sensor at 4000 ft altitude and 25 km range.

The output files generated after each run of the above files with the extension of r1 and r2 are included in Appendix I. Since the model uses the same file name for the output as the input, all output files have the same names as given above. The r2 extension files provided input for Windows Excel to produce the plots of the probability of discrimination given range parameters. These plots were also included in Appendix I along with the alphanumeric results.

As can be seen from the output file formats, they basically use three different summary sections to display the results. The first is the one containing information about the input ACQUIRE data file used, the second is the messages containing information about the sensor structure and a detailed examination of intermediate results. And the last section gives the discrimination ranges versus the given probabilities.

## H. COMPARISON OF WinEOTDA AND ACQUIRE MODEL OUTPUTS

The TDAs under study were compared under three different conditions. First, the original scenario parameters previously listed were used for range prediction in both codes. Second, WinEOTDA Met data were modified to get the same 4km transmissivity value as in ACQUIRE. Last, the two codes were compared for the same 4km transmissivities obtained by using the Beer's law approximation in the ACQUIRE model. This section will cover the procedure and the results related to the first condition.

The models were run for different sensor altitudes (500, 2000, and 4000ft) with the original scenario input parameters. The following results (Table 4.3) were obtained.

SENSOR HEIGHT (Ft)	WinEOTDA DETECTION RANGES (4 KM TRANSMISSIVITY = 0.60)				ACQUIRE DETECTION RANGES (4 KM TRANSMISSIVITY = 0.407)			
	SIDE VIEW (90 deg)		FRONT VIEW (0 deg)		SIDE VIEW (90 deg)		FRONT VIEW (0 deg)	
	NFOV	WFOV	NFOV	WFOV	NFOV	WFOV	NFOV	WFOV
500	44.1	18.4	44.1	18.4	26.26	19.65	22.27	14.18
2000	51.5	18.5	48.1	18.5	26.31	19.72	22.52	14.49
4000	55.5	18.6	55.5	18.6	26.38	19.81	22.80	14.87

Table 4.3 - WinEOTDA and ACQUIRE Detection Range Comparison Table With The Original Scenario Parameters for Different Sensor Altitudes

The obvious difference in Table 4.3 was found to be in 4km transmissivities calculated by two programs. This difference is due to the detailed input data structure of WinEOTDA model as opposed to ACQUIRE. Two crucial parameters, temperature and dew point temperature, for calculating relative humidity, which is an input for atmospheric extinction coefficient calculations, are not entered by the users in ACQUIRE atmospheric model (i.e. SeaRad in this study). Instead the atmospheric transmittance model uses the default values for the specified region. Additionally, the low cloud cover, which was not used in ACQUIRE, caused a difference in predictions.

The results in Table 4.3 showed that the two programs give different detection ranges with the same scenario input parameters. WinEOTDA predicted a longer-range performance especially for NFOV for both aspects. It output almost twice as long detection range as ACQUIRE at 500ft sensor altitude in NFOV detection. This was not observed for WFOV detection.

As seen in Table 4.3 WinEOTDA detection ranges vary with the changing sensor altitudes, but this is not observed for the ACQUIRE model, or at most the observed



change is very small. This is because of the difference in target modeling in the two programs. While WinEOTDA uses a powerful target signature model, TCM2, which calculates the mean temperature and projected areas within specified time intervals for a user defined period, ACQUIRE requires only a measured target signature and critical dimension value for off-menu targets, ignoring the changing sensor altitude effects. However, as analyzed before, the varying sensor height affects the projected area of the target and consequently critical dimension. In WinEOTDA, calculated total projected area is used in determining the sensor performance model detection ranges as a function of target spatial frequency.

On the other hand, background information which is useful for target signature calculation is ignored for user defined targets in ACQUIRE. Despite the convenience of describing off-menu targets in ACQUIRE by their measured parameters, this method depends heavily on the accountability of the reference used. However WinEOTDA lets the users enter a detailed background input data set that is used by the TCM2 model for target signature calculation. Thus the model can generate a more accurate target signature.

**I. COMPARISON OF WinEOTDA AND ACQUIRE OUTPUTS WITH THE MODIFIED WinEOTDA METEOROLOGICAL DATA**

The previous section showed that the models calculated different 4km transmissivity values for the same original scenario input parameters. In order to see whether the same transmissivity values will give the same results, some modifications were made in the WinEOTDA meteorological input data. Temperature and dew point temperature parameters were changed until the same 4km transmissivity as in ACQUIRE was found. After achieving the same value, the program was run for 500, 2000, and 4000 ft sensor altitudes and the results in the following table were obtained.

SENSOR HEIGHT (Ft)	WinEOTDA DETECTION RANGES (4 KM TRANSMISSIVITY = 0.41)				ACQUIRE DETECTION RANGES (4 KM TRANSMISSIVITY = 0.407)			
	SIDE VIEW (90 deg)		FRONT VIEW (0 deg)		SIDE VIEW (90 deg)		FRONT VIEW (0 deg)	
	NFOV	WFOV	NFOV	WFOV	NFOV	WFOV	NFOV	WFOV
500	31.9	18.4	29.9	18.4	26.26	19.65	22.27	14.18
2000	31.6	18.5	29.6	18.5	26.31	19.72	22.52	14.49
4000	28.9	18.6	27.6	18.6	26.38	19.81	22.80	14.87

Table 4.4 - WinEOTDA and ACQUIRE Detection Range Comparison With The Modified WinEOTDA Meteorological Parameters To Get The Same 4km Transmissivity Value As In the ACQUIRE for Different Sensor Altitudes

Table 4.4 shows that even if the same 4km transmissivities are used in both models, the predicted

detection ranges are still different from each other and WinEOTDA predicts longer-range performance for NFOV detection for both aspects. Since WinEOTDA still uses the Beer's law approximation in calculating transmissivities for the other ranges, this 4km transmissivity will be the only common value for WinEOTDA and ACQUIRE. This approximation along with a better target signature and critical dimension calculation in WinEOTDA cause the difference in the output ranges.

As seen from Table 4.4, the WinEOTDA detection ranges are reduced, as expected, when compared to those in Table 4.3. This is because the atmospheric model uses a lower 4km transmissivity as a reference to calculate the transmissivities for different ranges. The smaller transmissivities cause a decrease in the predicted ranges.

#### **J. COMPARISON OF WinEOTDA AND ACQUIRE OUTPUTS WITH THE USE OF BEER'S LAW APPROXIMATION IN ACQUIRE MODEL**

The predicted detection ranges of the WinEOTDA and ACQUIRE models were compared for the same 4km transmissivities as in the previous section. But this time the Beer's Law approximation was also used in the ACQUIRE atmospheric model. First the following table was built

using the ACQUIRE detection ranges in Table 4.3 and the outputs obtained after running the ACQUIRE model for different sensor altitudes (500, 2000, and 4000ft) with the transmittivities calculated by the Beer's Law approximation.

SENSOR HEIGHT (ft)	ACQUIRE DETECTION RANGES in Km (4 KM TRANSMISSIVITY = 0.407)				ACQUIRE DETECTION RANGES in Km (BEER'S LAW APPROXIMATION FOR 4 KM TRANSMISSIVITY = 0.407)			
	SIDE VIEW (90 deg)		FRONT VIEW (0 deg)		SIDE VIEW (90 deg)		FRONT VIEW (0 deg)	
	NFOV	WFOV	NFOV	WFOV	NFOV	WFOV	NFOV	WFOV
500	26.26	19.65	22.27	14.18	21.17	16.92	18.74	12.98
2000	26.31	19.72	22.52	14.49	21.22	16.97	18.90	13.22
4000	26.38	19.81	22.80	14.87	21.26	17.04	19.08	13.52

Table 4.5 - ACQUIRE Detection Range Comparison With The SeaRad Atmospheric Transmittance Parameters and Modified ACQUIRE Atmospheric Transmittance Parameters by Beer's Law Approximation for Different Sensor Altitudes.

Then the predicted ranges in Table 4.5 obtained by using Beer's law were utilized to compare the results of the two models for the same atmospheric model inputs. Table 4.6 displays the results of this procedure.

SENSOR HEIGHT (Ft)	WineOTDA DETECTION RANGES (4 KM TRANSMISSIVITY = 0.41)				ACQUIRE DETECTION RANGES (BEER'S LAW APPROXIMATION FOR 4 KM TRANSMISSIVITY = 0.407)			
	SIDE VIEW (90 deg)		FRONT VIEW (0 deg)		SIDE VIEW (90 deg)		FRONT VIEW (0 deg)	
	NFOV	WFOV	NFOV	WFOV	NFOV	WFOV	NFOV	WFOV
500	31.9	18.4	29.9	18.4	21.17	16.92	18.74	12.98
2000	31.6	18.5	29.6	18.5	21.22	16.97	18.90	13.22
4000	28.9	18.6	27.6	18.6	21.26	17.04	19.08	13.52

Table 4.6 - WineOTDA And ACQUIRE Detection Range Comparison Table With The Modified ACQUIRE Atmospheric Transmittance Parameters To Get The same 4km Transmissivity Value As In WineOTDA (Beer's Law Approximation) For Different Sensor Altitudes

As seen from Table 4.5, the Beer's law approximation reduced the range performance of ACQUIRE. This is an expected result, since the exponential Beer's law gives smaller transmissivity values than the SeaRad model. A MathCAD file was included in Appendix J to show that the Beer's law approximation gives smaller transmissivities than SeaRad model where  $\tau_0$  represents the transmissivities calculated by using the Beer's law approximation and  $\tau_{SeaRad}$  displays the outputs of SeaRad Radiance model for different ranges.

Table 4.6 shows that WineOTDA predicts better performance for both aspects in NFOV and WFOV with the same atmospheric model inputs. The difference is due to the better structure of the WineOTDA target model to calculate

the target signature and better approximation for calculating critical dimension of the target. These two parameters were frequently mentioned in the last sections of this thesis as the main causes of differences in predictions. However WFOV detection ranges do not vary according to the changing transmissivity values.



THIS PAGE INTENTIONALLY LEFT BLANK

## V. CONCLUSIONS AND RECOMMENDATIONS

This thesis has presented an analytical comparison between the Army FLIR TDA, ACQUIRE Version 1 dated 1995, and the infrared module of the Navy/Air Force TDA, WinEOTDA Version 1.3.3 dated 1998. The programs were compared with respect to different means they used to model target, atmosphere and sensor. They were analyzed for the same scenario conditions, in which the scenario parameters were chosen to reflect a beach environment within the concept of 'joint operations'.

The research questions addressed were to find the differences in the modeling of underlying physical principles, input parameters, and predicted detection ranges; suggestions were sought for modification of the codes that would lead to equivalent output for the same inputs. The following sections will give responses to these questions that may finally determine the possibility of using one of the codes under study as a standard TDA for all services.

## A. COMMON SET OF INPUT PARAMETERS

The common set of input parameters that can be used to operate both WinEOTDA and ACQUIRE can be grouped as target, atmosphere and sensor data. As studied in Chapter III these data form the inputs for the models, which are known by the same names, constituting both TDA codes. Although both programs have the same model structure, the treatment of inputs shows some differences that will be made clearer in the following sections.

The target models in this work were built using a naval target and its related backgrounds. The R/V POINT SUR, which happened to have the same dimensions as the Gunboat entry in WinEOTDA target look-up table and backgrounds depicting a beach environment formed the inputs for both models. While no external calculations for target signature and critical dimension were needed in WinEOTDA, ACQUIRE required these computations for this off-menu target. ACQUIRE's internal look-up table is useful for land targets only, while WinEOTDA can be directed at maritime and overland scenarios.

The atmospheric data were entered according to the scenario parameters. WinEOTDA required specific parameters

for its internal transmittance calculations. On the other hand in ACQUIRE these computations were externally handled by the user and the results were incorporated into the program.

The sensor models in both codes utilized the FLIR92 model outputs.

#### **B. DIFFERENCES IN THE PREDICTIONS OF CODES WITH THE COMMON INPUT PARAMETERS**

Using equivalent data the two programs yielded different detection ranges for different sensor altitudes. Table 4.3 in the previous Chapter provided these detection ranges of both codes. While varying sensor altitudes caused only a slight change in ACQUIRE detection ranges, WinEOTDA displayed significant differences for the same sensor altitudes.

WinEOTDA predicted a longer detection range than ACQUIRE 100% of the time. In particular, NFOV detection ranges of WinEOTDA were twice as long as the ranges in ACQUIRE. However, although the WFOV detection ranges of WinEOTDA displayed better performance than ACQUIRE, they seemed to be insensitive to differing aspect angles and showed a very small change for different sensor altitudes.

For ACQUIRE, WFOV detection ranges did not change as much with changing sensor altitude as did the NFOV detection ranges.

### **C. DIFFERENCES IN THE TREATMENT OF CODE INPUTS**

WinEOTDA and ACQUIRE have the same input models. However, there are some differences in the treatment of inputs, and these differences in the interaction of sensor and target give rise to the differences in predictions.

The WinEOTDA target model uses TCM2 to calculate the target signature. This model treats the target as a mesh of different nodes and calculates the resultant signature by considering the transfer of heat between these nodes. It also takes into account the atmospheric effects on the body heat of the target surface and calculates the signature according to the input meteorological data. It is believed to be the most accurate model available to calculate the target signature, and the results are certainly better than the ACQUIRE target model. The calculated target-to-background temperature difference at zero range will have a great effect on the discrimination of the targets. On the other hand, the ACQUIRE target model allows the user to input the critical dimension of the target and the measured

target-to-background temperature difference as the 'target signature' for off-menu targets.

There are some deficiencies in this method. In the case of target signature, the difference between the target's average surface temperature and the average immediate background temperatures at zero range are used for calculations and it cannot be as accurate as the TCM2 Model used in WinEOTDA. Further, only one value of critical dimension is required. However after the analysis of the critical dimension calculation by using aspect angles, it was noted that even though the impact of the change in altitude for longer ranges has a negligible effect on the critical dimension, it has a considerable effect at shorter ranges and the critical dimension changes significantly for shorter ranges at different altitudes. Although the longer ranges were used for critical dimension calculation in this thesis, varying sensor altitudes lead to differences in range predictions. As can be seen in Appendix H the critical dimensions at 25 km for 500, 2000, and 4000 ft altitudes are very close but not identical. These small differences cause the changes in detection ranges for varying sensor altitudes.



Due to the unavailability for analysis of the original ACQUIRE source code, the treatment for the targets included in the look-up table could not be examined. Thus comparison of the treatment of target models in the two codes could only be made for external targets in ACQUIRE. The author's suggestions are based on these results.

The WinEOTDA atmospheric model evaluates atmospheric transmittance values using a limited version of the LOWTRAN model according to the meteorological data input by the user, which implies that more detailed and accurate data can give better outputs. The transmittance value at 4km is calculated by LOWTRAN and then the extinction coefficient obtained for this range is used to calculate the other transmittance values using the Beer's Law approximation. But the use of the broadband Beer's law approximation is known to give erroneous results as discussed in Chapter II. Thus, this must be considered as a weakness of this code.

The range predictions of the two programs were compared for the same 4km transmittances obtained by modifying the meteorological data of WinEOTDA. But the Beer's law approximation was still used in WinEOTDA as opposed to SeaRad transmittance used in ACQUIRE. It was observed that the WinEOTDA NFOV detection ranges decreased

and got closer to ACQUIRE predictions. This change was due to the modification in temperature and dew point temperature parameters of the WinEOTDA meteorological data. Temperature was reduced and dew point temperature was increased, which caused an increase in RH. But the WFOV detections were unchanged and were insensitive to changing altitudes and transmissivity. Another significant result was the diminishing detection range with increasing sensor altitude in WinEOTDA NFOV detection. Here the only meteorological parameter modified was dew point temperature to get the desired change in relative humidity to match transmissivity between the models. This is thought to be the only effect that caused the change.

The ACQUIRE atmospheric model allows two different methods for calculating the atmospheric transmittance values. In the first method, the transmittances are calculated by the broadband Beer's law approximation, which has the same deficiencies as mentioned for the WinEOTDA model. In the second method, recommended by the ACQUIRE User Manual, one of the atmospheric transmittance codes is used to get the transmissivities. Then the resultant transmittance values are directly input into the ACQUIRE data file. The author thinks that this treatment is better

than the first and the method used in WinEOTDA. The second method was used in this thesis to get the required atmospheric transmittance values. Furthermore, different effects of the first and second methods on the model outputs were analyzed as described in Chapter IV.

ACQUIRE model atmospheric transmittances were calculated by using the Beer's law approximation as in WinEOTDA. For the same 4km transmissivity values and method for calculating the transmissivities for the other ranges, the detection ranges of both programs were compared. The outputs are shown in Table 4.5 and Table 4.6 in Chapter IV. The Beer's law approximation used in ACQUIRE reduced the detection ranges as expected. This caused a greater difference between the two codes' NFOV detection ranges. In the case of WFOV detections the insensitivity of WinEOTDA to varying sensor altitudes and aspect angles was still observed.

WinEOTDA sensor model utilized the FLIR92 outputs to build a sensor data file. The same procedure was also followed by ACQUIRE. Although the input parameters and sensor data file structure are similar in both codes, ACQUIRE predicts classification, recognition and

identification detection ranges in addition to WinEOTDA's particular detection range predictions.

#### **D. SUGGESTIONS FOR THE MODIFICATION OF CODES**

Some suggestions can be made about the modification of the codes that would lead to equivalent output for the same inputs. Firstly, since the FLIR92 model was commonly used to create a sensor data file for both codes and the sensor models have the same structure except for their different ways of handling the sensor data, FLIR92 can be incorporated into both programs for modeling the new sensors. In fact ACQUIRE currently uses the outputs of the FLIR92 Model, but WinEOTDA can also be integrated with FLIR92 for building new sensors either externally or internally. However the cost and time must be taken into consideration before the integration.

The WinEOTDA target model uses TCM2, which is seen as the best and the most accurate model available for target signature calculations. Thus, the only suggestion for the modification of target model might be to include more targets in its look-up table. On the other hand, since the ACQUIRE program code was not available for examination, the treatment of its target model for look-up table targets is

unknown and the suggestion will be to include more targets in the model. However for off-menu targets, a target signature model such as TCM2 can be included to get better and more accurate predictions.

Atmospheric transmittance values required by the WinEOTDA atmospheric model can be calculated completely by LOWTRAN/MODTRAN and used to find the apparent temperature difference of the target-to-background. This is expected to give more accurate results in the prediction of the model. However a trade-off analysis must be performed before the integration of the whole model, as in the sensor modeling case previously mentioned. The cost and time needed to run the program will increase and this will cause some problems. Especially when the importance of minimizing the time required to reach a decision is considered, it will not be easy just to decide on the integration of the whole program before an exhaustive analysis.

In the ACQUIRE atmospheric model use of the second method is recommended to avoid the erroneous results of the broadband Beer's law approximation in the predictions.



## E. CODE SELECTION FOR INTER-SERVICE USE

The WinEOTDA code seems to have a deficiency in its atmospheric model, which is not easy to fix for the reasons given in the previous section. But the target and sensor models are powerful and give accurate results.

On the other hand, ACQUIRE has some shortcomings in modeling targets and backgrounds, and in the method for transmittance calculation. Furthermore it is not user friendly, and requires some codes to be written in specific formats to run. It also requires an operator trained in IR theory and the operation of the code, which is not generally available in the operational environment envisaged for naval TDA use (i.e. ordnance selection and pre-sortie mission planning.).

Although the range predictions of the two programs compared in this work have not been validated by real world measurements, the better performance of WinEOTDA, its easy to use structure and powerful target model display an advantage in choosing a standard TDA for inter-service use. However the author believes that at the unclassified level without using the real sensor data and predicted ranges, it is not easy to decide on a standard code.



## F. RECOMMENDATIONS FOR FURTHER RESEARCH

The differences in the predicted ranges as shown in Chapter IV point out the need for field testing of the two programs to determine the accuracy of detection ranges. If the same results occur in a field test, one of the programs may show as better than the other. This could result in an improvement to the other program, or choosing the better one as a standard TDA for inter-service use.

The comparisons on an unclassified level might not reflect the actual performance of the codes. The real sensor parameters and predicted detection ranges can be more useful to prove the reliability of performance. Thus a classified level research study with all the needed real world parameters will give better information to decide on or modify a specific TDA code. This would require a measurement campaign on the level of the MAPTIP [Ref. 20] or EOPACE [Ref. 21] international measurement series.

The next level of comparisons must take place between ACQUIRE and the Target Acquisition Weather Software (TAWS), which is an upgrade to the EOTDA program. The summary information about TAWS and the comparison tables of delta T and detection ranges of WineOTDA and TAWS can be found in

Appendix K. A more systematic and detailed comparison of the two codes is recommended for future study.

THIS PAGE INTENTIONALLY LEFT BLANK

## APPENDIX A. FLIR92 MODEL OUTPUTS

```

U.S. Army CECOM NVESD FLIR92                Thu May 18 23:24:55 2000
output file: SADAI1.1  short listing
data file: SADAI1
command line arguments:  -d SADAI1 -o SADAI1 -p MRT
begin data file listing . . .
gen2: sample data file for 2nd generation FLIR with SADA II FPA
  >spectral
    spectral_cut_on           8.0      microns
    spectral_cut_off         12.0      microns
    diffraction_wavelength    0.0      microns
  >optics_1
    f_number                   0.0      --
    eff_focal_length          20.0      cm
    eff_aperture_diameter     10.0      cm
    optics_blur_spot          0.01     mrad
    average_optical_trans     0.7      --
  >optics_2
    HFOV:VFOV_aspect_ratio    0.0      --
    magnification              0.0      --
    frame_rate                 30.0      Hz
    fields_per_frame           1.0      --
  >detector
    horz_dimension_(active)    25.4      microns
    vert_dimension_(active)    25.4      microns
    peak_D_star                1.5e10    cm-sqrt(Hz) /W
    integration_time           0.007     microseconds
    1/f_knee_frequency         3.0      Hz
  >fpa_parallel
    #_detectors_in_TDI         4.0      --
    #_vert_detectors           480.0     --
    #_samples_per_HIFOV        2.0      --
    #_samples_per_VIFOV        2.0      --
    3dB_response_frequency     2032.0    Hz
    scan_efficiency            0.75     --
  >electronics
    high_pass_3db_cuton        1.0      Hz
    high_pass_filter_order     0.0      --
    low_pass_3db_cutoff        100000.0  Hz
    low_pass_filter_order      0.0      --
    boost_amplitude            0.0      --
    boost_frequency            0.0      Hz
    sample_and_hold             HORZ      NO_HORZ_VERT
  >display
    display_brightness         10.0     milli-Lamberts
    display_height              15.24    cm
    display_viewing_distance    30.0     cm
  >crt_display
    #_active_lines_on_CRT      480.0    --
    horz_crt_spot_sigma        0.0      mrad
    vert_crt_spot_sigma        0.0      mrad

```

```

>eye
  threshold_SNR          2.5      --
  eye_integration_time   0.1      sec
  MTF                    EXP      EXP_or_NL
>random_image_motion
  horz_rms_motion_amplitude 0.02   mrad
  vert_rms_motion_amplitude 0.02   mrad
>sinusoidal_image_motion
  horz_rms_motion_amplitude 0.0     mrad
  vert_rms_motion_amplitude 0.0     mrad
>3d_noise_default
  noise_level            MOD      NO_LO_MOD_or_HI
>spectral_detectivity
  #_points: 9           microns___detectivity
                        8.00      0.666
                        8.50      0.708
                        9.00      0.750
                        9.50      0.792
                        10.00     0.833
                        10.50     0.875
                        11.00     0.917
                        11.50     0.958
                        12.00     1.00

```

>end

end data file listing . . .

MESSAGES

```

diagnostic(): Using default 3D noise components.
diagnostic(): Using _MOD_ level 3D noise defaults.
diagnostic(): Diff. wavelength set to spectral band midpoint.
diagnostic(): HFOV:VFOV aspect ratio defaulted to 1.33.
diagnostic(): Fields-of-view calculated by model.
diagnostic(): Electronics high pass filter defaulted to order 1.
diagnostic(): Electronics low pass filter defaulted to order 1.

```

CALCULATED SYSTEM PARAMETERS

```

field-of-view:    2.323h x  1.746v degrees
                  40.54h x  30.48v mrad
magnification:    16.323
optics blur spot: 48.800 microns (diffraction-limited)
                  0.244 mrad
detector IFOV:   0.127h x  0.127v mrad
scan velocity:   1621.29 mrad/second
dwell time:      7.833e-005 seconds

```

TEMPERATURE DEPENDENCE

parameter	NETD @ 300 K	NETD @ 0 K	noise bandwidth
white NETD	0.185 deg C	0.000 deg C	1.003e+004 Hz
classical NETD	0.185 deg C	0.000 deg C	1.007e+004 Hz
sigma_TVH NETD	0.103 deg C	0.000 deg C	3.134e+003 Hz
sigma_TV NETD	0.077 deg C	0.000 deg C	
sigma_V NETD	0.077 deg C	0.000 deg C	

Planck integral 1.978e-004 0.000e+000 W/(cm\*cm\*K)  
 . . . w/D-star 2.439e+006 0.000e+000 sqrt(Hz)/(cm\*K)

PREFILTER VALUES AT NYQUIST

horz H\_PRE(7.87) = 0.000 vert H\_PRE(7.87) = 0.000

SAMPLING RATES

horizontal 15.75 samples/mr  
 vertical 15.75 samples/mr  
 effective 15.75 samples/mr

SENSOR LIMITING FREQUENCIES

	spatial	Nyquist
horizontal	7.87	7.87
vertical	7.87	7.87
effective	7.87	7.87

MRTD 3D NOISE CORRECTION (AVERAGE)

	300 K	0 K
horizontal	1.000	0.000
vertical	3.833	0.000

MRTD AT 300 K BACKGROUND TEMPERATURE

	cy/mr	horz		cy/mr	vert	cy/mr	2D
0.05	0.394	0.007	0.05	0.394	0.065	0.830	0.065
0.10	0.787	0.017	0.10	0.787	0.100	1.120	0.085
0.15	1.181	0.031	0.15	1.181	0.134	1.424	0.110
0.20	1.575	0.053	0.20	1.575	0.176	1.767	0.144
0.25	1.969	0.085	0.25	1.969	0.228	2.112	0.188
0.30	2.362	0.133	0.30	2.362	0.295	2.458	0.245
0.35	2.756	0.206	0.35	2.756	0.385	2.794	0.319
0.40	3.150	0.318	0.40	3.150	0.508	3.116	0.416
0.45	3.543	0.494	0.45	3.543	0.680	3.425	0.542
0.50	3.937	0.778	0.50	3.937	0.929	3.720	0.706
0.55	4.331	1.245	0.55	4.331	1.301	4.001	0.921
0.60	4.724	2.038	0.60	4.724	1.872	4.268	1.200
0.65	5.118	3.433	0.65	5.118	2.785	4.522	1.564
0.70	5.512	6.000	0.70	5.512	4.314	4.767	2.039
0.75	5.906	10.815	0.75	5.906	7.021	4.998	2.658
0.80	6.299	21.134	0.80	6.299	12.206	5.219	3.464
0.85	6.693	45.254	0.85	6.693	23.284	5.429	4.515
0.90	7.087	99.999	0.90	7.087	51.641	5.629	5.886
0.95	7.480	99.999	0.95	7.480	99.999	5.820	7.672
1.00	7.874	99.999	1.00	7.874	99.999	6.003	10.000

FLIR92. . . SADAI1.1: end of listing



output file: SADA1.1      short listing  
data file: SADAI1  
command line arguments: -d SADAI1 -o SADA1 -p MDT  
begin data file listing . . .  
gen2: sample data file for 2nd generation FLIR with SADA II FPA

## MDTD AT 300 K BACKGROUND TEMPERATURE

	1/mr	MDTD
0.20	39.370	27.084
0.40	19.685	6.867
0.60	13.123	3.123
0.80	9.843	1.811
1.00	7.874	1.203
1.20	6.562	0.872
1.40	5.624	0.672
1.60	4.921	0.540
1.80	4.374	0.450
2.00	3.937	0.384
2.20	3.579	0.335
2.40	3.281	0.296
2.60	3.028	0.266
2.80	2.812	0.241
3.00	2.625	0.221
3.20	2.461	0.204
3.40	2.316	0.190
3.60	2.187	0.178
3.80	2.072	0.167
4.00	1.969	0.158
4.20	1.875	0.150
4.40	1.790	0.142
4.60	1.712	0.136
4.80	1.640	0.130
5.00	1.575	0.125

FLIR92 . . . SADA1.1: end of listing

**APPENDIX B. FIGURES OF COMPARISON OF FLIR92 MODEL SENSOR  
OUTPUTS WITH THE OTHER SENSORS IN WinEOTDA MODEL**

No	Sns # (sensor number)	NETD	IFOVx (horizontal IFOV)	IFOVy (vertical IFOV)	f min (minimum spatial frequency)	MRT min (MRTD at min spatial frequency)	f max (maximum spatial frequency)	MRT max (MRTD at max spatial frequency)
1	100	0.175	0.0005	0.0005	0.06	0.15	2	99.9988
2	101	0.175	0.0005	0.0005	0.06	0.15	2	99.9988
3	102	0.539	0.0004	0.0004	0.25	0.31	2	99.9988
4	103	0.0805	0.0006	0.00041	0.2	0.082	0.96992	100
5	104	0.4515	0.0005	0.0005	0.25	0.17	2.95	100
6	105	0.3815	0.0008	0.0008	0.1	0.1	0.66981	1.2
7	106	0.2695	0.00066	0.00066	0.19	0.12	1.4	99.9
8	107	0.35	0.00105	0.00105	0.02	0.16	0.77008	100
9	108	0.1575	0.0005	0.000374	0.05	0.1	1.6	100
10	109	0.1995	0.000457	0.000689	0.044	0.12533	1.3	100
11	110	0.119	0.0006	0.0009	0.1	0.01	1.07	100
12	111	0.301	0.0015	0.0015	0.025	0.01467	0.65	100
13	112	0.2485	0.000307	0.000306	0.225	0.024	3.2	99.9
14	113	0.301	0.0015	0.0015	0.025	0.08	0.65	100
15	114	0.0875	0.000478	0.000717	0.25	0.05467	1.51009	100
16	115	0.119	0.0006	0.0009	0.143	0.064	1.15	100
17	116	0.5005	0.00134	0.00202	0.166	0.14067	0.7	100
18	117	0.329	0.00095	0.00113	0.04	0.06	0.8	100
19	118	0.1995	0.000402	0.000579	0.53	0.152	2	100
20	119	0.168	0.0006	0.00075	0.08	0.004	1.32982	92.8
21	120	0.1995	0.0012	0.0015	0.067	0.02867	0.6	31.7
22	121	0.1995	0.0006	0.00075	0.133	0.02867	1.2	31.7
23	122	0.0105	0.0003	0.000224	0.1	0.01133	2.5319	99.8
24	123	0.1015	0.000128	0.000104	0.1	0.01	2	99.9
25	124	0.1015	0.0008	0.00111	0.08	0.05	0.45	0.5
26	125	0.1015	0.00024	0.00033	0.28	0.05	1.61	0.5
27	126	0.175	0.0005	0.0005	0.06	0.15	2	99.9988
28	127	0.185	0.000127	0.000127	0.394	0.007	7.087	99.999

Table B.1 - WinEOTDA and FLIR92 Sensors Physical and  
Performance Parameters

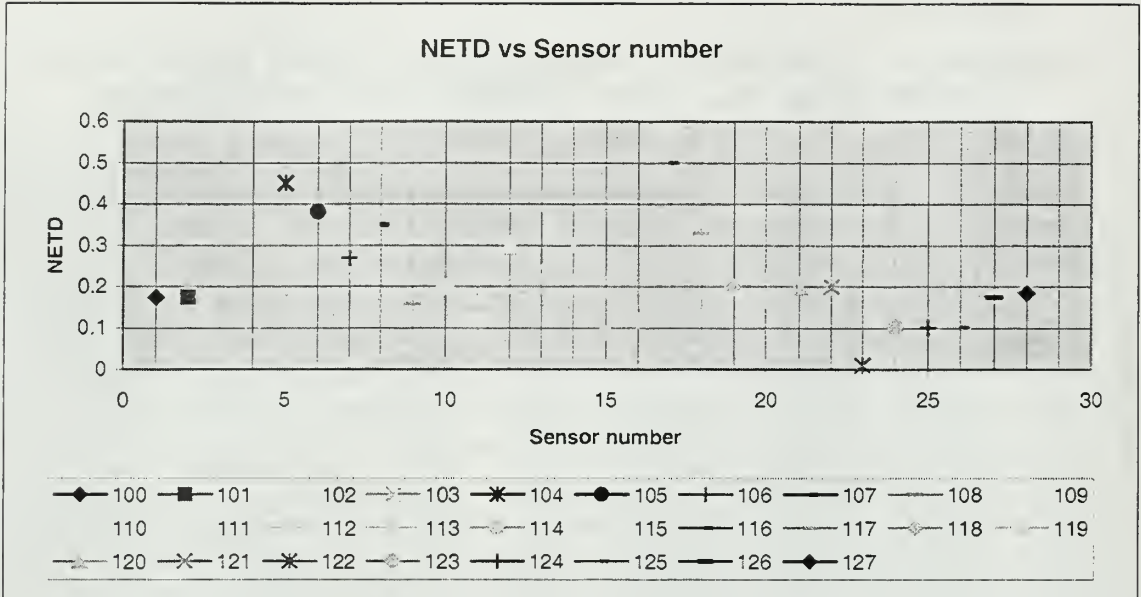


Figure B.1 - WinEOTDA and FLIR92 Sensors NETD Comparison

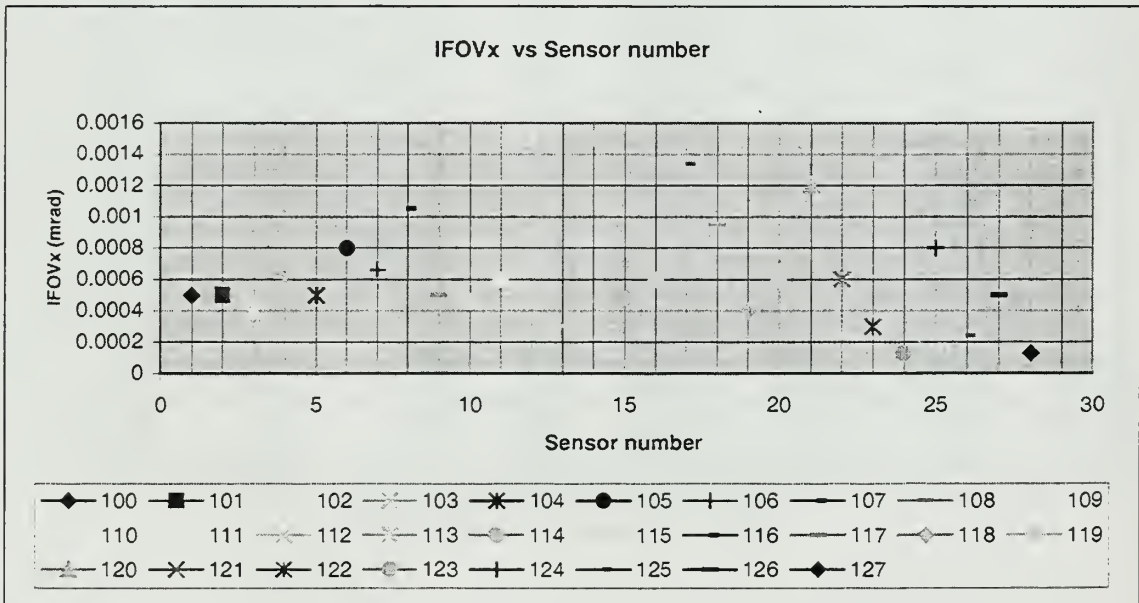


Figure B.2 - WinEOTDA and FLIR92 Sensors Horizontal IFOV Comparison

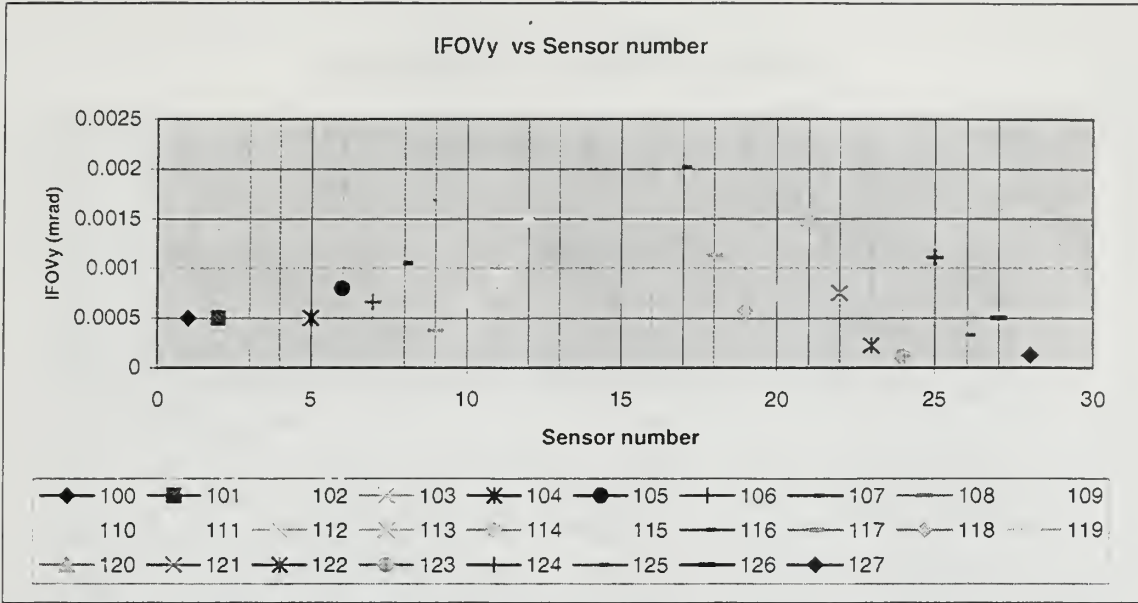


Figure B.3 - WinEOTDA and FLIR92 Sensors Vertical IFOV Comparison

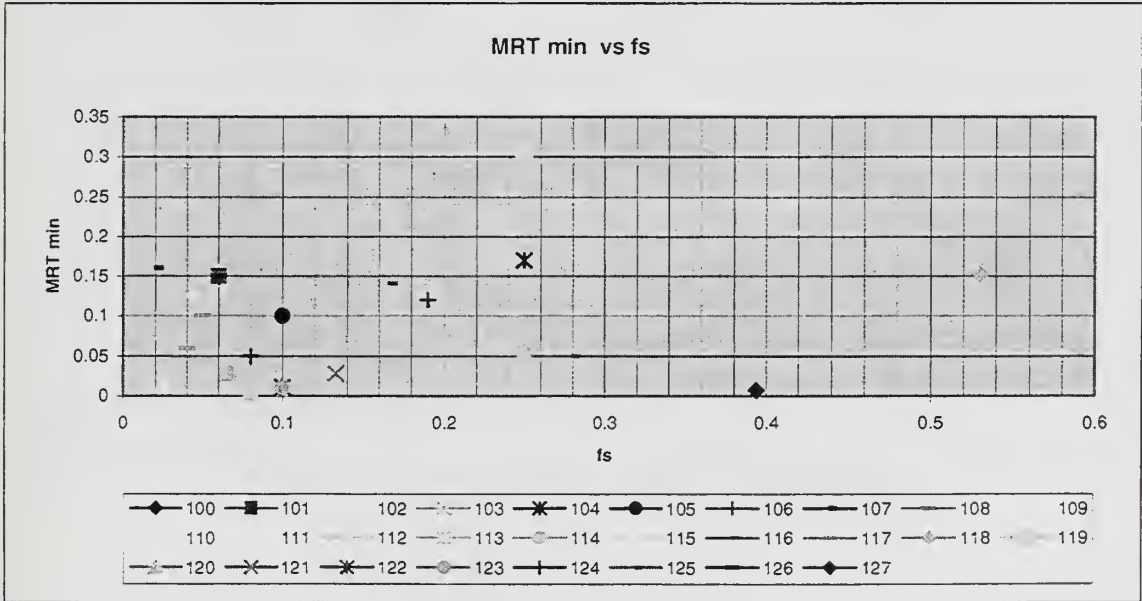


Figure B.4 - WinEOTDA and FLIR92 Sensors Minimum MRT vs. Spatial Frequency

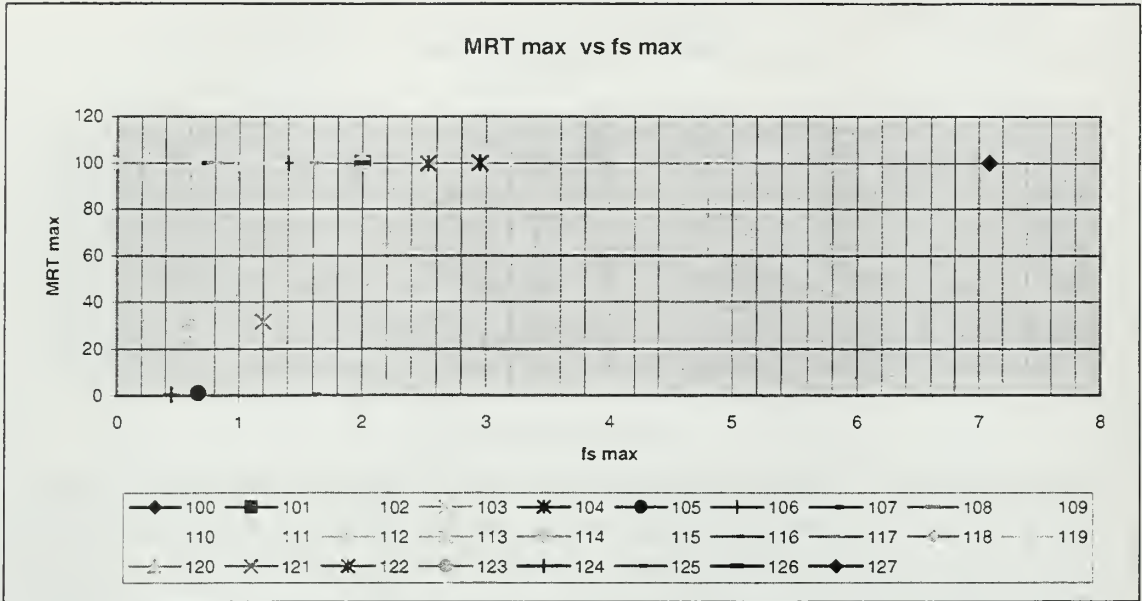


Figure B.5 - WinEOTDA and FLIR92 Sensors Maximum MRT vs. Spatial Frequency



### APPENDIX C. SEARAD INPUTS

1	INPUT FOR CARD 1:	
	MODEL	Mid-latitude summer
	ITYPE INDICATES THE TYPE OF ATMOSPHERIC PATH	Vertical or slant path between two altitudes
	IEMSCT DETERMINES THE MODE OF EXECUTION	Transmittance mode
	IMULT DETERMINES EXECUTION WITH OR WITHOUT MULTIPLE SCATTERING	Without multiple scattering
	TBOUND (K) IS THE BOUNDARY TEMPERATURE FOR SLANT PATH THAT INTERSECTS THE EARTH OR GREYBODY	294
2	INPUT FOR CARD 2:	
	IHAZE, ISEASN, IVULCN, ICSTL, ICLD, IVSA, VIS, WSS, WHH, RAINRT, GNDALT IHAZE SELECTS THE EXTINCTION TYPE AND THE DEFAULT VISIBILITY RANGE	3=Navy maritime extinction, set own visibility
	ICSTL IS THE AIR MASS CHARACTER (1 TO 10) USED ONLY WITH NAVY MARITIME MODEL	3=open ocean
	ICLD SPECIFIES THE CLOUD MODELS AND THE RAIN RATES TO BE USED	4=stratus/strato cu base
	VIS SPECIFIES THE METEOROLOGICAL RANGE	24.14km=15mi
	WSS SPECIFIES THE CURRENT WIND SPEED (AVAILABLE ONLY WHEN IHAZE=3/10)	2.57
	WSS SPECIFIES THE CURRENT WIND SPEED	2.57
3	INPUT FOR CARD 3:	
	H1 - SPECIFIES THE INITIAL ALTITUDE (KM)	0.01
	H2 SPECIFIES THE FINAL ALTITUDE (KM)	0.5
	RANGE SPECIFIES THE PATH LENGTH (KM)	0, .5, .75, 1, ..., 6, 8, ..., 30
	RO SPECIFIES THE RADIUS OF THE EARTH (KM) AT THE PARTICULAR GEOGRAPHICAL LOCATION	0
	SEAWITCH SELECTS WHETHER SEA MODIFICATIOIN WILL BE USED	F
4	INPUT FOR CARD 4 :	
	V1 = INITIAL FREQUENCY(WAVENUMBER CM-1)	1000
	V2 = FINAL FREQUENCY(WAVENUMBER CM-1 )	1333
	DV = FREQUENCY INCREMENT (OR STEP SIZE) (CM-1)	5
	IFWHM = INCREMENTAL FREQUENCY WIDTH AT HALF MAXIMUM (CM-1)	10

Table C.1 - SeaRad Input Parameters



THIS PAGE INTENTIONALLY LEFT BLANK

## APPENDIX D. SEARAD OUTPUTS

\*\*\*\*\* SEARAD \*\*\*\*\*

DATE: 05/16/2000

TIME: 01:41:29.25

TRANSMITTANCE MODE

SINGLE SCATTERING USED

MARINE AEROSOL MODEL USED

WIND SPEED = 2.57 M/SEC  
WIND SPEED = 2.57 M/SEC, 24 HR AVERAGE  
RELATIVE HUMIDITY = 76.11 PERCENT  
AIRMASS CHARACTER = 3.0  
VISIBILITY = 24.14 KM

SLANT PATH, H1 TO H2

H1 = .010 KM  
H2 = .500 KM  
ANGLE = .000 DEG  
RANGE = .500 KM  
BETA = .000 DEG  
LEN = 0

FREQUENCY RANGE

IV1 = 830 CM-1 (12.05 MICROMETERS)  
IV2 = 1250 CM-1 (8.00 MICROMETERS)  
IDV = 5 CM-1  
IFWHM = 10 CM-1  
IFILTER = 0

SUMMARY OF THE GEOMETRY CALCULATION

H1 = .010 KM  
H2 = .500 KM  
ANGLE = 11.479 DEG  
RANGE = .500 KM  
BETA = .001 DEG  
PHI = 168.521 DEG  
HMIN = .010 KM  
BENDING = .000 DEG  
LEN = 0

INTEGRATED ABSORPTION = 64.47 CM-1 FROM 830 TO 1250 CM-1  
AVERAGE TRANSMITTANCE = .8465

Range	Transmittance
0	1
0.5	0.8465
0.75	0.796
1	0.751
2	0.6049
3	0.4942
4	0.407
5	0.3371
6	0.2804
8	0.1959
10	0.1386
12	0.0986
14	0.0709
16	0.0511
18	0.0371
20	0.027
22	0.0197
24	0.0144
26	0.0106
28	0.0078

Table D.1 - SeaRad Outputs for Different Ranges

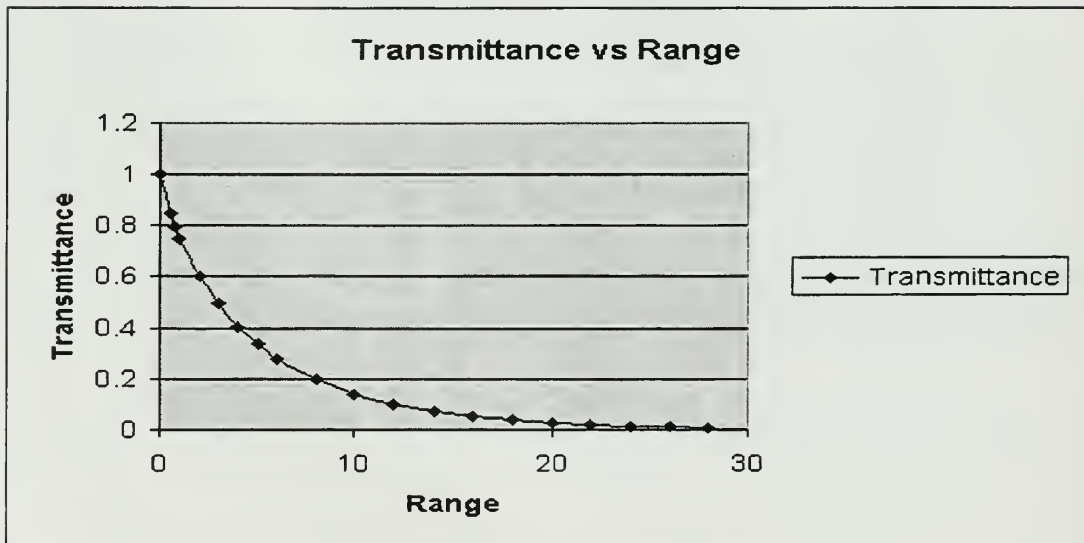


Figure D.1 - Searad Outputs For Mid-Latitude Summer Scenario Conditions

APPENDIX E. WINEOTDA MODEL DATA ENTRY FORMS

WinEOTDA - Targets

Target #1 Target #2

Target Gunboat

Heading 0

Position At Base

Op State Off

Speed (kts) 0

Target Elevation (ft MSL) 0

OK Cancel

Figure E.1 - WinEOTDA Target Entry Form

WinEOTDA Backgrounds

Background #1 Background #2 Background #3

Background Type : Water

Depth (ft) : 20

Clarity : Clear

N/A

Slope : Value 0 Direction 0

General Background ID

Continental  Urban  Desert  Ocean  Snow

OK Cancel

Figure E.2 - WinEOTDA Background Entry Form

**WinEOTDA - Time Over Target**

Planning Interval:  15  30  60

TOT - Date:  Hr:  Min:

January 1993

Sun	Mon	Tue	Wed	Thu	Fri	Sat
27	28	29	30	31	1	2
3	4	5	6	7	8	9
10	11	12	13	14	15	16
17	18	19	20	21	22	23
24	25	26	27	28	29	30
31	1	2	3	4	5	6

Select  Exec  Plan

Figure E.3 - WinEOTDA Time Over Target (TOT) Entry Form

**WinEOTDA - Sensor Data Entry Form**

Select  IR  TV  LAS

Sensor ID:

Sensor Height (ft AGL)

Scene Complexity  None  Low  Medium  High

View Direction (Deg)

Figure E.4 - WinEOTDA Sensor Entry Form



Met Input																				
Date - Jul	26																		27	
Time GMT (Hrs)	10	11	12	13	14	15	16	17	18	19	20	21	22	23	0	1	2	3	4	
Temperature (deg F)	51	49	47	45	45	45	47	49	51	55	57	61	64	66	69	71	71	71	69	6
Dew PT Temp (deg F)	47	45	44	43	43	43	44	45	47	49	50	51	53	55	57	57	57	57	57	5
Relative Humidity (%)	84	87	90	92	93	92	90	87	84	80	76	72	69	67	65	64	64	64	65	6
Aerosol Index	2	2	2	2	2	2	2	2	2	2	2	2	2	2	2	2	2	2	2	
BICs	0	0	0	0	0	0	0	0	0	0	0	0	0	0	0	0	0	0	0	
Visibility (mi)	6.2	6.2	6.2	6.2	6.2	6.2	6.2	6.2	6.2	6.2	6.2	6.2	6.2	6.2	6.2	6.2	6.2	6.2	6.2	6
Precipitation Index	0	0	0	0	0	0	0	0	0	0	0	0	0	0	0	0	0	0	0	
Rain Rate	0	0	0	0	0	0	0	0	0	0	0	0	0	0	0	0	0	0	0	
Wind Speed (kts)	10	10	10	10	10	10	26	15	15	15	28	15	15	15	15	15	15	15	15	1
Wind Direction (deg)	130	130	130	130	130	130	298	5	190	190	92	190	190	190	190	190	190	190	190	19
Boundary Layer Ht (hft)	150	150	150	150	150	150	150	150	150	150	150	150	150	150	150	1	150	150	150	15
Low Cloud Type	0	0	0	0	0	0	2	2	2	2	2	2	2	2	2	2	2	2	2	
Low Cloud Ht (hft)	0	0	0	0	0	0	40	40	40	40	40	40	40	40	40	40	40	40	40	4
Low Cloud Amount (8ths)	0	0	0	0	0	0	2	2	2	2	2	2	2	2	2	2	2	2	2	
Mid Cloud Type	3	3	3	3	3	3	3	3	3	3	3	3	3	3	3	3	3	3	3	
Mid Cloud Ht (hft)	150	150	150	150	150	150	120	120	120	120	120	120	120	120	120	120	120	120	120	12
Mid Cloud Amount (8ths)	1	1	1	1	1	1	1	1	1	1	1	1	1	1	1	1	1	1	1	
High Cloud Type	6	6	6	6	6	6	5	5	5	5	5	5	5	5	5	5	5	5	5	
High Cloud Ht (hft)	250	250	250	250	250	250	250	250	250	250	250	250	250	250	250	250	250	250	250	25
High Cloud Amount (8ths)	2	2	2	2	2	2	2	2	2	2	2	2	2	2	2	2	2	2	2	
Time GMT (Hrs)	10	11	12	13	14	15	16	17	18	19	20	21	22	23	0	1	2	3	4	
Date - Jul	26																		27	

Status: Min Temp: 45    Max Temp: 71

Figure E.5 - WinEOTDA Meteorology Data Entry Form



THIS PAGE INTENTIONALLY LEFT BLANK

## APPENDIX F. WINEOTDA MODEL OUTPUTS

### IR EOTDA EXECUTION SUMMARY

SYSTEM INPUT FILE NAME: C:\PROGRAM FILES\NRL-  
 MONTEREY\WINEOTDA\Data\local\EOTDA\State\SystemState.dat

TOT : 07 January 1993 1055 GMT (Z)  
 Absolute Humidity : 8.9 (g/m\*\*3)      4 km Transmissivity : 0.60  
 Sky Temperature : 243.4 (deg K)      IR Visibility : 066.3 (kft)

Latitude : 24 deg 15 min N      Longitude : 059 deg 45 min W  
 Sensor ID : 127      Sensor Ht : 2,000 feet  
 View Direction : 0      Complexity : None

#### TARGET INFORMATION

Target Elevation: 0 feet (MSL)

Target #1	Target #2
Target ID : Gunboat	Target ID : Gunboat
Target Heading : 0	Target Heading : 0
Operating State : 1	Operating State : 1
Target Speed : 0	Target Speed : 0

#### BACKGROUND INFORMATION

General Background Albedo: Ocean

Background #1 ID: Water  
 Background #2 ID: Soil  
 Background #3 ID: Vegetation

#### IR EOTDA OUTPUT

RANGES	Target #1 Gunboat		Background #1 Water		
View Dir (deg)	MRT Detection Range (km)		MDT Detection Range (km)		Lock-on Range
-----	NFOV	WFOV	NFOV	WFOV	(km)
-----	-----	-----	-----	-----	-----
000	48.1	18.5	31.8	33.7	0.0
045	51.5	18.5	31.3	38.6	0.0
090	51.5	18.5	31.5	39.5	0.0
135	51.0	18.5	34.6	38.4	0.0
180	45.1	18.5	28.8	31.8	0.0
225	49.1	18.5	30.1	36.9	0.0
270	49.8	18.5	31.1	38.2	0.0
315	50.4	18.5	31.3	38.0	0.0

THERMAL CONTRAST (Delta-T)			Target #1 Gunboat		Background #1 Water
View Dir	MRT Delta T (K)		MDT Delta T (K)		Lock-on Delta-T
(deg)	NFOV	WFOV	NFOV	WFOV	
000	31.3	28.2	33.3	15.4	0.0
045	28.8	25.8	31.0	22.2	0.0
090	27.1	24.2	31.2	24.8	0.0
135	25.9	23.0	28.6	21.7	0.0
180	21.5	18.8	22.7	11.3	0.0
225	21.0	18.3	27.0	18.0	0.0
270	21.3	18.5	29.8	20.7	0.0
315	24.4	21.6	31.0	20.9	0.0

TEMPERATURES (K)			Target #1 Gunboat		Background #1 Water	
View Dir	Bkgd Temp	MRT Temperature (K)		MDT Temperature (K)		Lock-on Temp
(deg)	(K)	NFOV	WFOV	NFOV	WFOV	(K)
000	273.5	304.9	304.6	307.7	289.7	300.0
045	273.5	302.2	302.2	305.4	296.1	300.0
090	273.5	300.5	300.5	305.6	298.7	300.0
135	273.5	299.4	299.4	302.9	295.7	300.0
180	273.5	295.3	295.4	297.5	285.9	300.0
225	273.5	294.8	294.9	301.8	292.3	300.0
270	273.5	295.0	295.1	304.5	294.9	300.0
315	273.5	298.0	298.0	305.5	294.9	300.0

RANGES			Target #1 Gunboat		Background #2 Soil
View Dir	MRT Detection Range (km)		MDT Detection Range (km)		Lock-on Range
(deg)	NFOV	WFOV	NFOV	WFOV	(km)
000	41.0	18.5	26.8	30.1	0.0
045	42.9	18.5	25.6	32.6	0.0
090	41.8	18.5	26.4	31.5	0.0
135	40.3	18.5	24.7	30.3	0.0
180	26.2	16.1	19.8	17.0	0.0
225	28.3	17.8	24.7	22.1	0.0
270	30.1	18.5	26.0	23.8	0.0
315	38.6	18.5	26.4	28.8	0.0

THERMAL CONTRAST (Delta-T)			Target #1 Gunboat		Background #2 Soil
View Dir	MRT Delta T (K)		MDT Delta T (K)		Lock-on Delta-T
(deg)	NFOV	WFOV	NFOV	WFOV	
000	10.7	10.5	14.8	6.8	0.0
045	8.1	8.1	12.8	8.4	0.0
090	6.4	6.4	13.8	7.4	0.0
135	5.3	5.3	11.3	6.4	0.0
180	1.2	1.3	6.0	2.0	0.0
225	0.8	0.8	11.1	2.2	0.0
270	0.9	1.0	11.4	2.8	0.0
315	3.9	3.9	11.4	5.3	0.0

TEMPERATURES (K)		Target #1 Gunboat		Background #2 Soil		
View Dir (deg)	Bkgd Temp (K)	MRT Temperature (K)	WFOV	MDT Temperature (K)	WFOV	Lock-on Temp (K)
		NFOV		NFOV		
000	294.1	304.8	304.6	308.9	300.9	300.0
045	294.1	302.2	302.2	307.0	302.5	300.0
090	294.1	300.5	300.5	307.9	301.5	300.0
135	294.1	299.4	299.4	305.4	300.5	300.0
180	294.1	295.4	295.4	300.1	296.1	300.0
225	294.1	294.9	294.9	305.2	296.3	300.0
270	294.1	295.0	295.1	305.5	296.9	300.0
315	294.1	298.0	298.0	305.5	299.4	300.0

RANGES		Target #1 Gunboat		Background #3 Vegetation	
View Dir (deg)	MRT Detection Range (km)	WFOV	MDT Detection Range (km)	WFOV	Lock-on Range (km)
	NFOV		NFOV		
000	34.1	18.5	23.6	25.8	0.0
045	31.3	18.5	22.1	21.9	0.0
090	24.7	15.9	23.4	25.3	0.0
135	32.0	18.5	22.5	25.6	0.0
180	36.5	18.5	24.9	27.3	0.0
225	41.0	18.5	29.4	31.1	0.0
270	41.2	18.5	23.2	31.1	0.0
315	36.9	18.5	26.8	27.5	0.0

THERMAL CONTRAST (Delta-T)		Target #1 Gunboat		Background #3 Vegetation	
View Dir (deg)	MRT Delta T (K)	WFOV	MDT Delta T (K)	WFOV	Lock-on Delta-T
	NFOV		NFOV		
000	3.9	3.7	9.1	3.3	0.0
045	1.3	1.3	7.6	2.0	0.0
090	-0.4	-0.4	9.0	-3.1	0.0
135	-1.5	-1.5	-7.4	-3.3	0.0
180	-5.5	-5.5	-7.6	-4.1	0.0
225	-6.0	-6.0	-7.6	-6.6	0.0
270	-5.9	-5.8	-8.4	-6.6	0.0
315	-2.9	-2.9	-7.6	-4.1	0.0

TEMPERATURES (K)		Target #1 Gunboat		Background #3 Vegetation		
View Dir (deg)	Bkgd Temp (K)	MRT Temperature (K)	WFOV	MDT Temperature (K)	WFOV	Lock-on Temp (K)
		NFOV		NFOV		
000	300.9	304.8	304.6	310.0	304.2	300.0
045	300.9	302.2	302.2	308.5	302.9	300.0
090	300.9	300.5	300.5	309.9	297.8	300.0
135	300.9	299.4	299.4	293.5	297.5	300.0
180	300.9	295.3	295.4	293.3	296.8	300.0
225	300.9	294.8	294.9	293.3	294.2	300.0
270	300.9	295.0	295.1	292.5	294.3	300.0
315	300.9	298.0	298.0	293.3	296.8	300.0

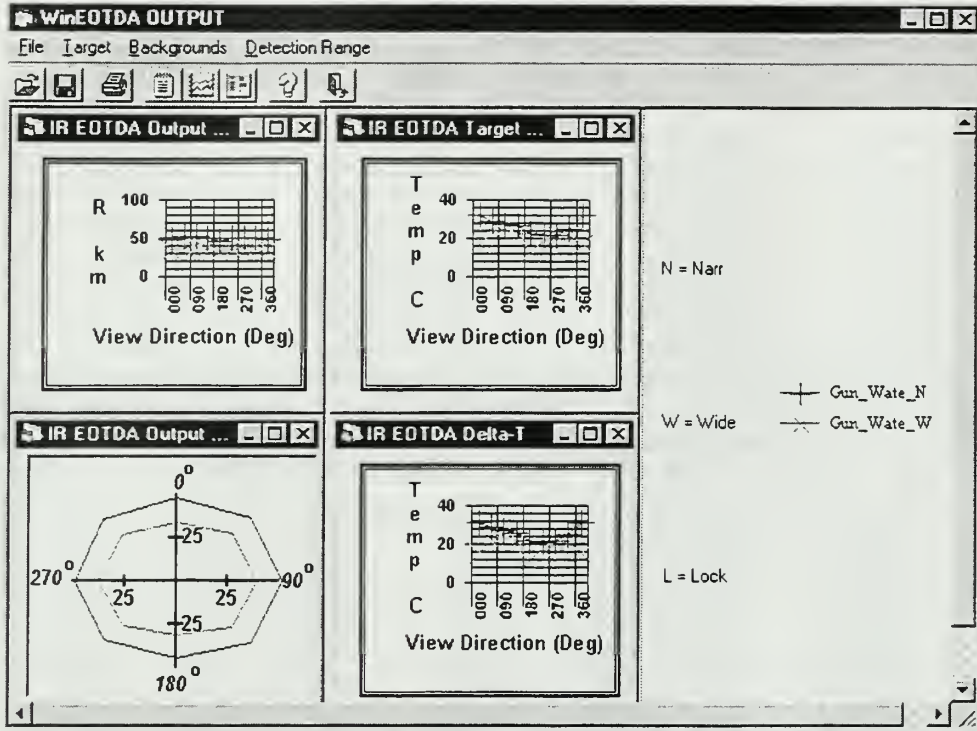


Figure F.1 - WinEOTDA Graphical Output

The figure shows the WinEOTDA OUTPUT - [Tabular Output] window. It displays the following table:

**IR EOTDA EXECUTION OUTPUT**

View Direction	Gunboat Range (kft)		Gunboat Range (kft)	
	NFDV	WFDV	NFDV	WFDV
000	157.9	110.6	157.9	110.6
045	169.0	126.6	169.0	126.6
090	169.0	129.6	169.0	129.6
135	167.2	126.0	167.2	126.0
180	148.1	104.4	148.1	104.4
225	161.0	121.0	161.0	121.0
270	163.5	125.3	163.5	125.3
315	165.3	124.7	165.3	124.7

0.0 --> No Value Computed  
-1.0 --> No Solution Possible

Figure F.2 - WinEOTDA Tabular Output



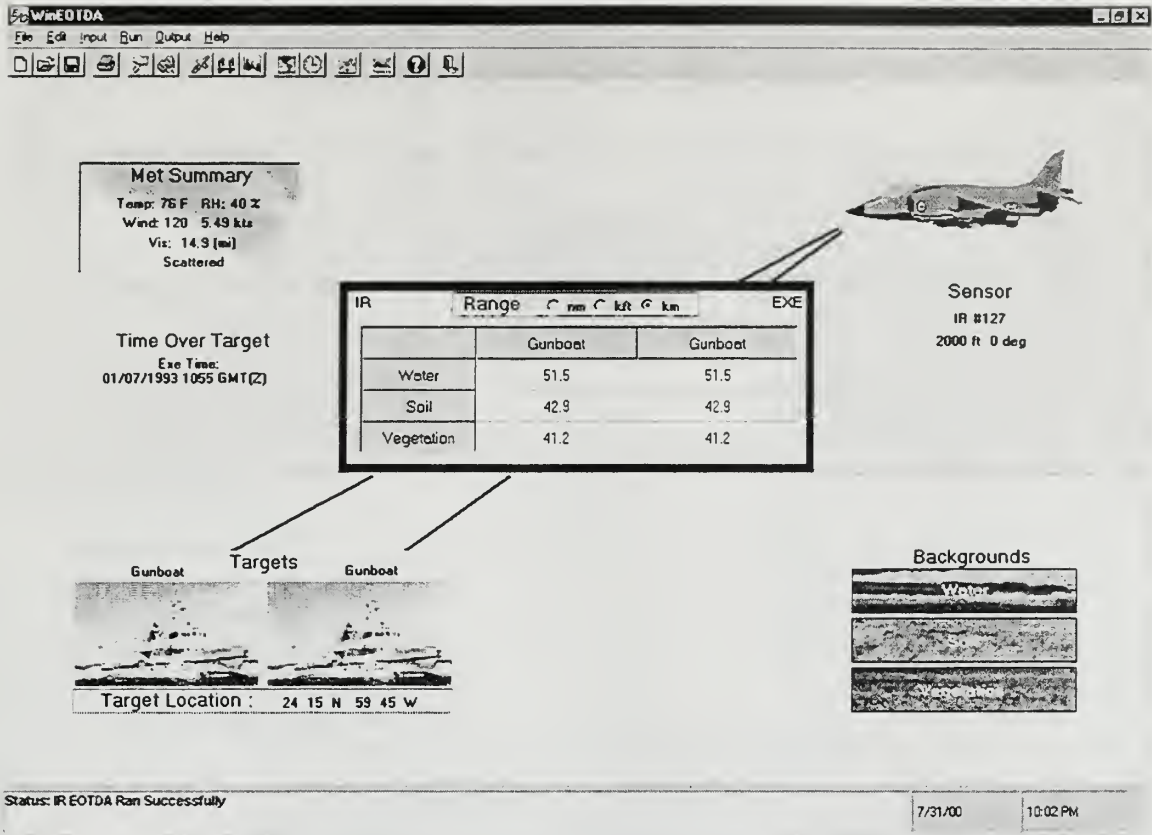


Figure F.3 - WinEOTDA Main Screen Output



THIS PAGE INTENTIONALLY LEFT BLANK

## APPENDIX G. ACQUIRE MODEL INPUTS

Acquire data file for front view of gunboat 2000ft at 25km

```
>sensor_lookup
  data_file_name      Sada.dat      ---
  sensor_id           gen2          ---
  performance_mode    MRT           MRT_MDT_MRC_OR_MDC

>target
  characteristic_size 9.78          meters
  target_signature    7.71          degrees_C

>cycle_criteria
  detection_n50        0.75          wfov
  detection_n50        0.75          nfov
  classification_n50  1.5           nfov
  recognition_n50     3.0           nfov
  identification_n50  6.0           nfov

>band-averaged_atmosphere
  #_points: 20      km.....transmittance
                   0.000e+00      1.000e+00
                   5.000e-01      8.465e-01
                   7.500e-01      7.960e-01
                   1.000e+00      7.510e-01
                   2.000e+00      6.049e-01
                   3.000e+00      4.942e-01
                   4.000e+00      4.070e-01
                   5.000e+00      3.371e-01
                   6.000e+00      2.804e-01
                   8.000e+00      1.959e-01
                   1.000e+01      1.386e-01
                   1.200e+01      9.860e-02
                   1.400e+01      7.090e-02
                   1.600e+01      5.110e-02
                   1.800e+01      3.710e-02
                   2.000e+01      2.700e-02
                   2.200e+01      1.970e-02
                   2.400e+01      1.440e-02
                   2.600e+01      1.060e-02
                   2.800e+01      7.800e-03

>end
```

THIS PAGE INTENTIONALLY LEFT BLANK

**APPENDIX H. CRITICAL DIMENSION ANALYSIS OF ACQUIRE TARGET  
MODEL**

<b>Range</b>	<b>Altitude 500 ft</b>	<b>Theta 500 ft</b>	<b>Area Front View</b>	<b>Critical Dimension Front View 500ft</b>	<b>Area Side View</b>	<b>Critical Dimension Side View 500ft</b>
1000	152.4	0.152996	146.4626	12.10217	422.5989	20.55721
2000	152.4	0.076274	116.383	10.78809	394.9706	19.87387
3000	152.4	0.050822	106.2442	10.30748	385.2834	19.62864
4000	152.4	0.038109	101.1539	10.05753	380.3511	19.50259
5000	152.4	0.030485	98.09311	9.904196	377.3633	19.42584
6000	152.4	0.025403	96.04979	9.8005	375.3596	19.3742
7000	152.4	0.021773	94.58893	9.725684	373.9227	19.33708
8000	152.4	0.019051	93.49254	9.669154	372.8418	19.30911
9000	152.4	0.016934	92.63935	9.624934	371.9993	19.28728
10000	152.4	0.015241	91.95652	9.589396	371.3241	19.26977
11000	152.4	0.013855	91.39766	9.560212	370.7708	19.25541
12000	152.4	0.0127	90.93182	9.535818	370.3093	19.24342
13000	152.4	0.011723	90.53755	9.515122	369.9184	19.23326
14000	152.4	0.010886	90.19955	9.497344	369.583	19.22454
15000	152.4	0.01016	89.90656	9.481907	369.2921	19.21698
16000	152.4	0.009525	89.65016	9.468377	369.0375	19.21035
17000	152.4	0.008965	89.4239	9.456421	368.8127	19.2045
18000	152.4	0.008467	89.22275	9.445779	368.6127	19.19929
19000	152.4	0.008021	89.04276	9.436247	368.4338	19.19463
20000	152.4	0.00762	88.88075	9.427659	368.2726	19.19043
21000	152.4	0.007257	88.73416	9.419881	368.1268	19.18663
22000	152.4	0.006927	88.60089	9.412805	367.9942	19.18317
23000	152.4	0.006626	88.4792	9.406338	367.8731	19.18002
24000	152.4	0.00635	88.36764	9.400406	367.762	19.17712
25000	152.4	0.006096	88.265	9.394945	367.6598	19.17446
26000	152.4	0.005862	88.17025	9.389902	367.5655	19.172
27000	152.4	0.005644	88.08252	9.385229	367.4781	19.16972
28000	152.4	0.005443	88.00105	9.380887	367.3969	19.1676
29000	152.4	0.005255	87.92519	9.376843	367.3213	19.16563
30000	152.4	0.00508	87.85439	9.373067	367.2508	19.16379

Table G.1. - Critical Dimension Analysis for 500ft Sensor  
Height

Range	Altitude 2000 ft	Theta 2000 ft	Area Front View	Critical Dimension Front View 2000ft	Area Side View	Critical Dimension Side View 2000ft
1000	609.6	0.655556	314.6738	17.73905	536.1568	23.15506
2000	609.6	0.309728	205.047	14.31946	471.1522	21.70604
3000	609.6	0.204625	166.2298	12.89301	439.8007	20.97143
4000	609.6	0.152996	146.4626	12.10217	422.5989	20.55721
5000	609.6	0.122224	134.4918	11.59706	411.8075	20.29304
6000	609.6	0.101776	126.4659	11.24571	404.4201	20.1102
7000	609.6	0.087196	120.7111	10.98686	399.0496	19.97623
8000	609.6	0.076274	116.383	10.78809	394.9706	19.87387
9000	609.6	0.067785	113.0096	10.6306	391.7679	19.79313
10000	609.6	0.060998	110.3064	10.50268	389.1867	19.72782
11000	609.6	0.055447	108.0917	10.39672	387.0624	19.6739
12000	609.6	0.050822	106.2442	10.30748	385.2834	19.62864
13000	609.6	0.04691	104.6794	10.2313	383.7721	19.5901
14000	609.6	0.043557	103.3372	10.16549	382.4722	19.5569
15000	609.6	0.040651	102.1731	10.10807	381.3423	19.52799
16000	609.6	0.038109	101.1539	10.05753	380.3511	19.50259
17000	609.6	0.035867	100.2542	10.0127	379.4745	19.48011
18000	609.6	0.033873	99.45408	9.972667	378.6938	19.46006
19000	609.6	0.03209	98.7379	9.936695	377.9941	19.44207
20000	609.6	0.030485	98.09311	9.904196	377.3633	19.42584
21000	609.6	0.029033	97.50953	9.874691	376.7918	19.41113
22000	609.6	0.027713	96.97885	9.847784	376.2716	19.39772
23000	609.6	0.026507	96.49418	9.823145	375.796	19.38546
24000	609.6	0.025403	96.04979	9.8005	375.3596	19.3742
25000	609.6	0.024386	95.64086	9.779615	374.9578	19.36383
26000	609.6	0.023448	95.26331	9.760293	374.5865	19.35424
27000	609.6	0.02258	94.91366	9.742364	374.2424	19.34535
28000	609.6	0.021773	94.58893	9.725684	373.9227	19.33708
29000	609.6	0.021022	94.28654	9.710126	373.6248	19.32938
30000	609.6	0.020321	94.00426	9.69558	373.3466	19.32218

Table G.2 - Critical Dimension Analysis for 2000ft Sensor Height

Range	Altitude 4000 ft	Theta 4000 ft	Area Front View	Critical Dimension Front View 4000ft	Area Side View	Critical Dimension Side View 4000ft
1000	1219.2					
2000	1219.2	0.655556	314.6738	17.73905	536.1568	23.15506
3000	1219.2	0.418511	242.8347	15.58315	498.1211	22.31863
4000	1219.2	0.309728	205.047	14.31946	471.1522	21.70604
5000	1219.2	0.246323	181.8739	13.48606	452.8404	21.28005
6000	1219.2	0.204625	166.2298	12.89301	439.8007	20.97143
7000	1219.2	0.175064	154.9627	12.4484	430.0922	20.73866
8000	1219.2	0.152996	146.4626	12.10217	422.5989	20.55721
9000	1219.2	0.135884	139.8223	11.82465	416.6468	20.41193
10000	1219.2	0.122224	134.4918	11.59706	411.8075	20.29304
11000	1219.2	0.111065	130.1185	11.40695	407.797	20.19399
12000	1219.2	0.101776	126.4659	11.24571	404.4201	20.1102
13000	1219.2	0.093923	123.3694	11.10718	401.538	20.03841
14000	1219.2	0.087196	120.7111	10.98686	399.0496	19.97623
15000	1219.2	0.08137	118.404	10.88136	396.8796	19.92184
16000	1219.2	0.076274	116.383	10.78809	394.9706	19.87387
17000	1219.2	0.071779	114.5978	10.70504	393.2784	19.83125
18000	1219.2	0.067785	113.0096	10.6306	391.7679	19.79313
19000	1219.2	0.064213	111.5873	10.56349	390.4115	19.75883
20000	1219.2	0.060998	110.3064	10.50268	389.1867	19.72782
21000	1219.2	0.05809	109.1466	10.44733	388.0754	19.69963
22000	1219.2	0.055447	108.0917	10.39672	387.0624	19.6739
23000	1219.2	0.053034	107.128	10.35027	386.1352	19.65032
24000	1219.2	0.050822	106.2442	10.30748	385.2834	19.62864
25000	1219.2	0.048787	105.4307	10.26794	384.4982	19.60863
26000	1219.2	0.04691	104.6794	10.2313	383.7721	19.5901
27000	1219.2	0.045171	103.9835	10.19723	383.0986	19.5729
28000	1219.2	0.043557	103.3372	10.16549	382.4722	19.5569
29000	1219.2	0.042054	102.7351	10.13583	381.8881	19.54196
30000	1219.2	0.040651	102.1731	10.10807	381.3423	19.52799

Table G.3 - Critical Dimension Analysis for 4000ft Sensor Height



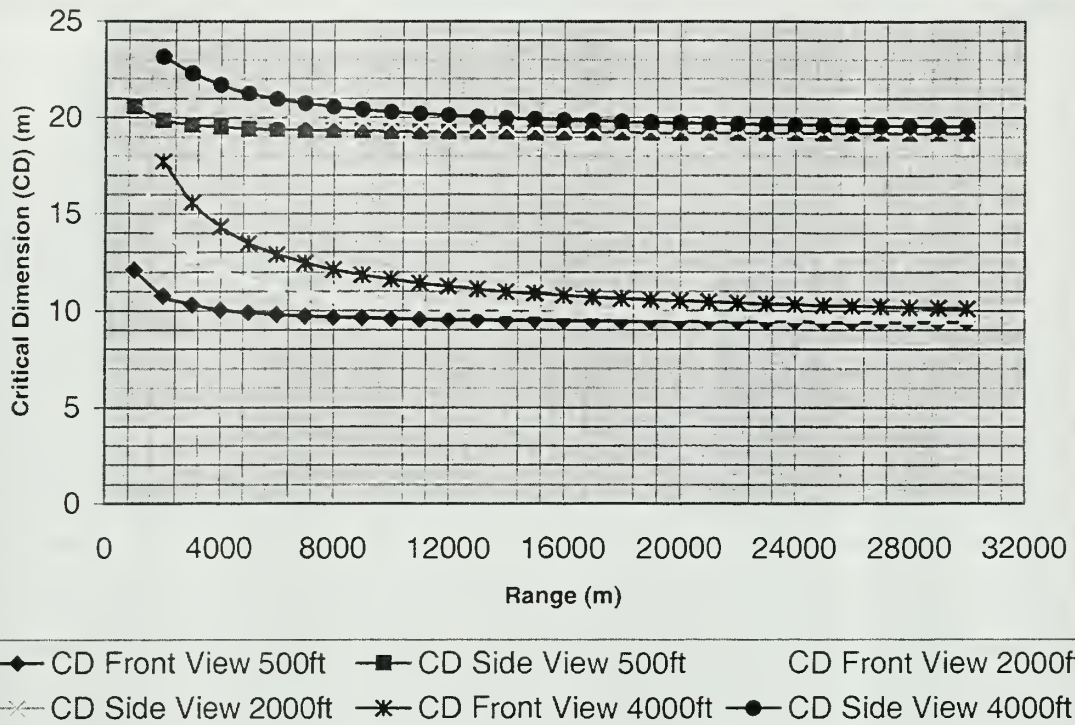


Figure G.1 - Critical Dimension Analysis for 500, 2000, and 4000ft Sensor Heights

## APPENDIX I. ACQUIRE MODEL OUTPUTS

run #1 Wed May 31 21:33:59 2000  
U.S. Army CECOM RDEC NVESD  
ACQUIRE version 1 (May 30 1995)

data file: sadaIifa  
command line: -d sadaIifa  
TARGET DISCRIMINATION RANGE PERFORMANCE  
begin parameter listing...  
Acquire data file for front view of gunboat 500ft at 25km

```
>sensor_lookup
  data_file_name      Sada.dat      ---
  sensor_id           gen2           ---
  performance_mode    MRT           MRT_MDT_MRC_OR_MDC
```

```
>target
  characteristic_size 9.39          meters
  target_signature    7.71          degrees_C
```

```
>cycle_criteria
  detection_n50        0.75          wfov
  detection_n50        0.75          nfov
  classification_n50   1.5           nfov
  recognition_n50      3.0           nfov
  identification_n50   6.0           nfov
```

```
>band-averaged_atmosphere
  #_points: 20      km.....transmittance
                   0.000e+00    1.000e+00
                   5.000e-01    8.465e-01
                   7.500e-01    7.960e-01
                   1.000e+00    7.510e-01
                   2.000e+00    6.049e-01
                   3.000e+00    4.942e-01
                   4.000e+00    4.070e-01
                   5.000e+00    3.371e-01
                   6.000e+00    2.804e-01
                   8.000e+00    1.959e-01
                   1.000e+01    1.386e-01
                   1.200e+01    9.860e-02
                   1.400e+01    7.090e-02
                   1.600e+01    5.110e-02
                   1.800e+01    3.710e-02
                   2.000e+01    2.700e-02
                   2.200e+01    1.970e-02
                   2.400e+01    1.440e-02
                   2.600e+01    1.060e-02
                   2.800e+01    7.800e-03
```

>end

end parameter listing...

MESSAGES

2D MRTD from lookup table

cyles/mrad	MRTD
8.300e-001	6.500e-002
1.120e+000	8.500e-002
1.424e+000	1.100e-001
1.767e+000	1.440e-001
2.112e+000	1.880e-001
2.458e+000	2.450e-001
2.794e+000	3.190e-001
3.116e+000	4.160e-001
3.425e+000	5.420e-001
3.720e+000	7.060e-001
4.001e+000	9.210e-001
4.268e+000	1.200e+000
4.522e+000	1.564e+000
4.767e+000	2.039e+000
4.998e+000	2.658e+000
5.219e+000	3.464e+000
5.429e+000	4.515e+000
5.629e+000	5.886e+000
5.820e+000	7.672e+000
6.003e+000	1.000e+001

Sky-to-ground ratio defaulted to 1 for thermal systems.

Last range for input atmospheric transmittance data is less than maximum range.

Loadline does not intersect MRTD/MRC above range 27.4 km, extend curve to lower frequencies and temperatures.

SENSOR

gen2 from Sada.dat

TARGET

characteristic dimension: 9.39 meters

inherent signature: 7.71 degrees C

OBSERVER ENSEMBLE PERFORMANCE

RANGE GIVEN PROBABILITY...

prob	WFOV	NFOV	NFOV	NFOV	NFOV
	N50=0.75	N50=0.75	N50=1.50	N50=3.00	N50=6.00
0.95	8.87 km	17.23 km	11.76 km	7.10 km	3.94 km
0.90	9.91	18.38	12.94	8.01	4.51
0.85	10.66	19.16	13.77	8.67	4.94
0.80	11.27	19.73	14.42	9.23	5.30
0.75	11.81	20.25	14.99	9.71	5.64
0.70	12.32	20.71	15.52	10.17	5.96
0.65	12.79	21.11	15.99	10.61	6.27
0.60	13.24	21.49	16.45	11.05	6.58
0.55	13.71	21.88	16.91	11.47	6.89
0.50	14.18	22.27	17.39	11.91	7.22
0.45	14.64	22.63	17.82	12.39	7.57
0.40	15.13	22.99	18.29	12.86	7.95
0.35	15.68	23.39	18.81	13.38	8.36
0.30	16.23	23.83	19.33	13.98	8.83
0.25	16.89	24.30	19.90	14.61	9.39
0.20	17.64	24.81	20.60	15.38	10.05
0.15	18.54	25.47	21.38	16.31	10.92
0.10	19.72	26.31	22.46	17.60	12.15
0.05	21.58	0.00	24.07	19.61	14.29

end of run 1 from sadaIifa

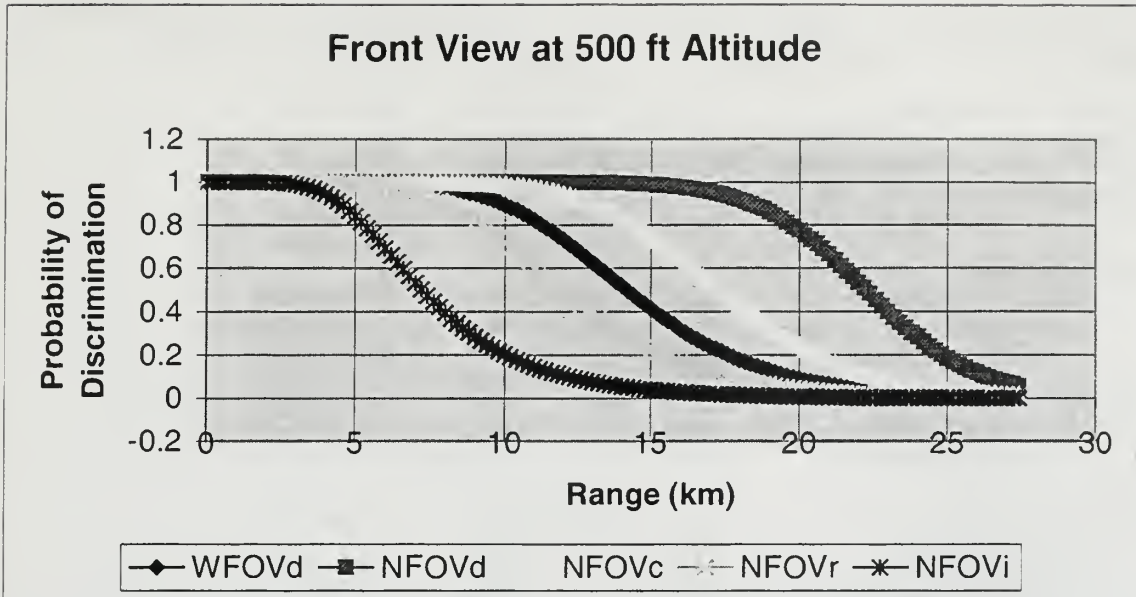


Figure H.1. Range Performance Gunboat Front View at 500 ft Sensor

run #1  
U.S. Army CECOM RDEC NVESD  
ACQUIRE version 1 (May 30 1995)

Wed May 31 21:23:47 2000

data file: sadaIIf  
command line: -d sadaIIf  
TARGET DISCRIMINATION RANGE PERFORMANCE  
begin parameter listing...  
Acquire data file for front view of gunboat 2000ft at 25km

```
>sensor_lookup
  data_file_name      Sada.dat      ---
  sensor_id           gen2          ---
  performance_mode    MRT           MRT_MDT_MRC_OR_MDC
```

```
>target
  characteristic_size  9.78          meters
  target_signature     7.71          degrees_C
```

```
>cycle_criteria
  detection_n50        0.75          wfov
  detection_n50        0.75          nfov
  classification_n50   1.5           nfov
  recognition_n50      3.0           nfov
  identification_n50   6.0           nfov
```

```
>band-averaged_atmosphere
  #_points: 20      km.....transmittance
                   0.000e+00    1.000e+00
                   5.000e-01    8.465e-01
                   7.500e-01    7.960e-01
                   1.000e+00    7.510e-01
                   2.000e+00    6.049e-01
                   3.000e+00    4.942e-01
                   4.000e+00    4.070e-01
                   5.000e+00    3.371e-01
                   6.000e+00    2.804e-01
                   8.000e+00    1.959e-01
                   1.000e+01    1.386e-01
                   1.200e+01    9.860e-02
                   1.400e+01    7.090e-02
                   1.600e+01    5.110e-02
                   1.800e+01    3.710e-02
                   2.000e+01    2.700e-02
                   2.200e+01    1.970e-02
                   2.400e+01    1.440e-02
                   2.600e+01    1.060e-02
                   2.800e+01    7.800e-03
```

>end

end parameter listing...

MESSAGES

2D MRTD from lookup table

cyles/mrad	MRTD
8.300e-001	6.500e-002
1.120e+000	8.500e-002
1.424e+000	1.100e-001
1.767e+000	1.440e-001
2.112e+000	1.880e-001
2.458e+000	2.450e-001
2.794e+000	3.190e-001
3.116e+000	4.160e-001
3.425e+000	5.420e-001
3.720e+000	7.060e-001
4.001e+000	9.210e-001
4.268e+000	1.200e+000
4.522e+000	1.564e+000
4.767e+000	2.039e+000
4.998e+000	2.658e+000
5.219e+000	3.464e+000
5.429e+000	4.515e+000
5.629e+000	5.886e+000
5.820e+000	7.672e+000
6.003e+000	1.000e+001

Sky-to-ground ratio defaulted to 1 for thermal systems.

Last range for input atmospheric transmittance data is less than maximum range.

Loadline does not intersect MRTD/MRC above range 27.4 km, extend curve to lower frequencies and temperatures.

SENSOR

gen2 from Sada.dat

TARGET

characteristic dimension: 9.78 meters

inherent signature: 7.71 degrees C

OBSERVER ENSEMBLE PERFORMANCE

RANGE GIVEN PROBABILITY...

prob	WFOV	NFOV	NFOV	NFOV	NFOV
	N50=0.75	N50=0.75	N50=1.50	N50=3.00	N50=6.00
0.95	9.14 km	17.53 km	12.07 km	7.33 km	4.08 km
0.90	10.20	18.69	13.26	8.26	4.68
0.85	10.97	19.44	14.10	8.94	5.12
0.80	11.57	20.02	14.74	9.50	5.49
0.75	12.12	20.55	15.32	9.99	5.83
0.70	12.63	20.97	15.84	10.46	6.16
0.65	13.10	21.37	16.31	10.92	6.48
0.60	13.57	21.76	16.77	11.34	6.79
0.55	14.04	22.15	17.25	11.78	7.12
0.50	14.49	22.52	17.68	12.23	7.46
0.45	14.96	22.87	18.13	12.70	7.82
0.40	15.47	23.23	18.60	13.17	8.19
0.35	15.99	23.63	19.11	13.71	8.62
0.30	16.55	24.07	19.61	14.29	9.11
0.25	17.22	24.51	20.19	14.93	9.66
0.20	17.94	25.03	20.87	15.71	10.34
0.15	18.86	25.69	21.65	16.63	11.22
0.10	20.00	26.52	22.69	17.90	12.47
0.05	21.85	0.00	24.29	19.90	14.60

end of run 1 from sadaIIf



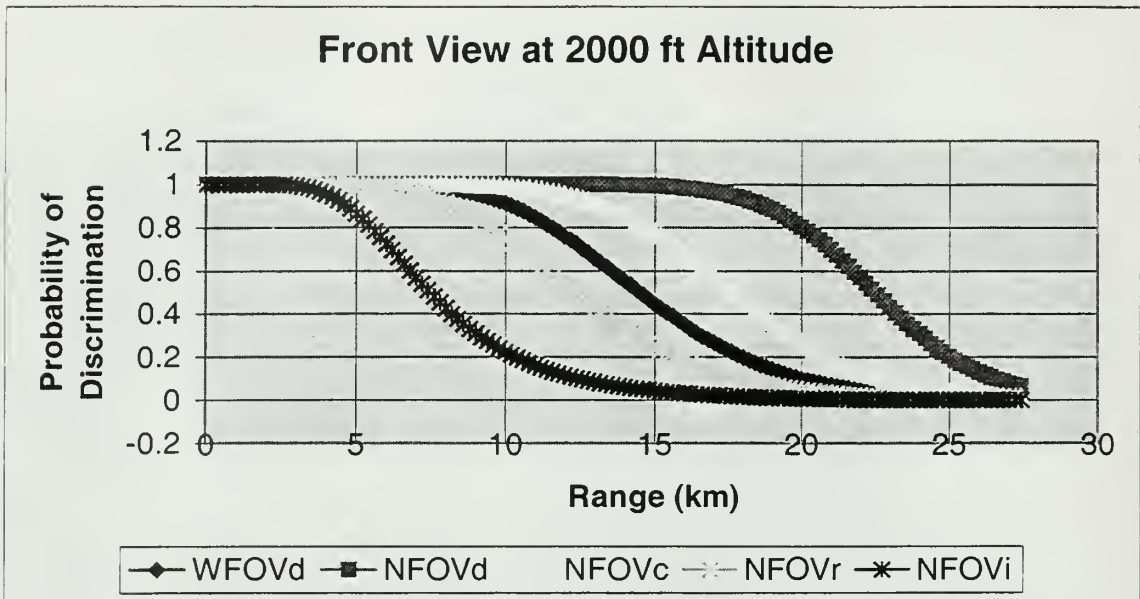


Figure H.2. Range Performance Gunboat Front View at 2000 ft Sensor

run #1  
U.S. Army CECOM RDEC NVESD  
ACQUIRE version 1 (May 30 1995)

Wed May 31 21:34:14 2000

data file: sadaIIfb  
command line: -d sadaIIfb  
TARGET DISCRIMINATION RANGE PERFORMANCE  
begin parameter listing...  
Acquire data file for front view of gunboat 4000ft at 25km

```
>sensor_lookup
  data_file_name      Sada.dat      ---
  sensor_id          gen2          ---
  performance_mode    MRT           MRT_MDT_MRC_OR_MDC
```

```
>target
  characteristic_size 10.27      meters
  target_signature    7.71        degrees_C
```

```
>cycle_criteria
  detection_n50       0.75        wfov
  detection_n50       0.75        nfov
  classification_n50 1.5         nfov
  recognition_n50     3.0         nfov
  identification_n50  6.0         nfov
```

```
>band-averaged_atmosphere
#_points: 20      km.....transmittance
0.000e+00        1.000e+00
5.000e-01        8.465e-01
7.500e-01        7.960e-01
1.000e+00        7.510e-01
2.000e+00        6.049e-01
3.000e+00        4.942e-01
4.000e+00        4.070e-01
5.000e+00        3.371e-01
6.000e+00        2.804e-01
8.000e+00        1.959e-01
1.000e+01        1.386e-01
1.200e+01        9.860e-02
1.400e+01        7.090e-02
1.600e+01        5.110e-02
1.800e+01        3.710e-02
2.000e+01        2.700e-02
2.200e+01        1.970e-02
2.400e+01        1.440e-02
2.600e+01        1.060e-02
2.800e+01        7.800e-03
```

>end

end parameter listing...

MESSAGES

2D MRTD from lookup table

cyles/mrad	MRTD
8.300e-001	6.500e-002
1.120e+000	8.500e-002
1.424e+000	1.100e-001
1.767e+000	1.440e-001
2.112e+000	1.880e-001
2.458e+000	2.450e-001
2.794e+000	3.190e-001
3.116e+000	4.160e-001
3.425e+000	5.420e-001
3.720e+000	7.060e-001
4.001e+000	9.210e-001
4.268e+000	1.200e+000
4.522e+000	1.564e+000
4.767e+000	2.039e+000
4.998e+000	2.658e+000
5.219e+000	3.464e+000
5.429e+000	4.515e+000
5.629e+000	5.886e+000
5.820e+000	7.672e+000
6.003e+000	1.000e+001

Sky-to-ground ratio defaulted to 1 for thermal systems.

Last range for input atmospheric transmittance data is less than maximum range.

Loadline does not intersect MRTD/MRC above range 27.4 km, extend curve to lower frequencies and temperatures.

SENSOR

gen2 from Sada.dat

TARGET

characteristic dimension: 10.27 meters

inherent signature: 7.71 degrees C

OBSERVER ENSEMBLE PERFORMANCE

RANGE GIVEN PROBABILITY...

prob	WFOV	NFOV	NFOV	NFOV	NFOV
	N50=0.75	N50=0.75	N50=1.50	N50=3.00	N50=6.00
0.95	9.48 km	17.89 km	12.46 km	7.63 km	4.26 km
0.90	10.56	19.06	13.65	8.57	4.88
0.85	11.32	19.78	14.48	9.27	5.33
0.80	11.94	20.38	15.13	9.83	5.72
0.75	12.51	20.87	15.72	10.34	6.08
0.70	13.00	21.29	16.21	10.83	6.42
0.65	13.48	21.69	16.69	11.27	6.74
0.60	13.97	22.09	17.17	11.71	7.06
0.55	14.42	22.46	17.61	12.16	7.40
0.50	14.87	22.80	18.04	12.61	7.75
0.45	15.36	23.15	18.50	13.07	8.11
0.40	15.86	23.53	18.99	13.56	8.50
0.35	16.36	23.93	19.44	14.11	8.94
0.30	16.95	24.33	19.96	14.67	9.44
0.25	17.59	24.78	20.55	15.33	10.00
0.20	18.31	25.30	21.18	16.08	10.70
0.15	19.20	25.94	21.97	17.03	11.58
0.10	20.36	26.76	22.98	18.27	12.84
0.05	22.18	0.00	24.55	20.25	14.99

end of run 1 from sadaIIfb

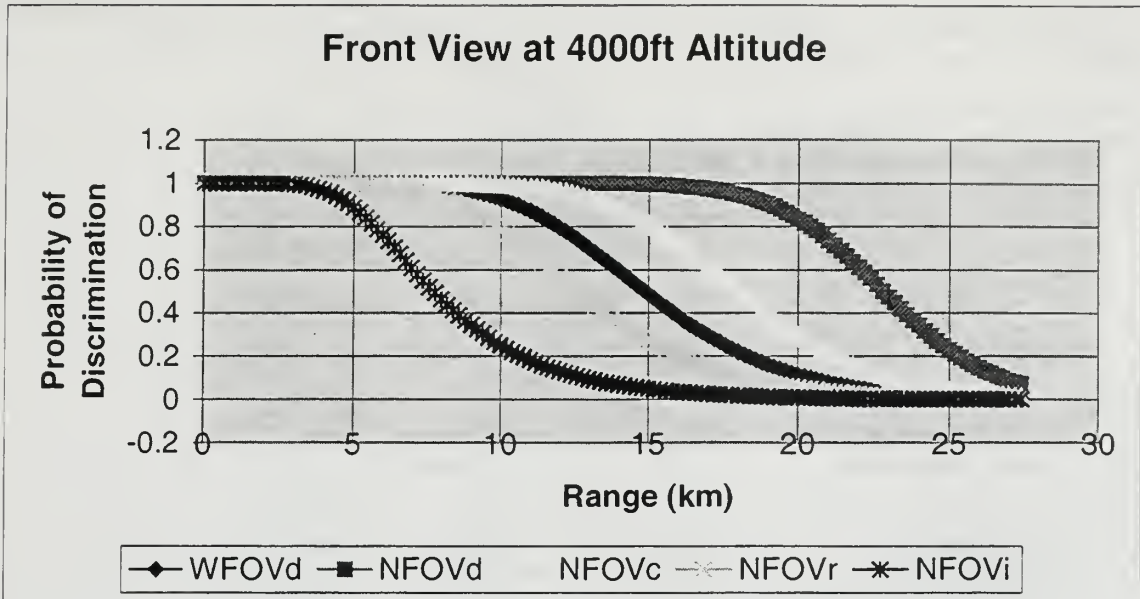


Figure H.3. Range Performance Gunboat Front View at 4000 ft Sensor

run #1  
U.S. Army CECOM RDEC NVESD  
ACQUIRE version 1 (May 30 1995)

Wed May 31 21:34:23 2000

data file: sadaIIsa  
command line: -d sadaIIsa  
TARGET DISCRIMINATION RANGE PERFORMANCE  
begin parameter listing...  
Acquire data file for side view of gunboat 500ft at 25km

```
>sensor_lookup
  data_file_name      Sada.dat      ---
  sensor_id          gen2          ---
  performance_mode    MRT          MRT_MDT_MRC_OR_MDC
```

```
>target
  characteristic_size 19.17      meters
  target_signature    7.71        degrees_C
```

```
>cycle_criteria
  detection_n50        0.75        wfov
  detection_n50        0.75        nfov
  classification_n50   1.5         nfov
  recognition_n50      3.0         nfov
  identification_n50   6.0         nfov
```

```
>band-averaged_atmosphere
  #_points: 20      km.....transmittance
                   0.000e+00    1.000e+00
                   5.000e-01    8.465e-01
                   7.500e-01    7.960e-01
                   1.000e+00    7.510e-01
                   2.000e+00    6.049e-01
                   3.000e+00    4.942e-01
                   4.000e+00    4.070e-01
                   5.000e+00    3.371e-01
                   6.000e+00    2.804e-01
                   8.000e+00    1.959e-01
                   1.000e+01    1.386e-01
                   1.200e+01    9.860e-02
                   1.400e+01    7.090e-02
                   1.600e+01    5.110e-02
                   1.800e+01    3.710e-02
                   2.000e+01    2.700e-02
                   2.200e+01    1.970e-02
                   2.400e+01    1.440e-02
                   2.600e+01    1.060e-02
                   2.800e+01    7.800e-03
```

>end

end parameter listing...

MESSAGES

2D MRTD from lookup table

cyles/mrad	MRTD
8.300e-001	6.500e-002
1.120e+000	8.500e-002
1.424e+000	1.100e-001
1.767e+000	1.440e-001
2.112e+000	1.880e-001
2.458e+000	2.450e-001
2.794e+000	3.190e-001
3.116e+000	4.160e-001
3.425e+000	5.420e-001
3.720e+000	7.060e-001
4.001e+000	9.210e-001
4.268e+000	1.200e+000
4.522e+000	1.564e+000
4.767e+000	2.039e+000
4.998e+000	2.658e+000
5.219e+000	3.464e+000
5.429e+000	4.515e+000
5.629e+000	5.886e+000
5.820e+000	7.672e+000
6.003e+000	1.000e+001

Sky-to-ground ratio defaulted to 1 for thermal systems.  
 Last range for input atmospheric transmittance data is less than maximum range.  
 Loadline does not intersect MRTD/MRC above range 27.4 km, extend curve to lower frequencies and temperatures.

SENSOR

gen2 from Sada.dat

TARGET

characteristic dimension: 19.17 meters  
 inherent signature: 7.71 degrees C

OBSERVER ENSEMBLE PERFORMANCE

RANGE GIVEN PROBABILITY...

prob	WFOV	NFOV	NFOV	NFOV	NFOV
	N50=0.75	N50=0.75	N50=1.50	N50=3.00	N50=6.00
0.95	14.18 km	22.27 km	17.39 km	11.91 km	7.22 km
0.90	15.39	23.18	18.53	13.10	8.14
0.85	16.20	23.80	19.30	13.94	8.80
0.80	16.86	24.28	19.88	14.58	9.37
0.75	17.44	24.66	20.40	15.15	9.85
0.70	17.91	25.02	20.85	15.69	10.31
0.65	18.37	25.35	21.24	16.15	10.77
0.60	18.83	25.68	21.63	16.61	11.19
0.55	19.25	25.97	22.02	17.08	11.62
0.50	19.65	26.26	22.40	17.53	12.07
0.45	20.08	26.56	22.75	17.97	12.54
0.40	20.53	26.88	23.12	18.45	13.02
0.35	20.97	27.20	23.51	18.97	13.54
0.30	21.44	0.00	23.95	19.47	14.14
0.25	21.99	0.00	24.40	20.05	14.77
0.20	22.60	0.00	24.93	20.74	15.55
0.15	23.31	0.00	25.58	21.51	16.48
0.10	24.26	0.00	26.41	22.57	17.75
0.05	25.75	0.00	0.00	24.18	19.75

end of run 1 from sadaIIsa



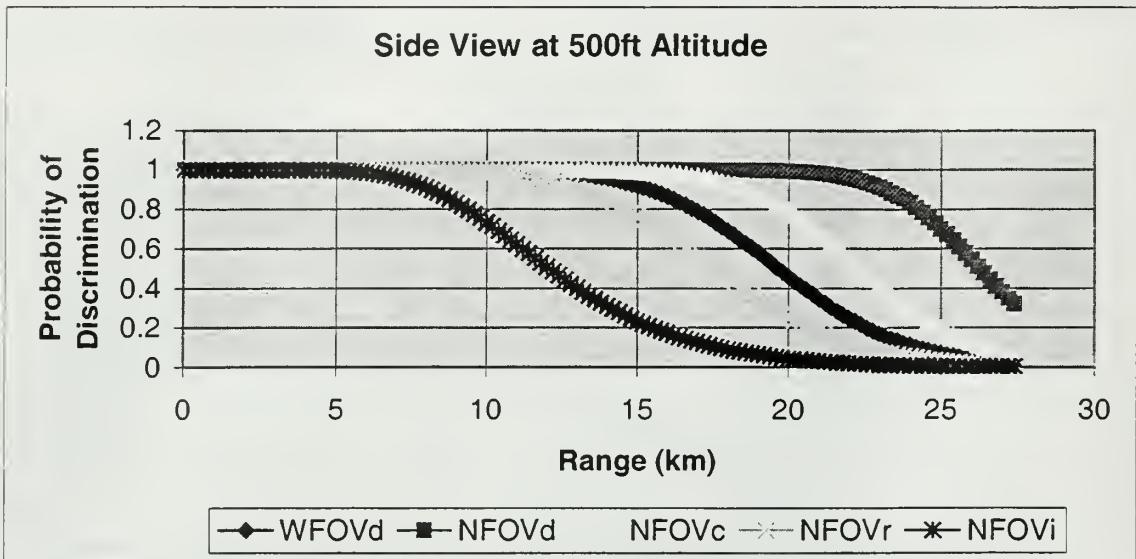


Figure H.4. Range Performance Gunboat Side View at 500 ft Sensor

run #1  
U.S. Army CECOM RDEC NVESD  
ACQUIRE version 1 (May 30 1995)

Wed May 31 21:27:14 2000

data file: sadaIIs  
command line: -d sadaIIs  
TARGET DISCRIMINATION RANGE PERFORMANCE  
begin parameter listing...  
Acquire data file for side view of gunboat 2000ft at 25km

```
>sensor_lookup
  data_file_name      Sada.dat      ---
  sensor_id           gen2          ---
  performance_mode    MRT           MRT_MDT_MRC_OR_MDC
```

```
>target
  characteristic_size 19.36      meters
  target_signature    7.71        degrees_C
```

```
>cycle_criteria
  detection_n50        0.75        wfov
  detection_n50        0.75        nfov
  classification_n50   1.5         nfov
  recognition_n50      3.0         nfov
  identification_n50   6.0         nfov
```

```
>band-averaged_atmosphere
#_points: 20      km.....transmittance
0.000e+00        1.000e+00
5.000e-01        8.465e-01
7.500e-01        7.960e-01
1.000e+00        7.510e-01
2.000e+00        6.049e-01
3.000e+00        4.942e-01
4.000e+00        4.070e-01
5.000e+00        3.371e-01
6.000e+00        2.804e-01
8.000e+00        1.959e-01
1.000e+01        1.386e-01
1.200e+01        9.860e-02
1.400e+01        7.090e-02
1.600e+01        5.110e-02
1.800e+01        3.710e-02
2.000e+01        2.700e-02
2.200e+01        1.970e-02
2.400e+01        1.440e-02
2.600e+01        1.060e-02
2.800e+01        7.800e-03
```

>end

end parameter listing...

MESSAGES

2D MRTD from lookup table

cyles/mrad	MRTD
8.300e-001	6.500e-002
1.120e+000	8.500e-002
1.424e+000	1.100e-001
1.767e+000	1.440e-001
2.112e+000	1.880e-001
2.458e+000	2.450e-001
2.794e+000	3.190e-001
3.116e+000	4.160e-001
3.425e+000	5.420e-001
3.720e+000	7.060e-001
4.001e+000	9.210e-001
4.268e+000	1.200e+000
4.522e+000	1.564e+000
4.767e+000	2.039e+000
4.998e+000	2.658e+000
5.219e+000	3.464e+000
5.429e+000	4.515e+000
5.629e+000	5.886e+000
5.820e+000	7.672e+000
6.003e+000	1.000e+001

Sky-to-ground ratio defaulted to 1 for thermal systems.

Last range for input atmospheric transmittance data is less than maximum range.

Loadline does not intersect MRTD/MRC above range 27.4 km, extend curve to lower frequencies and temperatures.

SENSOR

gen2 from Sada.dat

TARGET

characteristic dimension: 19.36 meters

inherent signature: 7.71 degrees C

OBSERVER ENSEMBLE PERFORMANCE

RANGE GIVEN PROBABILITY...

prob	WFOV	NFOV	NFOV	NFOV	NFOV
	N50=0.75	N50=0.75	N50=1.50	N50=3.00	N50=6.00
0.95	14.26 km	22.33 km	17.46 km	11.99 km	7.27 km
0.90	15.48	23.24	18.61	13.18	8.20
0.85	16.28	23.86	19.37	14.02	8.87
0.80	16.94	24.33	19.95	14.66	9.43
0.75	17.51	24.71	20.47	15.23	9.92
0.70	17.99	25.07	20.91	15.76	10.39
0.65	18.45	25.41	21.30	16.23	10.84
0.60	18.91	25.73	21.69	16.69	11.27
0.55	19.32	26.02	22.08	17.16	11.70
0.50	19.72	26.31	22.46	17.61	12.15
0.45	20.15	26.61	22.81	18.05	12.62
0.40	20.60	26.92	23.17	18.53	13.09
0.35	21.03	27.25	23.57	19.04	13.62
0.30	21.51	0.00	24.01	19.54	14.21
0.25	22.06	0.00	24.46	20.12	14.85
0.20	22.66	0.00	24.98	20.80	15.63
0.15	23.36	0.00	25.64	21.58	16.55
0.10	24.32	0.00	26.46	22.63	17.82
0.05	25.80	0.00	0.00	24.23	19.82

end of run 1 from sadaIIs

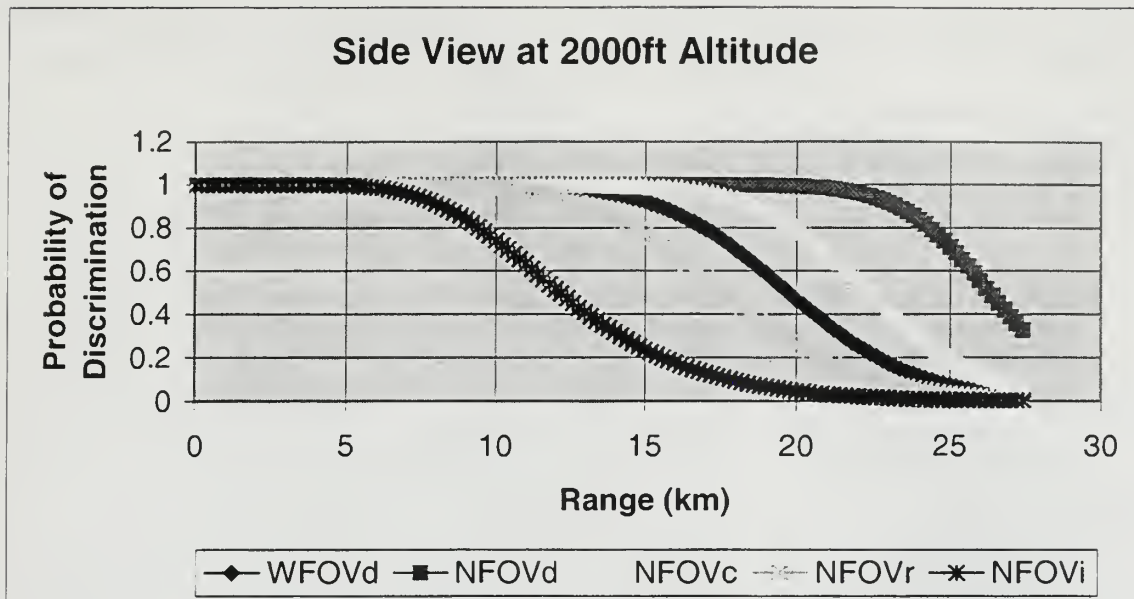


Figure H.5. Range Performance Gunboat Side View at 2000 ft Sensor

run #1  
U.S. Army CECOM RDEC NVESD  
ACQUIRE version 1 (May 30 1995)

Wed May 31 21:34:32 2000

data file: sadaIIsb  
command line: -d sadaIIsb  
TARGET DISCRIMINATION RANGE PERFORMANCE  
begin parameter listing...  
Acquire data file for side view of gunboat 4000ft at 25km

```
>sensor_lookup
  data_file_name      Sada.dat      ---
  sensor_id          gen2          ---
  performance_mode    MRT          MRT_MDT_MRC_OR_MDC
```

```
>target
  characteristic_size 19.61      meters
  target_signature    7.71      degrees_C
```

```
>cycle_criteria
  detection_n50        0.75      wfov
  detection_n50        0.75      nfov
  classification_n50  1.5       nfov
  recognition_n50     3.0       nfov
  identification_n50  6.0       nfov
```

```
>band-averaged_atmosphere
  #_points: 20      km.....transmittance
  0.000e+00        1.000e+00
  5.000e-01        8.465e-01
  7.500e-01        7.960e-01
  1.000e+00        7.510e-01
  2.000e+00        6.049e-01
  3.000e+00        4.942e-01
  4.000e+00        4.070e-01
  5.000e+00        3.371e-01
  6.000e+00        2.804e-01
  8.000e+00        1.959e-01
  1.000e+01        1.386e-01
  1.200e+01        9.860e-02
  1.400e+01        7.090e-02
  1.600e+01        5.110e-02
  1.800e+01        3.710e-02
  2.000e+01        2.700e-02
  2.200e+01        1.970e-02
  2.400e+01        1.440e-02
  2.600e+01        1.060e-02
  2.800e+01        7.800e-03
```

>end

end parameter listing...

MESSAGES

2D MRTD from lookup table

cycles/mrad	MRTD
8.300e-001	6.500e-002
1.120e+000	8.500e-002
1.424e+000	1.100e-001
1.767e+000	1.440e-001
2.112e+000	1.880e-001
2.458e+000	2.450e-001
2.794e+000	3.190e-001
3.116e+000	4.160e-001
3.425e+000	5.420e-001
3.720e+000	7.060e-001
4.001e+000	9.210e-001
4.268e+000	1.200e+000
4.522e+000	1.564e+000
4.767e+000	2.039e+000
4.998e+000	2.658e+000
5.219e+000	3.464e+000
5.429e+000	4.515e+000
5.629e+000	5.886e+000
5.820e+000	7.672e+000
6.003e+000	1.000e+001

Sky-to-ground ratio defaulted to 1 for thermal systems.  
 Last range for input atmospheric transmittance data is less than maximum range.  
 Loadline does not intersect MRTD/MRC above range 27.4 km, extend curve to lower frequencies and temperatures.

SENSOR

gen2 from Sada.dat

TARGET

characteristic dimension: 19.61 meters  
 inherent signature: 7.71 degrees C

OBSERVER ENSEMBLE PERFORMANCE  
 RANGE GIVEN PROBABILITY...

prob	WFOV N50=0.75	NFOV N50=0.75	NFOV N50=1.50	NFOV N50=3.00	NFOV N50=6.00	
	14.35 km	22.42 km	17.55 km	12.09 km	7.35 km	0.95
0.90	15.58	23.31	18.71	13.28	8.28	
0.85	16.38	23.94	19.46	14.12	8.95	
0.80	17.05	24.40	20.04	14.76	9.52	
0.75	17.60	24.78	20.57	15.34	10.01	
0.70	18.08	25.14	20.99	15.86	10.48	
0.65	18.55	25.48	21.39	16.33	10.93	
0.60	19.01	25.80	21.78	16.79	11.36	
0.55	19.40	26.09	22.17	17.27	11.80	
0.50	19.81	26.38	22.53	17.70	12.25	
0.45	20.24	26.68	22.88	18.15	12.71	
0.40	20.69	26.99	23.25	18.62	13.19	
0.35	21.12	27.31	23.65	19.13	13.73	
0.30	21.59	0.00	24.08	19.63	14.31	
0.25	22.15	0.00	24.53	20.21	14.95	
0.20	22.74	0.00	25.05	20.88	15.73	
0.15	23.44	0.00	25.71	21.66	16.65	
0.10	24.38	0.00	26.53	22.71	17.92	
0.05	25.86	0.00	0.00	24.30	19.91	

end of run 1 from sadaIIsb



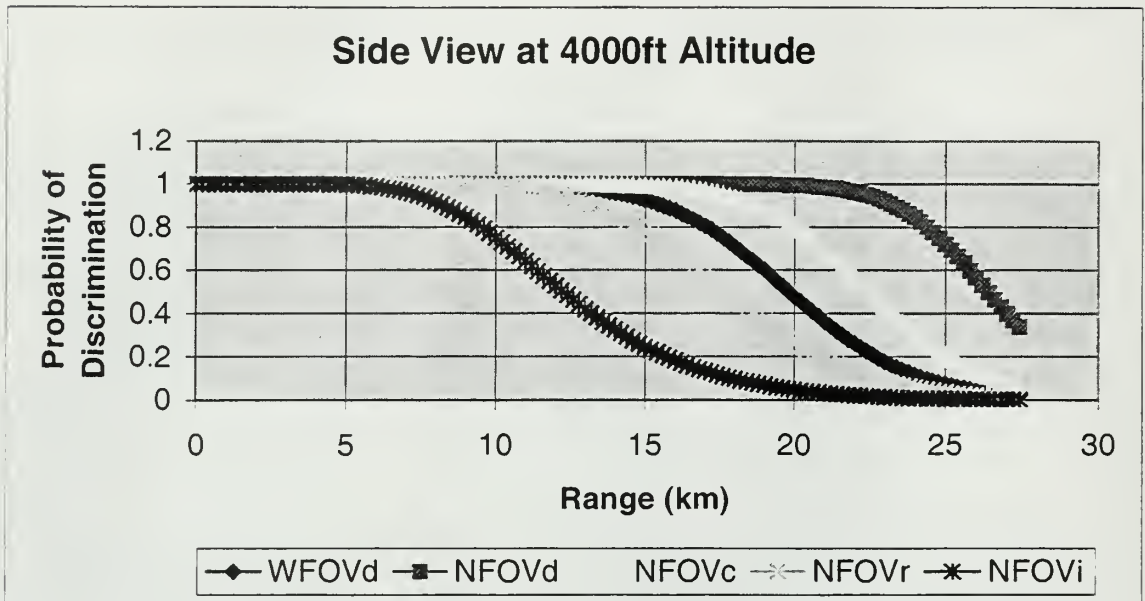


Figure H.6. Range Performance Gunboat Side View at 4000 ft Sensor

## APPENDIX J. COMPARISON OF BEER'S LAW AND SEARAD OUTPUTS

### BEER'S LAW APPROXIMATION FOR MIDLATITUDE SUMMER OUTPUTS OF SEARAD

The Beer's Law gives transmissivity ( $\tau$ ) as: 
$$\tau = \frac{I}{I_0} = e^{-\mu \cdot R}$$

The 4km transmissivity calculated by SeaRad is  $\tau_4 := 0.407$

The atmospheric extinction coefficient ( $\mu$ ) for 4km range (R)  $R := 4$  can be computed as:

$$\tau_4 := e^{-\mu \cdot R} \quad \ln(\tau_4) = -\mu \cdot R \quad \mu := \frac{-\ln(\tau_4)}{R} \quad \mu = 0.225$$

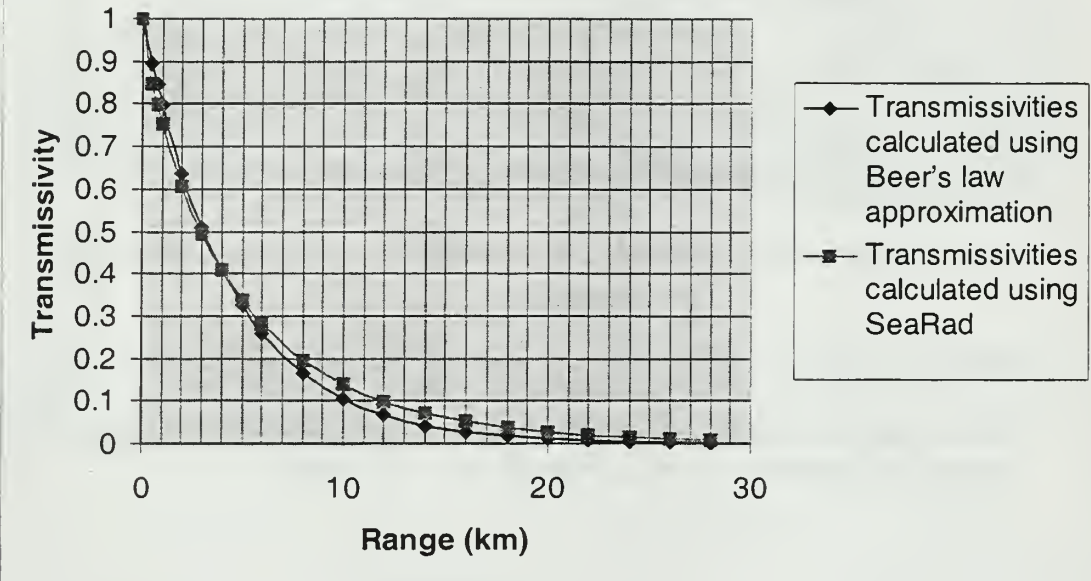
Then for  $\mu=0.225$ , the other transmissivities for different ranges can be found by using the Beer's Law approximation. (Ranges,  $R_i$ , are 0,0.5,0.75,1...6,8...28 km)

$I := 20$

$i := 0..I - 1$

0		0		1
0.5		0	1	0.8465
0.75		1	0.894	0.796
1		2	0.845	0.751
2		3	0.799	0.6049
3		4	0.638	0.4942
4		5	0.51	0.407
5		6	0.407	0.3371
6		7	0.325	0.2804
8		8	0.26	0.1959
10		9	0.166	0.1386
12		10	0.106	0.0986
14		11	0.067	0.0709
16		12	0.043	0.0511
18		13	0.027	0.0371
20		14	0.018	0.027
22		15	0.011	0.0197
24		16	$7.125 \cdot 10^{-3}$	0.0144
26		17	$4.545 \cdot 10^{-3}$	0.0106
28		18	$2.9 \cdot 10^{-3}$	0.0078
		19	$1.85 \cdot 10^{-3}$	

Comparison of Transmissivities Calculated Using Beer's Law Approximation and SeaRad (Common 4km Transmissivity)



## APPENDIX K. COMPARISON TABLES OF WINEOTDA AND TAWS OUTPUTS

### A. TAWS OVERVIEW

The Target Acquisition Weather Software (TAWS) predicts the performance of air-to-ground electro-optical weapon and navigation systems. The underlying algorithms are identical to those of EOTDA V. 3.1 and WinEOTDA, although some programming errors have been corrected. Performance is expressed primarily in terms of maximum detection or lock-on range. Results are displayed in graphic and tabular formats. The program is available through NRL or through AFRL.

TAWS supports systems in three regions of the spectrum: Infrared (3-5 micrometers; 8-12 micrometers); Visible (0.4 - 0.9 micrometers); and Laser (1.06 micrometers). The Visible includes both television (TV) and Night Vision Goggles (NVG) systems.

TAWS is designed to provide several types of analyses:

- Illumination Analysis: involves the computation of solar and lunar ephemeris information for a specified location. A mission planner, for example, might be interested in an illumination analysis to

determine the time of sunset for a particular mission date and location.

- **Single Point-Based Analysis:** involves detailed performance predictions for a particular location. A mission planner, for example, might be interested in a point-based analysis to predict detection range for a particularly important target as a function of time.
- **Multiple Map-Based Analysis:** involves detailed performance predictions for locations along a mission route. A mission planner, for example, might be interested in a map-based analysis to predict detection range for a series of key locations as a function of time.

TAWS runs on a PC under Microsoft Windows 95/NT/98.

## **B. COMPARISON OF TAWS AND WinEOTDA OUTPUTS**

TAWS was run with the same scenario input parameters used in WinEOTDA to observe the differences in delta T calculations and detection ranges. The delta T outputs of TAWS gave different values as seen in Table J.1. The

calculated temperature difference parameters were reduced significantly compared to WinEOTDA outputs.

SENSOR HEIGHT (Ft)	WinEOTDA DETECTION DELTA T (K) (4 km transmissivity = 0.60 absolute humidity = 8.9)				TAWS DETECTION DELTA T (K) (4 km transmissivity = 0.589 absolute humidity = 9.01)			
	SIDE VIEW (90 deg)		FRONT VIEW (0 deg)		SIDE VIEW (90 deg)		FRONT VIEW (0 deg)	
	NFOV	WFOV	NFOV	WFOV	NFOV	WFOV	NFOV	WFOV
500	28.9	28.3	33.4	32.7	19.1	19.2	19.6	11.5
2000	27.9	25.1	32.1	29.2	17.9	17.6	18.2	10.6
4000	26.6	21.7	30.8	25.4	16.7	10.0	17.1	6.3

Table J.1 - WinEOTDA And TAWS Detection Delta T Outputs Comparison For The Same Scenario Input Parameters For Different Sensor Altitudes

However, in the case of detection ranges, NFOV predictions were found to be the same except for the 2000ft sensor altitude. As can be seen in Table J.2, TAWS calculated different detection ranges for varying aspect angles and sensor altitudes in WFOV detection. This can be accepted as an improvement to the insensitivity of WinEOTDA to changing aspect angles and sensor altitudes in WFOV detection.

SENSOR HEIGHT (Ft)	WinEOTDA MRT DETECTION RANGE (4 km transmissivity = 0.60) (Km)				TAWS MRT DETECTION RANGE (4 km transmissivity =0.589) (Km)			
	SIDE VIEW (90 deg)		FRONT VIEW (0 deg)		SIDE VIEW (90 deg)		FRONT VIEW (0 deg)	
	NFOV	WFOV	NFOV	WFOV	NFOV	WFOV	NFOV	WFOV
500	44.1	18.4	44.1	18.4	44.1	36.1	43.2	30.8
2000	51.5	18.5	48.1	18.5	47.0	35.6	42.5	30.7
4000	55.5	18.6	55.5	18.6	55.5	48.6	55.5	38.6

Table J.2 - WinEOTDA And TAWS MRT Detection Range Comparison Table With The Original Scenario Parameters For Different Sensor Altitudes



THIS PAGE INTENTIONALLY LEFT BLANK

## LIST OF REFERENCES

1. Driggers, Ronald G., Cox, Paul, Edwards, Timothy, *Introduction to Infrared and Electro-Optical Systems*, Artech House, Inc. MA, 1999.
2. Schlessinger, Monroe, *Infrared Technology Fundamentals*, Marcel Dekker, Inc. New York, NY, 1995.
3. Cooper, A. W. and E.C Crittenden, Jr, *Electro-Optic Sensors and Systems*, Naval Postgraduate School, Monterey, CA, 1998.
4. Cooper, A. W., *SeaRad Radiance Model*, Class Notes, Naval Postgraduate School, Spring 1999.
5. Khalil Seyrafi and S. A. Hovanessian, *Introduction to Electro-Optical Imaging and Tracking Systems*, Artech House, Inc. MA, 1993.
6. Hudson, Richard D., *Infrared System Engineering*, John Wiley & Sons, New York, NY, 1969.
7. Zeisse, C. R., *SeaRad, A Sea Radiance Prediction Code*, Naval Command, Control and Ocean Surveillance Center RDT&E Division, San Diego, CA, November 1995.
8. Wagner, H. Daniel, *Naval Tactical Decision Aids, Lecture Notes*, Naval Postgraduate School, 1989.

9. Holst, Gerald C., *Electro-Optical Imaging System Performance*, JCD Publishing, FL, 1995.
10. Shumaker, David L., J. T. Wood and C. R. Thacker, *Infrared Imaging Systems Analysis*, The Environmental Research Institute of Michigan, 1993.
11. U.S. Army Night Vision and Electronic Sensors Directorate, *FLIR92 Thermal Imaging Systems Performance Model, Analyst's Reference Guide*, January 1993.
12. Gouveia, J. M., Hodges, D. B, *Electro-Optical Tactical Decision Aid (EOTDA), User's Manual Version 3.1*, 1994
13. *ACQUIRE User's Guide*, US Army CECOM RDEC, Night Vision and Electronic Sensors Directorate, 1995.
14. Goroch, Andreas K., Gush, Robert J., *Software Test Description for the EOTDA of Tactical Environmental Support System TESS(3)*, Naval Research Laboratory Marine Meteorology Division, Monterey, CA, 25 August 1994.
15. Ludwiszewski, Alan, *Standard Module Approach to Scanning Requirements for Second-generation Airborne FLIRs*, Proceedings of SPIE, Vol.2470/257, Bellingham, Washington, 1995.

16. Accetta, Joseph S., Shumaker, David L., *The Infrared and Electro-Optical Systems Handbook, Volume 4*, SPIE Optical Engineering Press, Bellingham, Washington, 1996.
17. Kneizys, F. X., Anderson G. P., Shettle E. P., Gallery W. O., Abreu L. W., Selby J. E. A., Chetwynd J. H., and Clough S. A., *Users Guide to LOWTRAN 7*, Air Force Geophysics Laboratory, Hanscom AFB, MA, 1988.
18. Berk, A., Bernstein L. S., and Robertson D. C., *MODTRAN: a moderate resolution model for LOWTRAN7*, Report No. GL-TR-89-0122, Geophysics Laboratory, Air Force Systems Command, Hanscom AFB, MA, 1989.
19. Johnson, J., *Analysis of Image Forming Systems*, in the Proceedings of the Image Intensifier Symposium, pp.249-273, Warfare Electrical Engineering Department, U.S. Army Research and Development Laboratory, Ft. Belvoir, VA, 1958.
20. Cooper, A. W., W. J. Lentz, P. L. Walker and P. M. Chan, *Infrared Polarization Measurements of Ship Signatures and Background Contrast*, In *Characterization and Propagation of Sources and Backgrounds*, Wendell W. Watkins and Dieter Clement, Eds., Proceedings SPIE Vol. 2223, pp. 300-309, 1994.

21. Jensen, D.R., *EO propagation assessment in the coastal environments*, NCCOSC RDTE DIV Code 543, San Diego, CA, Collection of EOPACE WORKSHOP REPORTS, May 1995.
22. Dreksler, S., Goroch, A.K., *Development of Windows NT Electro-Optical Meteorological Decision Aid (NT-EOMDA)*, Battlespace Atmospherics Conference, edited by K.D. Anderson, and J.H. Richter, San Diego, CA, 1997.

### INITIAL DISTRIBUTION LIST

1. Defense Technical Information Center ..... 2  
8725 John J. Kingman Rd., STE 0944  
Ft. Belvoir, VA 22060-6218
2. Dudley Knox Library ..... 2  
Naval Postgraduate School  
411 Dyer Rd.  
Monterey, CA 93943-5101
3. Professor Alfred W. Cooper ..... 3  
Code PH/Cr  
Naval Postgraduate School  
Monterey, CA 93943-5101
4. Dr. Andreas K. Goroeh ..... 1  
Naval Research Laboratory  
Monterey, CA 93940
5. Professor Kenneth Davidson ..... 1  
Code ME/Cr  
Naval Postgraduate School  
Monterey, CA 93943-5101
6. Celalettin Goksin ..... 2  
Buket Kent Oyak 8nci Kisim No: 9/6  
Cayyolu  
Ankara, Turkey 06530
7. Kara Harp Okulu Kutuphanesi ..... 1  
Bakanliklar  
Ankara, Turkey 06200
8. Kara Kuvvetleri K.ligi Kutuphanesi ..... 1  
Bakanliklar  
Ankara, Turkey 06200
9. Professor Dan Boger ..... 1  
Chairman, Code IW  
Naval Postgraduate School  
Monterey, CA 93943-5101







63 290NPG 2563  
TH  
6/02 22537 200











DUDLEY KNOX LIBRARY



3 2768 00379468 6